HIGHWAY RESEARCH RECORD

Number 396

Pavement Friction Characteristics and Water Depths

6 reports
prepared for the
51st Annual Meeting

Subject Areas

22 Highway Design
23 Highway Drainage
26 Pavement Performance
40 Maintenance, General
51 Highway Safety
53 Traffic Control and Operations

HIGHWAY RESEARCH BOARD
DIVISION OF ENGINEERING NATIONAL RESEARCH COUNCIL
NATIONAL ACADEMY OF SCIENCES—NATIONAL ACADEMY OF ENGINEERING

Washington, D.C. 1972

NOTICE

The studies reported herein were not undertaken under the aegis of the National Academy of Sciences or the National Research Council. The papers report research work of the authors done at the institution named by the authors. The papers were offered to the Highway Research Board of the National Research Council for publication and are published herein in the interest of the dissemination of information from research, one of the major functions of the HRB.

Before publication, each paper was reviewed by members of the HRB committee named as its sponsor and was accepted as objective, useful, and suitable for publication by NRC. The members of the committee were selected for their individual scholarly competence and judgment, with due consideration for the balance and breadth of disciplines. Responsibility for the publication of these reports rests with the sponsoring committee; however, the opinions and conclusions expressed in the reports are those of the individual authors and not necessarily those of the sponsoring committee, the HRB, or the NRC.

Although these reports are not submitted for approval to the Academy membership or to the Council of the Academy, each report is reviewed and processed according to procedures established and monitored by the Academy's Report Review Committee.

ISBN 0-309-02068-9

Price: $2.40

Available from

Highway Research Board
National Academy of Sciences
2101 Constitution Avenue, N. W.
Washington, D. C. 20418

CONTENTS

FOREWORD

The papers presented in this RECORD should be of interest to highway department engineers responsible for the design and maintenance of skid-resistant pavement surfaces. Information is presented on materials performance as well as on the effects of traffic volume, water depth, tire pressure and tread depth, de-icing salts, cross slope, surface texture, and other factors on the level of skid resistance. A correlation between the trailer and stopping-distance methods of measuring skid resistance is also presented.

Mahone and Runkle present the results of a three-phase study. The first phase involves a correlation between Virginia's skid trailer and stopping-distance car to provide a method of predicting automobile stopping distances from trailer results. The second phase of the study was concerned with the effects of traffic wear on three types of pavement surfaces. Bituminous pavements constructed with polish-resistant aggregates tended to retain a high skid resistance even after 30 million vehicle passes, portland cement concrete surfaces incorporating siliceous sand had lost much of their skid resistance after 25 million vehicle passes, and bituminous surfaces using limestone as the coarse aggregate were slippery after less than 2 million vehicle passes. The final phase of the study involved a correlation between the incidence of wet-pavement accidents and the level of skid resistance on Interstate highways in Virginia. The conclusion was that a skid number of 42 should be provided in traffic lanes and a skid number of 48 should be provided in the passing lanes of Interstate highways.

Kearney, McAlpin, and Burnett discuss the results of skid resistance tests on bituminous pavements in the state of New York during the past 10 years. The wearing characteristics of various aggregates as they affect the skid resistance of surfaces were of primary concern to these investigators. The results of the study showed that an aggregate must have a minimum of 20 percent noncarbonate material or 10 percent sand-sized impurities to provide an adequate level of skid resistance that would last for the life of the pavement. As a result of these tests, a specification has been written to require that aggregates not meeting these criteria be blended with a minimum of 20 percent noncarbonate stone.

Glennon describes a research project conducted to determine the frictional requirements for passing maneuvers. He concludes that wet-weather speed limits should be imposed along with minimum skid resistance requirements to provide adequate skid resistance for accomplishing passing maneuvers on wet pavements.

Martinez, Lewis, and Stocker discuss the phenomenon of hydroplaning as it applies to highway pavement surfaces. A parameter involving the degree of wheel spin-down as a vehicle travels through a known depth of water was used as the criterion to study the effects of water depth, tire pressure, tread depth, and wheel load on the hydroplaning susceptibility of portland cement concrete and gravel seal coat surfaces. They recommend that vehicle speed be reduced to 50 mph to prevent hydroplaning where water accumulates to a depth of 0.1 in. or more during wet weather.

Mortimer and Ludema call attention to the hidden wetness of pavement surfaces that may appear to be dry. This condition is present during the drying period immediately after a rainfall and on those surfaces that have been coated with de-icing salts, due to the affinity, particularly of calcium chloride, for moisture in the air. Equations are presented that predict fluid film drying rates and the influence on skid resistance.

The effects of the roadway cross slope, rain intensity, surface texture, and drainage path length on water film depth are assessed by Gallaway, Rose, and Schiller. An equation is developed to assist geometric design and pavement materials engineers in providing an acceptable friction level based on a design for adequate surface water runoff. Kao and Hutchinson, in discussing this research, point out that wind velocity and direction and raindrop impact also have a considerable effect on water film depth.

—A. B. Moore

PAVEMENT FRICTION NEEDS

David C. Mahone and Stephen N. Runkle, Virginia Highway Research Council

At 61 sites, skid trailer and stopping-distance tests were performed to establish a correlation between Virginia's skid trailer and the stopping-distance car. The regression analyses performed indicate that the trailer and the car are equivalent at a skid number of 30; however, as the pavement friction increases, the trailer gives progressively higher numbers than the car. We determined the relationship between accumulated traffic volumes and friction levels by conducting tests at 46 sites. It was found that (a) bituminous mixes manufactured from polish-resistant materials still had high skid resistance after 30 million vehicle passes, (b) portland cement concrete surfaces manufactured from silica sands had lost much of their skid resistance after 25 million passes, and (c) bituminous mixes manufactured from limestone approached a slippery condition after fewer than 2 million vehicle passes. We studied 521 sections, totaling 312.8 miles, on Virginia's Interstate System to determine the relationship between the percentage of wet pavement accidents and the predicted stopping-distance skid numbers. The sites were separated into four categories: open roadway, non-open roadway, open interchanges, and non-open interchanges. It was found that the minimum predicted stopping-distance skid number for the traffic and passing lanes of Interstate roadways with mean traffic speeds of 65 and 70 mph should be 42 and 48 respectively.

•THE PURPOSE of the investigation reported here was to provide the state of Virginia with information for determining the wet friction levels needed for various traffic conditions on its Interstate System (1). All pavement friction data for the analyses were obtained with the Virginia Highway Research Council's skid-test trailer (2).

Machine correlation and regression analyses were performed on the data obtained with the Council's skid trailer and stop meter stopping-distance car so that data collected by the skid trailer (reported as SN) could be used to predict the stopping-distance skid numbers that would have been obtained had the stopping-distance car (reported as PSDN) been used.

An analysis of the traffic volume-PSDN relationship was made for data obtained on roads constructed of three paving materials: portland cement concrete manufactured from silica sand, polish-susceptible bituminous mixes, and polish-resistant bituminous mixes.

In the compilation of the information for determining the wet friction values needed for various traffic conditions, prime consideration was given to ascertaining the relationship between the percentage of wet accidents and the PSDN. To the extent possible, the geometric configurations of the roadways were considered. Only data for the Interstate System were analyzed. The compiled wet-pavement accident data were not limited to skidding accident statistics, inasmuch as inadequate friction could promote accidents not involving skidding, e.g., breakway and non-locked-wheel deceleration accidents. In addition, it is sometimes impossible to determine from the accident reports whether skidding was a major contributing factor.

The greatest limitation of the study was the inability to collect rapidly, and in a usable form, the amount of roadway geometric and pavement surface descriptive data

Sponsored by Committee on Surface Properties-Vehicle Interaction.

necessary to determine the wet friction levels needed for various traffic conditions. Of all the data needed, the skid data might be the easiest to collect; the difficulty is locating and reducing the supporting data into a form compatible with the skid data. In addition to the difficulty cited, the following problems are noted:

1. On roads carrying over 1,000 vehicles per day, Virginia generally does not permit the use of polish-susceptible aggregates. Thus the lower range of skid numbers is not included in this study. Although this is an admirable situation for a highway department to be in, it does reduce the effectiveness of this type of research.
2. As a general rule, Virginia does not have any really harsh textures on its high traffic volume roads. In the past, portland cement concrete roads have been finished with one coverage of a burlap drag, and the high traffic bituminous roads have all been hot plant mixes laid with a regular paving machine. In addition, the gradation has been such that for even the coarsest of the surface mixtures the finished surface has been rather smooth. Some intermediate mixes were included in the study. These mixes are coarser than surface mixes but not so coarse as base mixes, and they are usually used in a leveling course between the base and the surface course. However, they are found only on low traffic volume roads.

MACHINE CORRELATION AND REGRESSION ANALYSES

In the opinion of the authors, skid data are more meaningful if analyzed and reported as predicted stopping-distance skid numbers. For this reason, several regression analyses were performed with the trailer skid number as the independent variable and the car stop meter skid number as the dependent variable. (The data were obtained from correlation tests made at six times between April 1968 and May 1970.) Later these equations will be used to determine predicted car skid numbers. Each data point used in the various analyses is an average value of five tests for both the car and the trailer.

Tests with the skid trailer were conducted at various speeds at the 62 sites, and the stopping-distance car was used to obtain tests at 40 mph and in some cases at other speeds at 61 sites. The data are given in Table 1.

As mentioned the data were collected and regression analyses made in six different groups. Even though the results did change from group to group, there did not appear to be any orderly change with regard to time. Regression analyses from each group for the trailer at 40 mph and the car at 40 mph are shown in Figure 1 and given in Table 2. Because no noticeable effect of time could be established, the 40-mph analysis for all 62 sites was used for predicting the stopping-distance skid numbers. The curve for this analysis is shown in Figure 2.

It should be noted that the Virginia trailer and the car are equivalent at an SN of 30; however, contrary to what was expected, the trailer gives progressively higher numbers than the car as the pavement friction increases. It will be shown later that the correlation between many other trailers and the stopping-distance car is about 1:1.

RELATIONSHIP BETWEEN TRAFFIC VOLUME AND PSDN

Table 3 gives the relationship of accumulated traffic volume to stopping-distance number (both actual and predicted) at 40 mph for Virginia S-4 and S-5 mixes (Appendix) composed of nonpolishing aggregate, portland cement concrete composed of nonpolishing aggregate, and I-2 and I-3 mixes composed of 100 percent limestone.

For the determination of accumulated traffic volume by lane, a computer program was written in which the lane volume breakdown was based on information contained in the Highway Capacity Manual (3). In this program, trucks were considered to be 2.5 automobiles. The results of this analysis are shown in Figure 3. For the I-2 and I-3 mixes the accumulated volume is plotted versus actual SDNs (at 40 mph) rather than PSDNs.

As can be seen from Figure 3, the limestone mixes drop drastically and reach stopping-distance skid numbers in the low forties, with an accumulated volume of only 1.6 million. The S-4 and S-5 mixes still retain PSDNs in the mid to high forties and seem to level off after 25 to 30 million vehicle passes. The portland cement concrete mixes also level off but decrease more rapidly and reach values in the mid to low forties at 20 to 25 million vehicle passes.

Table 1. Skid numbers obtained with stopping-distance car and with skid trailer.

Site	Mix Type	Car Distances (ft) by Speed (mph)				Trailer Distances (ft) by Speed (mph)			
		20	30	40	50	20	30	40	50
1	I-2			46		67	62	56	50
2	I-3			42		66	58	54	51
3	I-2			46		68	62	52	50
4	I-3	40	42	36	32	50	48	41	36
5	I-3	48	46	46	44	66	60	51	46
6	I-2	54	54	55	53	78	68	60	57
7	Weblite		61	65	65		88	84	81
8	Weblite		64	61	61		84	73	72
9	Weblite		54	52	48		59	52	48
10	Weblite		52	45	44		69	60	55
11	Weblite		56	52	45		75	70	57
12	Weblite		57	54	51		78	66	66
13	I-2		42	42			54	52	
14	I-3		39	41			57	53	
15	I-2		47	46	45		58	54	48
16	Sprinkle Weblite		62	58			82	70	
17	I-2 Sprinkle Granite		52	51			72	60	
18	Sprinkle Weblite		63	58			78	60	
19	Sprinkle No. 8 slag		64	63			83	79	
20	Sprinkle Slag sand		64	64			89	83	
21	Sprinkle Fine weblite		63	64			89	78	
22	Sprinkle No. 8 crushed gravel		63	62			82	67	
23	I-3		47	44			56	50	
24	I-2		51	48			63	58	
25	I-3		34	34			44	36	
26	Weblite		56	52	40		75	70	48

Site	Mix Type	Car Distances (ft) by Speed (mph)			Trailer Distances (ft) by Speed (mph)				
		30	40	50	20	30	40	50	60
27	Weblite	64	59	58		88	80	78	
28	Weblite	59	55	52		80	73	68	
29	Weblite	51	45	40		67	57	48	
30	Weblite	69	67	66		96	93	92	
31	Concrete		59		80		64		52
32	Concrete		63		98		80		60
33	Concrete		54		82		66		54
34	Concrete		61		96		76		56
35	S-4		56		91		73		60
36	S-4		60		98		82		68
37	S-4		53		77		65		52
38	S-4		61		94		78		62
39	S-5		60		89		74		55
40	S-5		64		95		78		62
41	Concrete		40		71		58		49
42	Concrete		46		79		65		53
43	Concrete		51		85		71		60
44	S-4		55		85		71		62
45	S-4		57		86		76		65
46	Concrete		44		71		58		49
47	Concrete		52		79		65		53
48	Concrete		57		83		68		59
49	Concrete		48		71		60		50
50	Concrete		54		77		64		51
51	Concrete		55		82		66		55
52	S-4					70	64		
53	Concrete		53		82		68		60
54	Concrete		57		88		75		64
55	Concrete		48		74		61		49
56	Concrete		54		88		68		56
57	Concrete		41		64		49		41
58	Concrete		44		70		47		40
59	Concrete		48		76		61		52
60	Concrete		52		85		64		54
61	Concrete		40		67		48		37
62	Concrete		51		85		62		47

Figure 1. Stopping-distance car versus trailer regression curves.

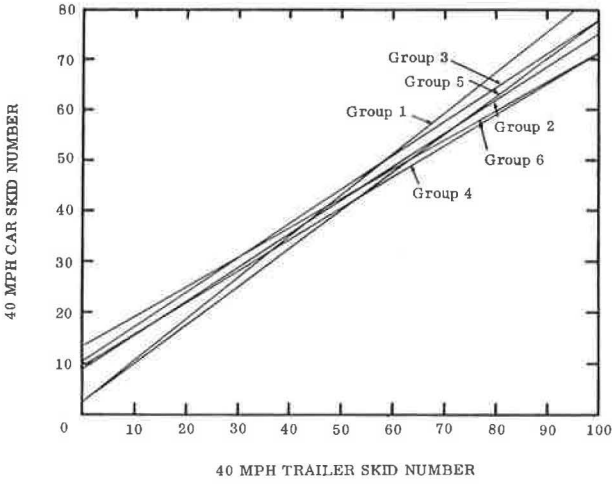

Table 2. Regression analyses by groups.

Group	Sites	Time Tested	Equation[a]	Sample Size	Correlation Coefficient	Standard Error
1	1 to 6	April to May 1968	y = 0.81x + 2.7	12	0.83	3.51
2	7 to 15	Aug. to Sept. 1968	y = 0.66x + 9.1	12	0.91	3.64
3	16 to 25	Sept. 1968	y = 0.67x + 10.7	16	0.94	3.57
4	26 to 30	May 1969	y = 0.62x + 9.6	5	0.99	0.52
5	31 to 51	March 1970	y = 0.75x + 2.9	25	0.85	3.29
6	52 to 62	April to May 1970	y = 0.58x + 13.4	15	0.96	1.55
1 to 4	1 to 30		y = 0.63x + 11.6	45	0.92	3.56
1 to 6	1 to 62		y = 0.63x + 11.2	112	0.92	3.01

[a]y is stopping distance number.

Figure 2. Regression curve for stopping-distance car versus trailer at 40 mph.

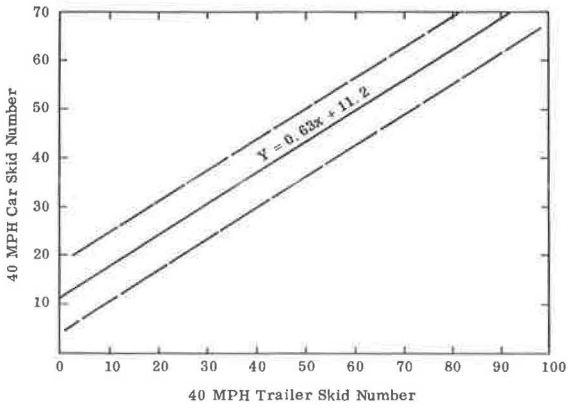

Table 3. Traffic volume versus stopping-distance number (at 40 mph).

Site	Portland Cement Concrete		S-4 and S-5 Mixes		I-2 and I-3 Mixes		Site	Portland Cement Concrete		S-4 and S-5 Mixes	
	Accumulated Traffic (millions)	PSDN	Accumulated Traffic (millions)	PSDN	Accumulated Traffic (millions)	SDN		Accumulated Traffic (millions)	PSDN	Accumulated Traffic (millions)	PSDN
1	10.9	52	12.7	50	1.12	46	26	8.6	48	0.6	65
2	2.2	61	2.5	57	1.57	42	27	21.9	42	2.6	61
3	12.4	48	13.9	49	0.74	46	28	8.6	50	0.5	64
4	2.5	63	2.9	57	0.86	46	29			3.4	65
5	14.7	48	14.0	50	0.59	55	30			0.7	68
6	2.9	65	3.0	57	1.12	42	31			0.8	65
7	15.5	48	28.4	46	1.57	41	32			0.3	65
8	3.1	63	12.4	52	0.74	46	33			2.6	65
9	24.6	45	6.2	63	0.86	44	34			0.6	67
10	9.0	50	1.2	67	0.59	48	35			2.6	65
11	24.3	42	5.2	65			36			0.6	70
12	8.8	45	0.9	67			37			1.8	66
13	24.5	43	30.2	47			38			0.4	67
14	8.9	47	14.5	52			39			1.8	65
15	24.1	43	28.4	46			40			0.4	68
16	8.6	50	12.4	51			41			1.8	65
17	21.4	44	3.2	59			42			0.4	67
18	8.1	53	0.6	63			43			2.2	65
19	21.8	42	3.1	59			44			0.5	72
20	8.5	50	0.6	62			45			2.8	65
21	21.8	42	3.2	59			46			0.6	70
22	8.5	49	0.6	65			47			2.8	65
23	21.9	44	5.2	60			48			0.6	69
24	8.6	49	0.6	63			49			3.4	65
25	21.9	42	3.3	59			50			6.7	70

Figure 3. Traffic volume versus PSDN.

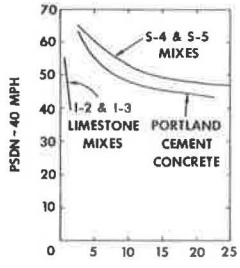

RELATIONSHIP BETWEEN PERCENTAGE OF WET-PAVEMENT ACCIDENTS AND FRICTION

We studied 521 sections on Virginia's Interstate System, totaling 312.8 miles, to determine the relationship between the percentage of wet-pavement accidents and PSDNs. The sites were separated into 4 categories: open roadway (level and tangent areas not at interchanges), non-open roadway (vertical or horizontal curves or both not at interchanges), open interchanges (level and tangent areas at interchanges), and non-open interchanges (vertical or horizontal curves or both at interchanges). Initially, consideration was given to using more categories broken down in more detail, but because of the difficulty in classifying sites it was decided to use the broad ones outlined here. Classifying a site as open or non-open was very difficult. Geometric data were not readily available, so the authors drove over each site and classified it according to their combined judgment. Sight distance was considered of prime importance. Therefore, areas with gentle horizontal or vertical curves that afforded good sight distance were classified as open roadway.

Sites not at interchange areas generally were ½ mile in length. Sites at interchange areas were usually longer, generally about 1 mile, and were determined by starting $\frac{1}{10}$ mile before the exit ramp and ending $\frac{1}{10}$ mile beyond the entrance ramp.

The percentage of wet-pavement accidents (the ratio of wet-pavement accidents to total accidents) was selected as the factor for analysis for two reasons. First, it was the only meaningful wet-accident figure easily obtainable, inasmuch as wet-accident rates were almost impossible to compute. Second, it was hoped that by selecting this factor the effect of traffic volume would be reduced. It is pointed out that one basic assumption was made in this analysis; namely, the amount of time the pavement was wet was considered to be essentially equal for all sections tested.

The possible effects of traffic volume were also taken into account by subdividing each classification into four lane-traffic volume groups: 0 to 3,999 average vehicles daily (AVD) per lane, 4,000 to 7,999 AVD per lane, 8,000 to 11,999 AVD per lane, and 12,000 to 15,999 AVD per lane.

Because there is no way of ensuring in which lane a car was driving at the initial stage of the wet accident, a weighted PSDN was obtained for each site. Trailer skid tests were taken at 40 mph in each lane (generally a site consisted of two passing and two traffic lanes), and averages were obtained for the traffic and passing lanes. A weighted trailer skid number was then usually obtained by summing 80 percent of the average skid number for the traffic lane and 20 percent of the average number for the passing lane. These factors were used because the normal traffic for the sites was 80 percent in the traffic lanes and 20 percent in the passing lanes. Other weighted factors based on traffic volume and number of lanes were used when appropriate. The general 40-mph regression equation discussed earlier was then used to predict the weighted 40-mph stopping-distance skid number for the site. Finally, because the passing lane is likely to demand more friction than the traffic lane due to passing maneuvers and to higher average speed, the relationships of percentage of wet accidents on all lanes and friction on the traffic lane only and the passing lane only were studied. It might also be economically feasible to maintain a higher friction value on passing lanes than on traffic lanes.

After weighted PSDNs were obtained for each site, the 1969 accident data were used to determine the percentage of wet accidents for each site. These data are given in Table 4. Figure 4 shows the data in a more summarized form, where percentage of wet accidents for the skid number groups 40 to 44, 45 to 49, 50 to 54, and 55 and above are plotted versus the average group skid number. It is pointed out that for sites at interchanges the accident data included only those accidents occurring on the main road.

Notice in Table 5 that, in effect, only three of the AVD groups were applicable for each classification because very few data fell in the highest group. Also, the ranges in skid data were not the same between traffic volume groups and skid number groups, obviously because the higher volume sites usually had more accumulated traffic and therefore lower skid numbers.

Two things are evident from the data given in Table 5 and shown in Figure 4. First, in most cases there was a definite negative slope, i.e., the percentage of wet accidents,

Table 4. Skid number versus percentage of wet accidents.

Weighted SN	0 to 3,999 AVD					4,000 to 7,999 AVD					8,000 to 11,999 AVD					12,000 to 15,999 AVD				
	Section		Accidents			Section		Accidents			Section		Accidents			Section		Accidents		
				Wet					Wet					Wet					Wet	
	No.	Miles	Total	No.	Percent	No.	Miles	Total	No.	Percent	No.	Miles	Total	No.	Percent	No.	Miles	Total	No.	Percent
Open Roadway																				
41											4	2.4	29	9	31					
42						5	2.6	39	20	51	5	2.5	9	0	0	4	1.9	8	1	12
43						16	8.5	48	14	29										
44	2	1.0	3	1	33	13	6.4	41	8	20	1	0.7	13	2	15	2	0.8	16	0	0
45						12	7.9	49	6	14	3	1.5	9	1	11					
46	4	2.0	4	1	25	20	11.1	102	10	10	3	1.3	8	0	0					
47	2	1.0	9	3	33	21	10.9	75	8	11	9	1.9	35	11	32					
48	3	1.3	5	1	20	11	5.4	40	4	10	8	3.8	44	6	13					
49	2	1.1	2	0	0	6	3.2	13	1	8										
50	11	6.0	15	3	20	4	1.8	6	2	33										
51	8	4.3	10	0	0															
52	6	3.0	4	1	25	5	3.7	42	9	21	9	2.0	35	3	8					
53	12	5.8	30	6	20															
57	27	15.0	19	0	0															
62	36	18.5	34	5	15															
63	35	20.4	36	2	6															
Non-Open Roadway																				
40											3	1.5	18	8	44					
41											12	6.6	96	42	44					
42						4	2.1	42	14	33										
43	1	0.4	2	0	0	1	0.5	1	0	0										
44						9	5.2	82	22	27	4	2.0	25	8	33	3	2.0	21	3	14
45						3	1.6	25	5	20	5	3.1	27	3	11					
46	1	0.5	1	0	0	7	3.8	67	19	28	6	3.5	56	9	16					
47	3	1.6	7	3	43	8	7.9	45	13	29	6	1.2	45	10	22					
48						4	2.3	10	4	40	2	1.3	18	0	0					
49						1	0.7	3	0	0										
50	4	2.2	14	3	21	2	1.2	4	0	0	3	1.5	26	3	12					
52	1	0.5	4	2	50															
53	2	1.1	7	2	29															
57	3	2.1	6	0	0															
62	3	2.0	3	1	33															
63	11	5.1	7	2	29															
Open Interchanges																				
41											2	1.1	47	21	45					
42						1	0.8	10	1	10	1	1.0	7	3	43					
43						3	2.3	22	2	9										
44											1	0.5	2	1	50					
45						2	1.3	17	1	6										
46						4	3.2	38	5	13										
47	1	0.6	9	1	11	6	4.9	51	8	16	2	1.6	32	5	16					
48	1	0.5	2	0	0	3	1.9	23	2	9										
49	2	1.5	16	5	31	1	0.4	3	1	33										
50	5	3.4	26	6	23	1	0.8	2	0	0	1	0.8	19	2	11					
51	2	1.3	19	5	26															
52	2	1.0	7	3	43	2	0.9	5	2	40	1	0.7	18	5	28					
57	6	4.0	7	0	0															
62	5	2.8	9	2	22															
63	6	4.6	15	6	40															
Non-Open Interchanges																				
41											1	0.7	11	6	54					
42																2	0.7	18	1	5
43						4	3.9	137	63	46										
44						5	6.1	158	47	30	1	1.1	28	7	25	1	0.8	20	6	30
45	1	0.7	12	6	50	2	1.6	19	4	21										
46						3	2.0	27	3	11	3	2.4	47	11	23	1	0.8	21	1	5
47						3	3.0	12	0	0	4	3.6	109	34	31					
48	2	1.6	29	9	31	3	2.4	28	8	29	1	1.0	9	3	33					
49	1	0.6	4	1	25	1	0.5	3	1	33	1	6.8	189	52	28					
51	1	1.0	3	0	0	1	0.8	12	2	17										
52	2	1.8	11	1	9						1	0.5	9	0	0					
57	5	3.3	15	6	40															
62	3	2.5	13	2	15															

Figure 4. Skid number versus percentage of wet accidents.

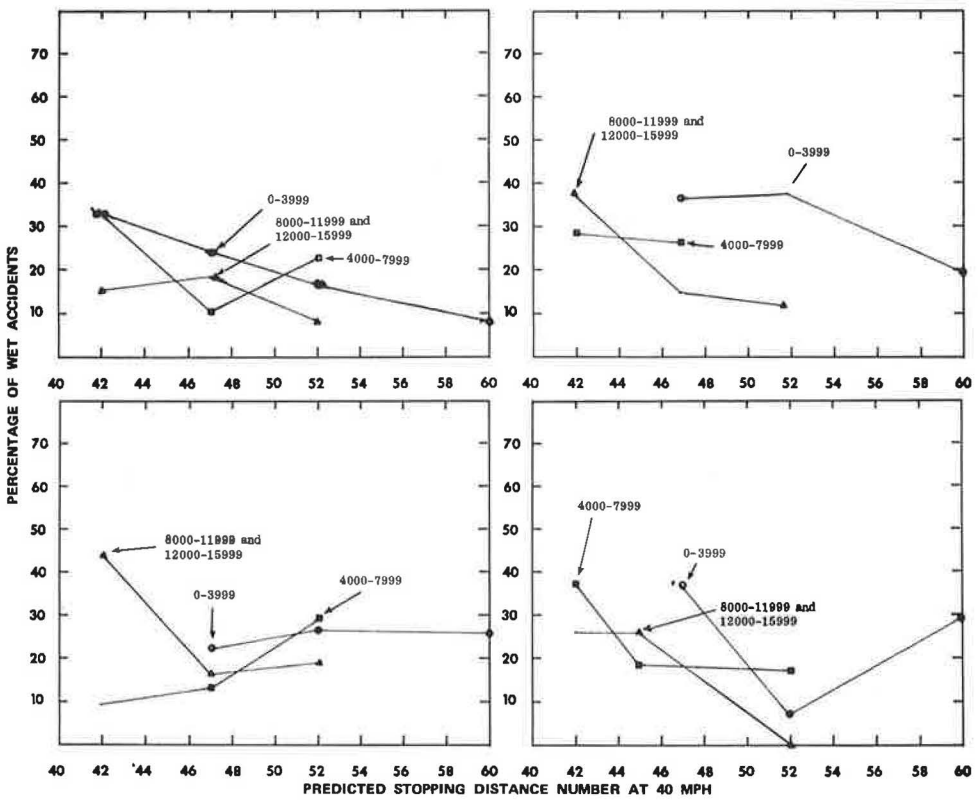

Table 5. Summary of skid number versus percentage of wet accidents.

Weighted SN	Open Roadway					Non-Open Roadway					Open Interchanges					Non-Open Interchanges				
	Section		Accidents			Section		Accidents			Section		Accidents			Section		Accidents		
				Wet					Wet					Wet					Wet	
	No.	Miles	Total	No.	Per-cent	No.	Miles	Total	No.	Per-cent	No.	Miles	Total	No.	Per-cent	No.	Miles	Total	No.	Per-cent
40						3	1.5	18	8	44										
41	4	2.4	29	9	31	12	6.6	96	42	44	2	1.1	47	21	45	1	0.7	11	6	54
42	14	7.0	56	21	38	4	2.1	42	14	33	2	1.8	17	4	24	2	0.7	18	1	5
43	16	8.5	48	14	29	2	0.9	1	0	0	3	2.3	22	2	9	4	3.9	137	63	46
44	18	8.9	73	27	37	16	9.4	128	33	26	1	0.5	2	1	50	7	8.0	206	60	29
45	15	9.9	58	7	12	8	4.7	52	8	15	2	1.3	17	1	6	3	2.3	31	10	32
46	27	14.4	114	11	10	14	7.8	124	28	23	4	3.2	38	5	13	7	5.2	95	15	16
47	27	13.3	114	22	18	13	10.7	97	26	27	9	7.1	92	14	15	7	6.6	121	34	28
48	22	8.5	89	11	12	6	3.6	18	4	22	4	2.4	25	2	8	6	5.0	66	20	30
49	8	4.3	15	1	7	1	0.7	3	0	0	3	1.9	19	6	32	3	7.9	196	54	28
50	15	7.8	21	5	24	9	4.9	44	6	14	7	5.0	47	8	17					
51	8	4.3	10	0	0	1	0.5	4	2	50	2	1.3	19	5	26	2	1.8	15	2	13
52	15	8.7	81	13	16	2	1.1	7	2	29	5	2.6	30	10	33	3	2.3	20	1	5
53	12	5.8	30	6	20															
57	27	15.0	19	0	0	3	2.1	6	0	0	6	4.0	7	0	0	5	3.3	15	6	40
62	36	18.5	34	5	15	3	2.0	3	1	33	5	2.8	9	2	22	3	2.5	13	2	15
63	35	20.4	36	2	6	11	5.1	7	2	29	6	4.6	15	6	40					

decreased as the PSDN increased. Second, if volume were a factor, it appears that on the average the percentage of wet accidents was lower with increased volumes. In many cases the data are erratic, probably because of the small number of accidents the percentages were based on. The authors feel that certainly at least 50, and preferably 100 or more, total accidents per skid number group (e.g., 40 to 44) would be necessary to provide fairly accurate results. It is obvious in Table 5 that many skid number groups have less than 50 total accidents. However, the consistency of the negative slope and the smaller percentage of wet accidents with the higher volume for each of the classifications indicate that these are defensible results.

The decrease in percentage of wet accidents with an increase in the PSDN was, of course, expected. However, the lower percentage of wet accidents associated with the higher volumes of traffic was not expected. This finding perhaps can be explained by the fact that the roads with the lowest traffic volumes had less traffic than they were designed for; thus drivers could make errors without becoming involved in accidents. This, of course, would hold the total number of accidents to a minimum, which in turn might make the wet to dry ratio high, even with a few wet accidents.

The data in each AVD group for each site category were combined so that a better estimate could be made of the shape and location of the percentage of wet accidents versus PSDN curve (Table 5 and Fig. 5). The curves shown in Figure 5 were developed by starting at the lowest PSDN for each category and adding PSDNs until at least 50 total accidents were available. This percentage of wet accidents was then plotted versus the average PSDN of the group from which the percentage was computed. It was felt that the possible effect of volume on percentage of wet accidents shown previously should not prevent the combining of data in the manner described, inasmuch as the vast majority of data fell in the two middle volume groups.

The following conclusions can be drawn from data in Figure 5:

1. There is very little difference in the shapes and locations of the four curves. There does, however, seem to be some tendency for the curves to move up and to the right with the complexity of the roadway situation; i.e., the percentage of wet accidents is usually at least slightly lower at any given PSDN for the open roadway condition than for the other conditions. The order of complexity in this case would be open roadway, non-open roadway and open interchange about equal, and then non-open interchange.
2. The breaking point for all four curves, i.e., the point with the greatest change in slope, appears to be at about a PSDN of 45. Again the curve seems to increase slightly with the complexity as mentioned in number 1. This point at which the greatest change in slope occurs should be selected as a guideline for a minimum PSDN.

Obviously, these results are averages, and to apply them to a particular existing roadway situation as a general remedy for areas having a high percentage of wet accidents would not always be appropriate without considering factors such as the total wet-accident history. However, it is felt that the results could be used in the development of general design guidelines for the PSDNs needed on new construction. Also, they could be incorporated in a general policy regarding resurfacing or other corrective action when a site has a PSDN lower than the guideline and a history of a high percentage of wet accidents, particularly if it is an accident-prone location in terms of the total number of accidents or the accident rate.

When these findings are used as guidelines, it should be remembered that the PSDNs shown are weighted. Actually, in a guideline for design or maintenance of a skid-resistant pavement, actual traffic lane and passing lane skid numbers would be of prime importance. Therefore, Figure 6 shows the actual wet accident-skid number curves for the traffic and passing lanes for all locations where there were only two lanes in one direction. The breaking point is a PSDN of 48 for the traffic lane and a PSDN of 42 for the passing lane. Because the passing lane would experience more acceleration during passing maneuvers, it is logical that the friction demand would be higher.

It is obvious that additional work is needed with more definitive geometric data describing each site. It is felt by the authors that one possible reason that the curves did not differ more was the very general way in which the site categories were derived.

Figure 5. Summary of skid numbers versus percentage of wet accidents for all four site categories.

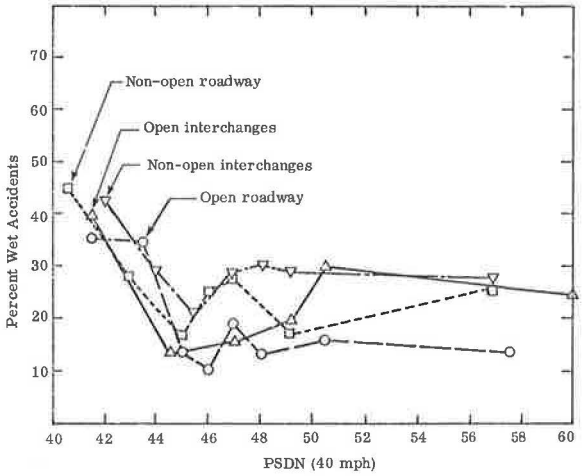

Figure 6. Traffic lane and passing lane PSDNs versus percentage of wet accidents.

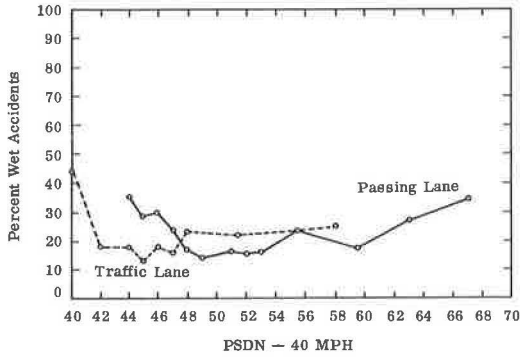

Figure 7. Relationship between stopping-distance skid number and trailer skid number.

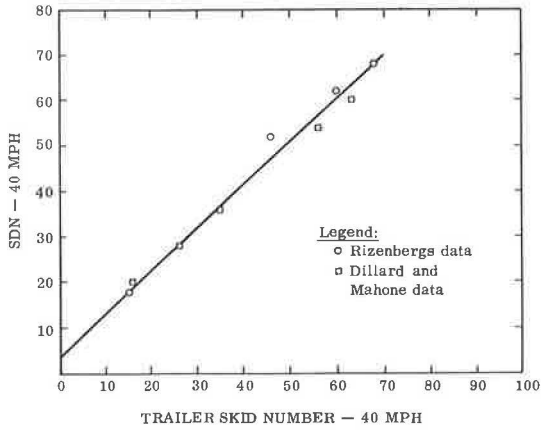

A comparison of the 42 PSDN (40 mph) found in this study with the recommended minimum interim stopping-distance skid number requirements reported by Kummer and Meyer (4, Table 19) seems to indicate a discrepancy. However, it should be noted that the 42 PSDN applies to the Virginia Interstate System, which is designed for a 70-mph traffic speed. Also, unpublished data available from other researchers at the Virginia Highway Research Council indicate average speeds on many of the sites included in the study to be between 65 and 70 mph. Therefore, based on the mean traffic speed, the stopping-distance number proposed by Kummer and Meyer would be about 55 to 57 or 13 to 15 numbers higher than the number established in this study.

The authors feel that part of this apparent discrepancy is due to the relationship between the trailer and stopping-distance methods used by Kummer and Meyer to obtain the stopping-distance numbers. The relationship they used was based on research results obtained in a study by Dillard and Allen (5) in 1958, and none of the trailers used in that study is still in service.

Correlation studies undertaken since 1965 indicate a somewhat different relationship. Data taken from a report by Dillard and Mahone (6, Fig. 17) and from a report by Rizenbergs (7, Fig. 8) are shown in Figure 7. These data indicate an approximate 1:1 relationship.

Based on Kummer and Meyer's recommended skid trailer values and the correlation shown in Figure 7, the minimum stopping-distance number required for a mean speed of 70 mph would be 47 instead of 57. This, of course, would bring the findings of this study into closer agreement with those of Kummer and Meyer, particularly with regard to the passing lane, which as shown in Figure 6 is 48, as well as with the recent guidelines set forth by the U.S. Department of Transportation (8).

This value of 42 is also in disagreement with the findings of McCullough and Hankins (9), which indicate an SN of 40 (at 20 mph) and an SN of 30 (at 50 mph) to be desirable. The SN (40 mph) by extrapolation would be about 35, which is much lower than the 42 indicated earlier as desirable. Of course, there is no way of knowing how the skid trailer used by McCullough and Hankins might relate to those used in the Tappahannock (6) and Florida (7) correlation studies. This uncertainty is one reason that the authors feel it is very important to develop regression equations for individual skid trailer skid numbers versus stopping-distance skid numbers, particularly because data from the Florida correlation study indicate that the variability between skid numbers obtained by several stopping-distance cars was much less than that obtained by the trailers.

CONCLUSIONS

1. The regression analyses performed on the stopping-distance car data and the trailer data indicate a relationship of 1:1 at an SN of 30; however, as the pavement friction increases, the trailer gives progressively higher numbers than the car. The Tappahannock and Florida correlation studies indicate that there is an approximate 1:1 relationship between the SN for many skid trailers and the SDN for the extent of the correlation curve.
2. The accumulated traffic-PSDN relationships indicate that nonpolishing S-4 and S-5 mixes retain an average PSDN of 48 after 25 to 30 million vehicle passes. Nonpolishing portland cement concrete mixes lose resistance more rapidly than do nonpolishing S-4 and S-5 mixes, and on the average portland cement concrete mixes have a PSDN of about 44 after 20 to 25 million vehicle passes. The PSDNs for I-2 and I-3 limestone mixes decrease more rapidly than those for the S-4, S-5, and portland cement mixes and reach an average of 42 after 1.6 million vehicle passes.
3. Based on the analysis of percentage of wet accidents versus PSDN, it appears that a minimum traffic lane PSDN of 42 and a passing lane PSDN of 48 are desirable for Interstate roads with a mean traffic speed of about 65 to 70 mph. It can be demonstrated that the passing lane values are in agreement with those recommended by Kummer and Meyer, assuming that a different relationship exists between skid trailers and the stopping-distance method that they used.

REFERENCES

1. Mahone, D. C. Slipperiness of Highway Pavements—Phase I. Virginia Highway Research Council, June 1968.
2. Cook, L. M., and Dancy, W. H., Jr. Development and Fabrication of the Virginia Skid-Resistance Measurement Vehicle (Model 2). Virginia Highway Research Council, VHRC 70-R15, Oct. 1970.
3. Highway Capacity Manual—1965. HRB Spec. Rept. 87, 1965.
4. Kummer, H. W., and Meyer, W. E. Tentative Skid-Resistance Requirements for Main Rural Highways. NCHRP Rept. 37, 1967.
5. Dillard, J. H., and Allen, T. M. Correlation Study—Comparison of Several Methods of Measuring Road Surface Friction. Proc., First Internat. Skid Prevention Conf., Part II, Virginia Council of Highway Investigation and Research, Aug. 1959.
6. Dillard, J. H., and Mahone, D. C. Measuring Road Surface Slipperiness. ASTM, STP 366, 1965.
7. Rizenbergs, R. L. Florida Skid Correlation Study of 1967—Skid Testing With Automobiles. ASTM, STP 456, 1968.
8. Highway Design, Construction and Maintenance. In Highway Safety Program Manual, Vol. 12, U.S. Dept. of Transportation, Federal Highway Administration, March 1971.
9. McCullough, B. F., and Hankins, K. D. Skid Resistance Guidelines for Surface Improvements on Texas Highways. Highway Research Record 131, 1966, pp. 204-217.

APPENDIX

BITUMINOUS CONCRETE MIXTURES

Type	Percentage by Weight Passing Square Mesh Sieves*										Percent Bituminous Materials	Mix Temperature (At Plant)
	1½	1	¾	½	⅜	No. 4	No. 8	No. 30	No. 50	No. 200		
S-1						100	95-100	50-95	25-65	0-8	8.5-10.5	225-300°F
S-2					100	95-100	60-85	20-40	10-30	2-10	9.5-12.0	225-300°F
S-3					100	90-100	70-95	25-55	15-35	2-12	6.5-10.5	200-240°F
S-4				100	90-100		60-80	25-45	10-30	2-10	5.5- 9.5	225-300°F
S-5/I-3				100	80-100		35-55	15-30	7-22	2-10	5.0- 8.5	225-300°F
I-1		100	90-100		85-100	75-100	60-95	25-60	12-35	2-12	5.0- 7.5	225-300°F
I-2		100	95-100		60-80	40-60	25-45		5-14	1-7	4.5- 8.0	225-300°F

*In inches except where otherwise indicated. Numbered Sieves are those of the U. S. Standard Sieve Series.

DEVELOPMENT OF SPECIFICATIONS FOR SKID-RESISTANT ASPHALT CONCRETE

Edward J. Kearney, George W. McAlpin, and William C. Burnett,
New York State Department of Transportation

This paper summarizes 10 years of research in New York State on the skid resistance of asphalt pavements. Skid numbers measured by a two-wheeled trailer are related to cumulative vehicle passes for the state's geologic formations that are sources of coarse aggregate for asphalt concrete. Mixes with coarse aggregate containing at least 20 percent noncarbonate stone—or 10 percent sand-sized impurities embedded in a carbonate matrix—remain skid resistant for the life of the pavement. Specifications have been written to require aggregates not meeting these requirements to be upgraded by blending them with 20 percent noncarbonate stone.

• FROM 1961 through 1966, the death toll on U. S. highways increased annually by an average of 6.9 percent, from 38,093 to 53,041 persons. The National Safety Council (1) estimated that 1966 motor vehicle accidents cost the country more than $10 billion in lost wages, medical and hospital fees, insurance administrative and claims settlement costs, and property damage.

Such statistics prompted the Congress to pass the Highway Safety Act of 1966. As a result, on June 27, 1967, the Highway Safety Bureau of the U. S. Department of Transportation issued 13 highway safety program standards that were "designed to reduce traffic accidents and deaths, injuries, and property damage resulting therefrom." One of these standards (No. 4.4.12) required that every state "have a program of highway design, construction, and maintenance to improve highway safety."

Because as many as 33 percent of all wet-weather accidents involved or were caused by skidding (2, 3), two of the 11 minimum requirements of this standard call for every state to have "standards for pavement design and construction with specific provisions for high skid resistance qualities," and "a program for resurfacing or other surface treatment with emphasis on correction of locations or sections of streets or highways with low skid resistance and high or potentially high accident rates susceptible to reduction by providing improved surfaces."

To fulfill the second requirement, the engineering research and development bureau of the New York State Department of Transportation completed a statewide inventory of the skid resistance of the entire state highway system in 1968 and 1969. During this survey, the skid number (wet 40-mph coefficient of friction × 100) was measured once per mile on nearly all the 14,000 miles of state highways, and the locations of most pavement sections with low skid resistance were determined.

Before conducting the statewide skid survey, the bureau had an ongoing research program to determine which pavement variables affected the skid resistance of asphalt concrete plant mixes. Previously reported New York research (4) had shown this skid resistance to be governed by the following factors:

1. Cumulative traffic the pavement had carried,
2. Vehicle speed,
3. Pavement and tire temperatures, and
4. Polishing resistance of the larger mix aggregates.

Sponsored by Committee on Surface Properties-Vehicle Interaction.

Skid resistance was not significantly influenced by mix type (for mixes containing 15 to 70 percent aggregate greater than $\frac{1}{8}$ in.) or by the type of fine (less than $\frac{1}{8}$ in.) aggregate. (Natural silica sand and manufactured carbonate fines performed nearly the same as similar coarse aggregate.)

New York State specifications require the use of crushed-stone coarse aggregate (greater than $\frac{1}{8}$ in.) in asphalt concrete, but the aggregate particle shape and its orientation in the pavement surface caused variations in the time required to wear the asphalt coating off the individual stones, and thus large variations in skid resistance were observed during the first million vehicle passes on asphalt concrete pavements. After the asphalt had worn off, additional traffic caused a logarithmic decrease in skid resistance due to aggregate polishing.

Previous research (4) showed a correlation between pavement skid resistance and the percentage of acid-insoluble material in the coarse aggregate of asphalt concrete pavements that had carried over 5 million vehicles. The amount of acid-insoluble residue was determined by the method described in the Appendix. In all cases, limestone and dolomite aggregates with less than 10 percent acid-insoluble residue produced pavements with inadequate skid resistance. A pavement was considered skid resistant if it maintained a skid number (wet at 40 mph) of 32 or more for 10 million vehicle passes. This number was selected as a guide because it corresponded to the skid resistance assumed by AASHO for calculating stopping distances used in highway design (5). At skid numbers above 32, a normal driver will be able to perceive an object in his path, apply his brakes, and stop his vehicle before striking that object. Because many New York State stone suppliers produce aggregates with less than 10 percent acid-insoluble residue, further research was initiated to determine the most practical and economical way to upgrade these aggregates so as to produce skid-resistant asphalt concrete pavements.

TEST PROCEDURE AND RESULTS

Procedure

In all skid testing, the New York State two-wheeled drag force trailer was used in a procedure conforming to ASTM Designation E 274-70. A standard test tire (ASTM Designation E 249-66) was used. Tests were usually made on level, tangent road sections because of the uncertainty in weight transfer onto or off the test wheel when traversing a curve. This weight transfer changed the magnitude of load carried by the test tire, from which the coefficient of friction was computed. Previous reports (4, 6) documented the reliability of the skid-trailer measuring system and its ability to correlate with the distance required to stop a car traveling at 40 mph.

During the 10 years of research, many thousands of skid tests have been performed on pavements containing aggregates from nearly every crushed-stone source that supplies asphalt concrete producers in New York State. In addition, over 10,000 asphalt pavements were tested during the 1968 and 1969 skid inventory of the state highway system. With the assistance of the department's highway maintenance subdivision and regional materials engineers, coarse aggregate sources were determined for almost all asphalt concrete pavements that had been skid tested. Surface course age was also checked, and the cumulative vehicle passes were calculated. Acid-insoluble residue tests were conducted on all geologic formations that were sources of coarse aggregate for asphalt concrete in New York. Carbonate staining tests were conducted on all Onondaga limestones. The methods used for both of these tests are given in the Appendix.

In addition, 51 experimental surfaces were placed on state highways in three regions. These contained varying quantities of hard acid-insoluble materials, and the mix types ranged from fine sheet asphalts to dense-graded asphalt concrete with up to 30 percent aggregate of $\frac{1}{4}$ to $\frac{1}{2}$ in. size.

Results

To relate pavement skid number to coarse aggregate geologic formations we conducted detailed analyses on all available skid test data on asphalt concrete pavements.

Figure 1 shows skid number as a function of cumulative traffic (on a log scale) in millions of vehicles per lane for pavements containing limestone coarse aggregate from the Manlius, Coeymans, Tully, and Cobourg formations and the Chazy and Black River groups from quarries located in central and north central New York. Limestones from these six geologic formations are high in calcium carbonate and contain only minor quantities of hard sand-sized impurities (less than 10 percent acid-insoluble residue). The figure shows the best-fit line and the 80 percent confidence lines. After 10 million vehicle passes, only 10 percent of the roads containing these coarse aggregates would be expected to be skid resistant, i.e., to have skid numbers above 32. The two confidence lines in Figure 1A are used as reference lines in Figure 1B and the other three figures. Also, each point on these graphs represents an average of seven or eight skid tests on one pavement section.

Figure 1B shows a similar plot for skid data representative of the Oak Orchard member of the Lockport dolomite formation, in the western part of the state. The Oak Orchard dolomite is high in carbonates (over 90 percent) and low in quartz (less than 2 percent). While the data are very few, the skid numbers are in the same range as the high-carbonate limestones in Figure 1A.

Figure 2 shows a comparison of the high-impurity dolomites with the relatively pure limestones of Figure 1A. These dolomites include the Penfield, Goat Island, and Gasport members of the Lockport formation and a special unit of the Lockport identified as the Brockport Lentil. Also included are the Beckmantown, Cranesville, and Little Falls formations. The Penfield member and the Brockport Lentil are characterized by high silica contents. In the Goat Island and Gasport members, the silica content varies both laterally and vertically. In general, however, the percentage of silica is slightly higher in the Goat Island and Gasport members than in the Oak Orchard member (Fig. 1B) but considerably less than in the Penfield one. The Beckmantown, Cranesville, and Little Falls formations have noncarbonate contents exceeding 15 percent. These dolomites, all containing more than 10 percent hard sand-sized impurities, have higher skid resistance than the low-impurity limestones or dolomites. About 10 percent of the pavements containing these dolomites had skid numbers in the unacceptable range of the low-impurity limestones.

One of the most extensive sources of coarse aggregate in New York State is the Onondaga limestone formation, which occurs in an east-west band from the vicinity of Albany to Buffalo. The Onondaga formation contains chert (a flint-like quartz) nodules in varying quantities: a relatively low percentage at Syracuse but increasing to 40 percent or more westward near Buffalo. The chert does not appear in the softer limestone matrix but rather in a variety of forms ranging from whole pieces of crushed aggregate to a small chip on the edge of a piece of limestone aggregate. The percentage of chert was determined by the staining procedure rather than by the acid-insoluble residue test.

Figure 3 shows a plot of skid numbers versus traffic for 93 pavements in which the coarse aggregate was Onondaga limestone. The extreme ranges of skid resistance on these pavements were attributable to the varying percentages of chert particles in the coarse aggregate. The pavements with skid numbers in the same range as the pure limestones contained aggregates with less than 15 percent chert (open circles), whereas those with higher skid numbers (solid circles) ranged from 20 to 50 percent chert.

Sandstone, granite, and traprock (diabase) are grouped for this analysis because they are all noncarbonates. All sandstones are of the Graywacke type in either the Catskill or Rensselaer formations and are quarried in the southern and eastern part of the state. The granites are quarried mostly in the Adirondack Mountains in northern New York, but one granite quarry is located just north of New York City. Traprock occurs in the lower Hudson River Valley and is also imported from New Jersey and Connecticut. The acid-insoluble residues for these aggregates ranged from 93.0 to 99.6 percent. Figure 4 shows the skid resistance of noncarbonates and pure limestones at various traffic volumes. The noncarbonates are clearly superior, even after 10 million vehicle passes.

Figure 1. Skid resistance change with traffic for pavements containing coarse aggregates with low acid-insoluble contents (A—91 pavements; B—6 pavements).

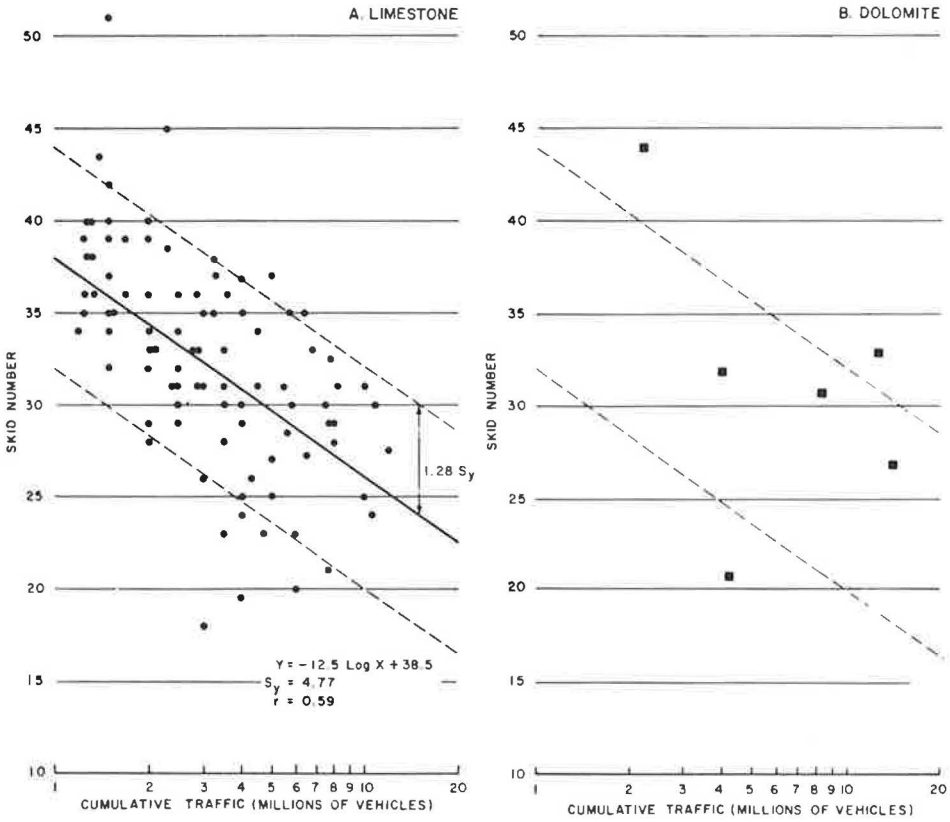

Figure 2. Skid resistance change with traffic for pavements containing low-impurity limestones and dolomites having more than 10 percent acid-insoluble residue (169 pavements).

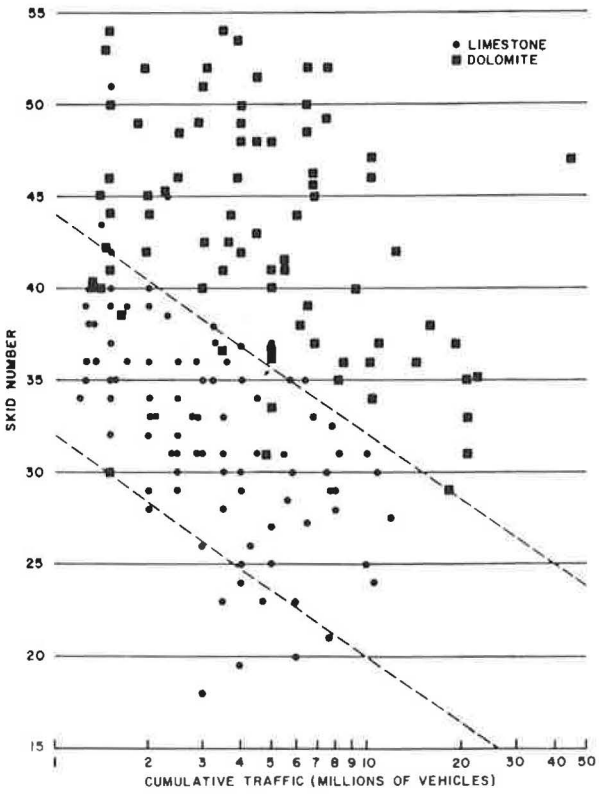

Figure 3. Skid resistance change with traffic for pavements containing limestones varying in percentage of noncarbonate material (93 pavements).

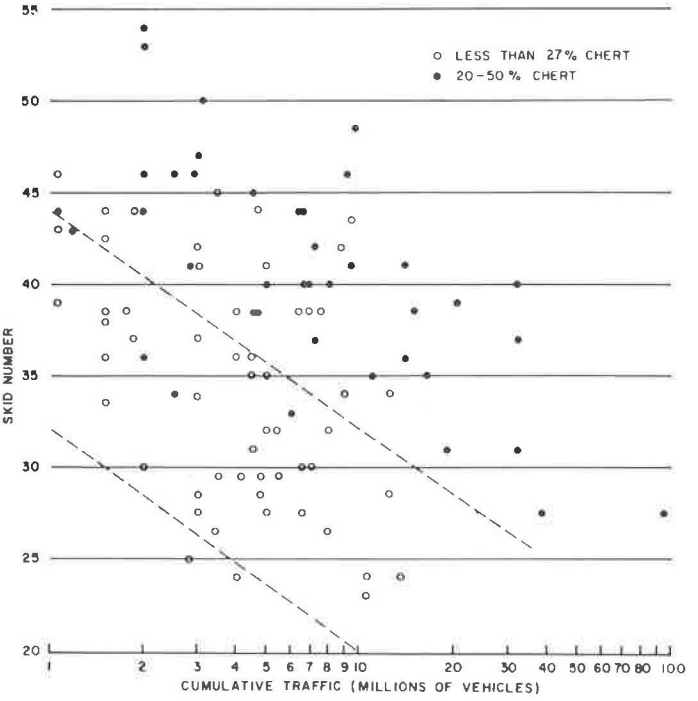

Figure 4. Skid resistance change with traffic for pavements containing low-impurity limestones and noncarbonates (117 pavements).

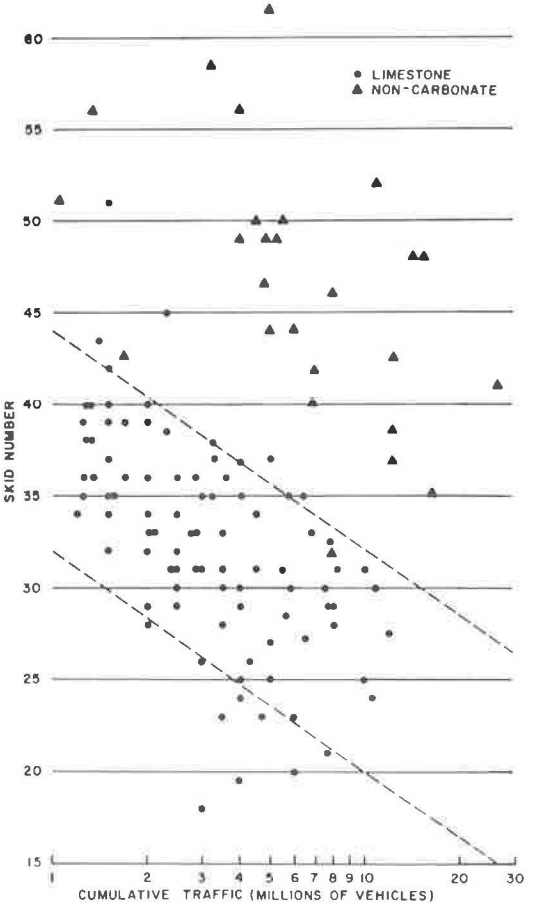

Table 1. New York State coarse aggregate suppliers.

Item	No. of Suppliers	Total
Quarried material		
Limestone	38	
Dolomite	24	
Sandstone, traprock, and granite	27	89
Geologic formations		22
Operating asphalt mix plants		182

Table 2. Mix proportions in New York State Types 1A and 1AC asphalt concrete plant mixes.

Material	Type 1A (percent)	Type 1AC (percent)
+¼ in. stone	20	—
+⅛ in. stone	35	45
-⅛ in. fines	45	55
Asphalt cement	6.5	7

IMPLEMENTATION OF RESULTS

Analyzing the long-term skid resistance of asphalt concrete mixes as related to the mineralogy of the coarse aggregate has permitted the following classification of aggregate:

1. Carbonates with less than 10 percent sand-sized impurities,
2. Mixtures of carbonate and noncarbonate aggregates with less than 20 percent noncarbonates,
3. Carbonates with more than 10 percent impurities,
4. Mixtures (carbonates and noncarbonates) with more than 20 percent noncarbonates, and
5. Noncarbonates, defined as any aggregate with more than 80 percent acid-insoluble residue.

Aggregates in the first two categories have been judged incapable of providing long-term skid resistance (up to 10 million vehicle passes) in asphalt mixes. Aggregates in any of the other categories will produce pavements generally resisting polishing throughout their lives.

A breakdown of coarse aggregate suppliers by type of stone being quarried is given in Table 1. At present, two-thirds of the total 89 quarries produce carbonate rock (limestone and dolomite). It is readily apparent that any specifications affecting the suitability of carbonate rock aggregate in New York could have serious consequences in increased costs of asphalt concrete and shortages of acceptable coarse aggregate. Consequently, care was necessary to ensure that the department did not make requirements more stringent than necessary for adequate long-term skid resistance.

After a thorough analysis of research data and due consideration for the aggregate resources available in New York State, the following specification was prepared to ensure long-term skid resistance of asphalt pavements. It applies only to the coarse aggregates used in surface course mixes placed on roads where the anticipated cumulative traffic per lane during the design life of the pavement surface exceeds 1 million. All other department specifications governing the mixing plant, materials, and construction details must still be followed. The specification was written to cover Types 1A and 1AC asphalt plant mixes, which are the most frequently used surface courses in New York. Typical mix proportions are given in Table 2.

The new specification requires that coarse aggregates be from approved sources and that they meet one of the following requirements:

1. They may be limestone from the Onondaga formation, but must contain at least 20 percent chert particles;
2. They may be either from a dolomite formation or from a limestone formation other than Onondaga, but they must contain at least 10 percent sand-sized acid-insoluble impurities; or
3. They may be noncarbonate crushed stone such as sandstone, granite, traprock, slag, or similar materials.

Aggregates not meeting any of these requirements naturally must be upgraded by blending them with noncarbonates and are covered under the following requirement:

4. The coarse aggregate may be a blend of carbonates (limestone or dolomites) and noncarbonates (sandstone, granite, traprock, slag, etc.) provided (a) that 20 percent of all stone over $\frac{1}{8}$ in. is noncarbonate and (b) that, if stone over $\frac{1}{4}$ in. is included, 20 percent of it is also noncarbonate.

The producer has the option to upgrade with noncarbonate stone from $\frac{1}{4}$ to $\frac{1}{2}$ in. in a Type 1A mix, but in the final mix the total aggregate over $\frac{1}{8}$ in. must have at least 20 percent noncarbonate particles. When the aggregates are from more than one source, or of more than one type of material, they must be proportioned and blended to provide a uniform mixture. If lightweight aggregate or slag is used as the noncarbonate, the requirement of 20 percent by weight must be adjusted for the different specific gravities.

Because this specification has been in force only two complete construction seasons, long-term effects on skid resistance cannot yet be evaluated. During these 2 years, 29 pavements containing blended aggregates have been sampled and will serve as test sections to determine whether additional specification changes are needed. Some dolomite sources that just meet part of this specification are being monitored to see whether the 10 percent acid-insoluble impurity requirement can or should be modified.

ACKNOWLEDGMENTS

The research project reported here was initiated by and progressed for the first 5 years after its approval with the support of the Federal Highway Administration under the supervision of John L. Gibson, senior civil engineer, now assigned to the staff of this department's Region 1. Under his direction and that of the senior author, the following technicians were responsible for field skid testing: Anthony J. Datri, Ronald Lorini, Raymond J. Mazuryk, David J. Rothaupt, James H. Tanski, and Thomas F. VanBramer. The resulting data were reduced and plotted by Nancy B. Couture.

Geological information was furnished by George D. Toung, assisted by Paul J. St. John and Edward A. McGrady, each from the materials bureau. The following regional materials engineers assisted in determining the aggregate sources for numerous pavements tested and in selecting sites for the experimental pavement sections: Frank A. DeFazio and John J. Pinto, Region 2; John P. Russell and Lawrence A. Colelli, Region 3; Alfred R. D'Annunzio and M. Dwight Vail, Region 4; James W. Foersch, Region 5; Eugene N. Thiebeau, Region 7; Donald F. Fullam, Region 8; Charles F. Donahue, Region 9; and Leland C. Fitts and William Thornwell, Region 10.

The assistance of the technical committee of the New York State Crushed Stone Association and the New York State Bituminous Producers Association in preparing the new specification is also gratefully acknowledged.

REFERENCES

1. Accident Facts. National Safety Council, Chicago, 1967.
2. Mills, J. P., Jr., and Shelton, W. B. Virginia Accident Information Relating to Skidding. Proc., First Internat. Skid Prevention Conf., Part 1, 1959, pp. 9-20.
3. Kummer, H. W., and Meyer, W. E. Tentative Skid-Resistance Requirements for Main Rural Highways. NCHRP Rept. 37, 1967.
4. Burnett, W. C., Gibson, J. L., and Kearney, E. J. Skid Resistance of Bituminous Concrete. Bureau of Physical Research, New York State Dept. of Transportation, Res. Rept. 67-3, Oct. 1967.
5. A Policy on Geometric Design of Rural Highways: 1965. American Association of State Highway Officials, 1966, pp. 134-140.
6. Skid Test Trailer: Development and Evaluation. Bureau of Physical Research, New York State Dept. of Public Works, Res. Rept. 61-7, Dec. 1961.

APPENDIX

EXTRACTS FROM NEW YORK STATE MATERIALS TEST METHODS

A. Test for Acid-Insoluble Residue (Coarse Aggregate)

1. Scope
   Determine the resistance of aggregates to loss when exposed to a hydrochloric acid solution.
2. Test Solutions
   a. 2*N* hydrochloric acid (5 parts distilled water and 1 part 12*N* hydrochloric acid, reagent grade).
   b. 6*N* hydrochloric acid (1 part distilled water and 1 part 12*N* hydrochloric acid, reagent grade).
3. Procedure
   a. A representative sample of the aggregate is screened over $\frac{1}{2}$- and $\frac{1}{8}$-in. sieves. The aggregate retained on the $\frac{1}{8}$-in. sieve is reduced to a test sample having a minimum size of 300 particles and weighing a minimum of 50 grams, after excluding any chert or other similar siliceous rock particles.

b. The sample is thoroughly cleaned by washing with potable tap water and dried to a constant weight in an oven at 221 to 230 F (105 to 110 C). Then the clean sample is weighed to the nearest 0.1 gram and placed in the glass container.
c. The aggregate sample is subjected to a 2 *N* hydrochloric acid solution until the chemical reaction ceases. Temperatures of the aggregate and the acid should be between 70 and 80 F at the beginning of test. Decant and repeat the addition of fresh 2 *N* acid. Repeat this step of decanting the spent acid and adding fresh acid until there is no further reaction.
d. When reaction with the 2 *N* hydrochloric acid stops, repeat the same procedure using 6 *N* hydrochloric acid. When all reaction stops, the acid solubility test is complete.
e. Decant the acid solution and rinse the aggregate thoroughly with water in the glass container. The residue in the container should have a pH (as indicated by pH paper) of more than 5.5 after washing.
f. Carefully transfer the residue from the container to a No. 200 sieve and wash thoroughly.
g. Dry the acid-insoluble residue to a constant weight in an oven at 221 to 230 F (105 to 110 C) to determine the percentage insoluble.

4. Calculations

$$\text{Percent insoluble residue} = \frac{\text{Weight retained on the No. 200 sieve}}{\text{Weight of the original test sample}}$$

B. Test for Percentage of Noncarbonate Particles in a Coarse Aggregate Mixture (Carbonate Staining Method)

1. Scope
Determine the percentage of noncarbonate rock in a coarse aggregate mixture by a staining technique, to separate the carbonate particles from the noncarbonates.

2. Definition of Terms
A carbonate particle is defined as one with 60 percent or more of its surface area stained after test, and a noncarbonate particle as one having less than 60 percent stained.

3. Test Solutions
a. Copper nitrate (molar solution), 1 liter of the molar solution being prepared by adding the indicated amounts of one of the following nitrates to 1,000 grams of distilled water: 188 grams of $Cu(NO_3)_2$; 225 grams of $Cu(NO_3)_2 \cdot 3H_2O$; or 332 grams of $Cu(NO_3)_2 \cdot 6H_2O$.
b. Ammonium hydroxide (concentrated commercial grade), NH_4OH_3.

4. Procedure
a. A representative sample of the aggregate must meet the following size requirements:

Size	Minimum No. of Particles	Minimum Weight (gram)
+1/4 in.	200	300
+1/8 in.	300	50

b. The retained sample of aggregate is thoroughly washed with potable tap water, and dried to a constant weight in an oven at 221 to 230 F (105 to 110 C).
c. The sample is weighed to the nearest 0.1 gram and placed in a glass or polyethylene container.
d. The aggregate is completely covered with the copper nitrate solution for a minimum of 4 hours.
e. Decant the copper nitrate solution, and immediately add the concentrated ammonium hydroxide. Allow the sample to remain immersed for at least 1 min.
f. Decant the ammonium hydroxide, and carefully wash the sample with potable tap water.
g. Limestone is stained blue or bluish-green. Dolomite is only slightly affected. Separate all stained limestone (carbonate) particles and all dolomite particles (by visual examination by a geologist) as defined under item 2.
h. Dry the noncarbonate portion of the sample to a constant weight in an oven at 221 to 230 F (105 to 110 C) to determine the percentage of noncarbonate particles.

5. Calculations
Compute the noncarbonate percentage as follows:

$$\text{Percentage of noncarbonate} = \frac{W_{ncp} \times F \times 100}{W_o}$$

where

W_{ncp} = weight of oven-dry noncarbonate particles,

W_o = weight of oven-dry original test sample, and

F = adjustment factor for differing specific gravities of noncarbonate rocks.

Select the proper F-value in the following table:

Noncarbonate Material	Specific Gravity	F-Value[a]
Iron ore tailings	3.10	0.871
Traprock	2.90	0.931
Chert	2.70	1.000
Granite	2.70	1.000
Sandstone	2.67	1.011
Blast furnace slag	2.45	1.102
Sinopal	2.18	1.239
Lightweight aggregates	1.60	1.688

[a]*The F-value may be used with carbonate particles having a specific gravity range of 2.67 to 2.73. For any carbonate rock having a specific gravity outside this range, the F-value must be computed using the following equation:*

$$F = \frac{\text{Carbonate specific gravity}}{\text{Noncarbonate specific gravity}}$$

THE FRICTIONAL REQUIREMENTS OF PASSING VEHICLES

John C. Glennon, Texas Transportation Institute, Texas A&M University

This research determines the tire-pavement friction demands of vehicles performing passing maneuvers. These frictional demands were found by photographing and analyzing passing maneuvers performed under actual highway conditions. Critical friction requirements are proposed for application to skidding accident prevention programs that incorporate minimum skid resistance levels and wet-weather speed limits.

•SLIPPERY PAVEMENTS have existed for many years, but the causes of slipperiness, its measurement, and its effect on traffic safety were not of great concern before 1950. Although reliable skidding accident data are hard to find, those in existence suggest that the skidding accident rate has increased and has reached proportions that may no longer be ignored. This trend may be partly due to improved accident reporting but is also undoubtedly a reflection of increased vehicle speeds and traffic volumes (1).

More rapid accelerations, higher travel speeds, and faster decelerations made possible by modern highway and vehicle design have raised the frictional demands on the tire-pavement interface. Larger forces are required to keep the vehicle on its intended path. On the other hand, for wet pavements, the frictional capability of the tire-pavement interface decreases with increasing speed. In addition, higher traffic volumes and speeds promote a fast degradation in the frictional capability of the pavement.

From the technological standpoint, the slipperiness problem appears amenable to solutions that either reduce the frictional demand (improved geometric design and lower speed limits for wet conditions) or increase the frictional capability (improved pavement surface design, improved tire design, and improved vehicle inspection procedures).

Passing maneuvers probably account for the highest frequency of critical tire pavement friction demands encountered on our rural two-lane highways. Not only are passing maneuvers performed at relatively high speeds, but also they may involve critical combinations of cornering and forward acceleration. In addition, passing vehicle path maneuvers are generally performed adverse (negative superelevation) to the pavement cross slope.

This research study was conducted to determine the frictional demands of vehicles performing high-speed passing maneuvers. Identification of critical friction requirements should provide a basis for determining minimum skid resistance requirements and also ascertain the need and basis for wet-weather speed limits.

FIELD MEASUREMENTS

The general procedure involved the use of an impeding vehicle and an observation vehicle equipped with a 16-mm movie camera. Sample vehicles approaching the study sites through a striped no-passing zone were impeded at selected speeds by the impeding vehicle. The observation vehicle followed immediately behind the sample vehicle. Upon entering the passing zone, the impeding vehicle maintained a constant speed while the sample vehicle's passing maneuver was filmed from the observation vehicle.

Sponsored by Committee on Surface Properties-Vehicle Interaction.

Study Sites

Two study sites having passing zone lengths of 1,360 and 2,680 ft were selected within a 20-mile radius of College Station, Texas. The study sites were selected to be free of external distractions that might alter the driver's normal operating procedure. That is, the driver was not subjected to drastic changes in environment or highway geometry, nor were there any intersections, railroad crossings, narrow bridges, or other such unique features. Each site was preceded by several miles of relatively unrestricted geometry. Drivers approaching each site, therefore, were accustomed to relatively unrestricted passing opportunities and, with minor exceptions, to free-flowing traffic conditions.

Because there were no major access points close to the study sites, traffic flow was fairly consistent. The average daily traffic (ADT) was 1,500 vehicles for site A and 3,600 vehicles for site B. The posted speed on both highways is 70 mph. Speed distributions at the sites were very similar to the statewide distributions found by the Texas Highway Department in 1968, which showed the average 85th percentile speed to be 70 mph and the average 15th percentile speed to be 54 mph. When only the speed characteristics are considered the passing maneuvers observed at the study sites should be indicative of those expected on similar facilities.

Immediately before each site, passing was restricted by a double yellow barrier stripe. No-passing zone lengths were 1,770 ft for site A and 3,000 for site B.

Passing zones at both sites began on the downgrade of a crest, extended through a sag vertical curve, and terminated on the upward grade of a crest. The approaches to the sites differed; whereas the sight distance prior to site A was restricted by a horizontal curve, the sight distance prior to site B was restricted by a crest vertical curve.

Site B, located 12 miles south of College Station on Texas-6, has 13-ft lanes and 8-ft shoulders. Site A, located 20 miles northeast of College Station on Texas-21, has 12-ft lanes and a short 8-ft shoulder on one side of the site. The rights-of-way at both locations received normal maintanance by the Texas Highway Department, were clear of all large vegetation, and were mowed throughout the study area.

Equipment

Three major elements composed the test equipment: an impeding vehicle, an observation vehicle, and a 16-mm camera.

A 1969 Plymouth sedan was used to impede subjects through the study sites. During the first several days, it became apparent that drivers were hesitant to pass the impedance vehicle, even when there was ample passing distance. It was suggested that drivers might have presumed the impeding vehicle to be a highway patrol vehicle because it was white and displayed the official State of Texas-exempt license plates. Therefore, all identifying Texas Transportation Institute door legends were masked, and conventional license plates were substituted during data collection periods. To an overtaking driver, the impeding vehicle then appeared to be simply another passenger car.

A 1970 Ford ½-ton pickup was used as the observation vehicle. So that test subjects would be unaware that their maneuvers were being photographed, the camera and operator were concealed. Because normal operating characteristics could be altered by the obvious presence of photographic equipment, a box resembling a handmade tool shed was placed in the pickup bed immediately behind the cab, extending 24 in. above the cab roof line. The box contained a small front window over the driver's side of the cab through which the subject's passing maneuver was photographed. Because the subject's attention was directed toward the impeding vehicle and the available passing distance and also because the small photographing window was above the line of sight through his rear vision mirror, it is doubtful that drivers were aware of the camera. Because the window was the only opening and because light was reflected from the glass, the interior of the box appeared dark and unoccupied. The observation vehicle is shown in Figure 1.

An Arriflex 16-mm camera was used to photograph the passing maneuvers. Power was supplied by an 8-V battery to a governor-controlled motor to produce a constant

24-frames/sec film advance. Black and white Plus-X reversal film (Kodak ASA 50) on 400-ft rolls was used. Subject vehicles were photographed with a zoom lens (17.5-mm to 70-mm) so that the camera operator could maintain full field of view under varying distance requirements. The camera, mounted on a "ball-head" rigid base mount attached to a shelf, is shown in Figure 2.

Calibration Marks

The plan was to measure the lateral placement of the subject vehicle's left-rear tire at intervals throughout the passing maneuver, using the highway centerline as a geometric base reference. Therefore, 2-ft lengths of 6-in. wide temporary traffic line pavement markings were placed perpendicular to, and centered on, the centerline at 40-ft intervals throughout the site. The 2-ft markers gave a length calibration that was always pictured on the film frame where lateral placement measurements were taken. The 40-ft interval gave a longitudinal reference system for speed and radius calculations.

Sample Size

The study was concerned primarily with high-speed passing maneuvers. Approximately 300 completed passing maneuvers were photographed during the field study. The sample consisted of about 45 maneuvers at each site for impeding speeds of 50, 55, and 60 mph. In addition, about 35 maneuvers were photographed at a 65-mph impeding speed at site B. Of this sample, 164 maneuvers were on film of high enough quality to permit precision measurement. Several filmed maneuvers were discarded because of poor field of view or because shadows prohibited film measurements.

The number of tests had no statistical basis but was set by the time and monetary constraints for data collection and film analysis. In excess of 2,000 subjects were photographed to achieve the desired number of completed passing maneuvers. Because approaching traffic was not stopped during the field studies, many potential passing opportunities were negated. Filming was initiated before the point where passing sight distance unfolded, and, hence, the presence of opposing traffic near the zone could not be determined in advance.

Study Procedure

After each photographic sample was taken, the two test vehicles returned to their starting stations upstream from the passing site. The observation vehicle was parked on the shoulder about 1 mile upstream from the impeding zone, and the impeding vehicle was parked on the shoulder near the beginning of the impeding zone.

The next subject selected was the first high-speed (generally greater than 55 mph) vehicle that had enough clear distance to the rear to permit the observation vehicle to safely move in behind. The impeding driver was notified by radio that a subject had been selected and was approaching at a specific speed. The impeding driver then moved from the shoulder to the traveled lane and accelerated to the predetermined impeding speed.

The subject driver was forced to follow the impeding vehicle through the no-passing zone (or illegally cross the double yellow stripe). During this time, the observation vehicle caught and trailed the two vehicles through the remainder of the impeding zone. Figure 3 shows the relative positions of the three vehicles during a test.

Filming was initiated at the first calibration mark and was continued throughout the passing zone or until it was obvious that the subject had declined the passing opportunity. The impeding vehicle maintained constant speed throughout the passing zone.

Opposing traffic was not stopped during the study. Many more passing maneuvers would have been performed had there been no opposing traffic in the passing zone, but it was believed that the presence of opposing traffic was a variable with which a passing driver must contend, and to remove this would introduce bias.

FILM ANALYSIS

The film was analyzed with a Vanguard motion analyzer. This device is a portable film reader for measuring displacements on photographic projections. It consists of a

Figure 1. Photographic observation vehicle.

Figure 2. Study camera and mounting.

Figure 3. Relative vehicle positions during test.

Figure 4. General path of passing vehicle.

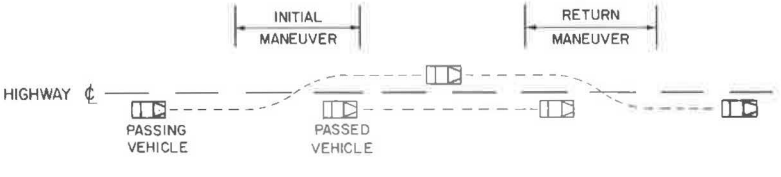

projection head, projection case, and measurement screen.

The 16-mm projection head permits forward and reverse motion of film on 400-ft reels. A variable-speed mechanism moves the image across the projection screen at from 0 to 30 frames/sec. A counter on the projection head displays frame numbers. If the camera speed is known, then, by noting elapsed frames, displacement over time (speed) can be calculated.

The measurement screen has an X-Y cross-hair system that measures displacement in 0.001-in. increments on the projected image. Rotation of the measurement screen permits angular alignment of the cross hairs with the projected image. Two counters display the numerical positions of the movable cross hairs. Conversion of image measurements to real measurements requires a calibration mark of known length in the plane of the photographed object. In other words, the 2-ft marker used at the study sites were measured in machine units on the film image to give a calibration for converting image length to real length.

To analyze the vehicle path of the samples, we always used the left edge of the left-rear tire as the lateral vehicle position reference. Lateral placement at each reference marker was measured from the frame where the left-rear tire was nearest the marker. After recording calibration readings on the left and right edge of the reference marker, we recorded the position reading of the left-rear tire. These readings, along with the 2-ft known length, gave the data necessary for calculating the actual lateral placement.

MATHEMATICAL ANALYSIS

The Vanguard data were used in a computer program to calculate vehicle speed, left-rear tire lateral placement, vehicle path radius, and lateral g acceleration (f). These estimates were calculated for each sample at each reference marker within the initial pull-out maneuver and the return maneuver. The general path of the passing vehicle is shown in Figure 4.

Vehicle Speed

The estimate of vehicle speed at each calibration marker was obtained as the average speed over the 80-ft interval centered on the marker. The speed estimate, V, was calculated using the following equation:

$$V = \frac{\text{film speed} \times \text{analysis interval}}{\text{elapsed frames}}$$

Because the frame count estimate was to the nearest integer, the greatest frame count error for the analysis interval was one frame. For the 24-frames/sec film speed used, this yields an acceptable maximum error of the speed estimate, ranging from about 4 percent at 50 mph to 7 percent at 80 mph.

Vehicle Path Radius

The computer program calculated the lateral placement of the left edge of the left-rear tire at each calibration marker. The instantaneous vehicle path radius was then estimated by computing the radius of the circular arc through three successive tire positions, the center position being the calibration marker under consideration. Because a circular arc is the minimum path through three points, the radius so calculated is a conservative estimate of the smallest instantaneous radius for the interval.

Figure 5 shows the three basic geometric configurations of three successive tire positions. Points A, B, and C represent left-rear tire positions spaced at 40-ft intervals, and d_A, d_B, and d_C are the respective lateral placements. From the law of sines, the radius of the vehicle path is the radius of the circle that circumscribes triangle ABC:

$$R_v = \frac{AC}{2 \sin \theta}$$

where θ is the angle ABC.

The length AC is determined by the law of cosines:

$$AC = \sqrt{(AB)^2 + (BC)^2 - 2(AB)(BC)\cos \theta}$$

The values for α, β, AB, and BC are calculated as follows:

$$\alpha = \tan^{-1} 40/|d_A - d_B|$$

$$\beta = \tan^{-1} 40/|d_B - d_C|$$

$$AB = 40/\sin \alpha$$

$$BC = 40/\sin \beta$$

The angle θ varies for the three cases shown in Figure 5 as follows:

Case	Value of θ
I	$\alpha + \beta$
II	$180 + \beta - \alpha$
III	$180 + \alpha - \beta$

The accuracy of the radius estimate is an important aspect of this analysis. Any error in the radius estimate would, of course, come from an error in the lateral placement estimate. Although study control was exerted, small errors were possible from several sources including (a) lateral discrepancy in placing the calibration marker, (b) length discrepancy of the calibration marker, (c) sampling error due to taking lateral placement readings up to one-half frame away from the calibration marker, (d) equipment error, and (e) human error in reading and recording lateral placement measurements.

Estimating the distribution of error values for lateral placement estimates was not possible. Because all the error sources could be either positive or negative, however, some error cancelation normally would be expected. In addition, all error sources would not be expected to reach maximum in the same direction at the same time.

Error sensitivity was checked by assuming that the maximum error ranged between 0.05 and 0.10 ft. For this analysis, the lateral placement of the two outside points was assumed to be equal, and the center lateral placement varied an increment of d_x greater. Thus, in reference to Figure 5, the increments $|d_A - d_B|$ and $|d_B - d_C|$ are equivalent to d_x. Figure 6 shows the maximum percentage of error of the radius estimate for various lateral placement differentials and their corresponding radii.

Lateral Acceleration

The lateral g acceleration (friction demand, f) at the tire-pavement interface was estimated at each calibration marker for each sample by using the centripetal force equation, $f = (V^2/15R) - e$. The superelevation, e, in this case, corresponds to the pavement cross slope, which was assumed equal to 0.02. The computer program was designed to monitor the direction of the vehicle path estimate and determine whether e was positive or negative for that path.

Forward Acceleration

Unfortunately, the film speed (24 frames/sec) and the analysis interval (80 ft) did not permit reasonable estimates of instantaneous forward acceleration and its corresponding friction demand. To obtain reasonable estimates required a much shorter analysis interval and a considerably greater film speed. Neither was feasible for this study.

RESULTS

The result of the computer application was the printing of several sets of lateral placement, speed, instantaneous radius, and lateral g acceleration data for each passing vehicle sampled. As mentioned previously, these variables were computed throughout both the initial pull-out maneuver and the return maneuver. The point of maximum lateral g acceleration was selected to represent the critical point for each maneuver.

Figure 5. Geometric descriptions of vehicle radius calculations.

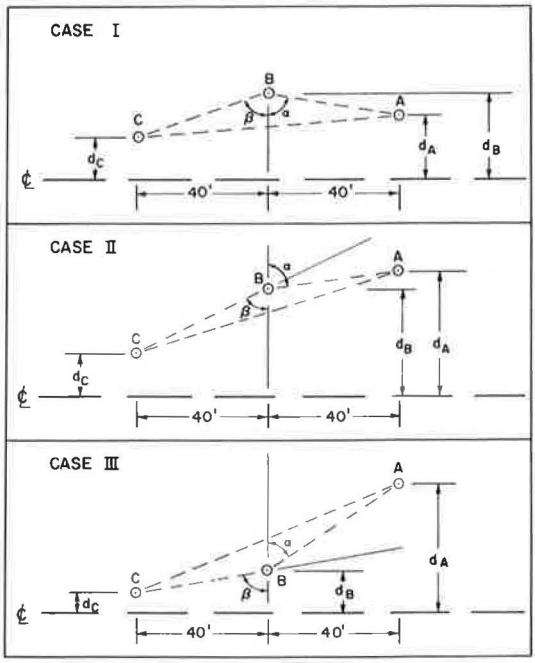

Figure 6. Error sensitivity of estimated radius.

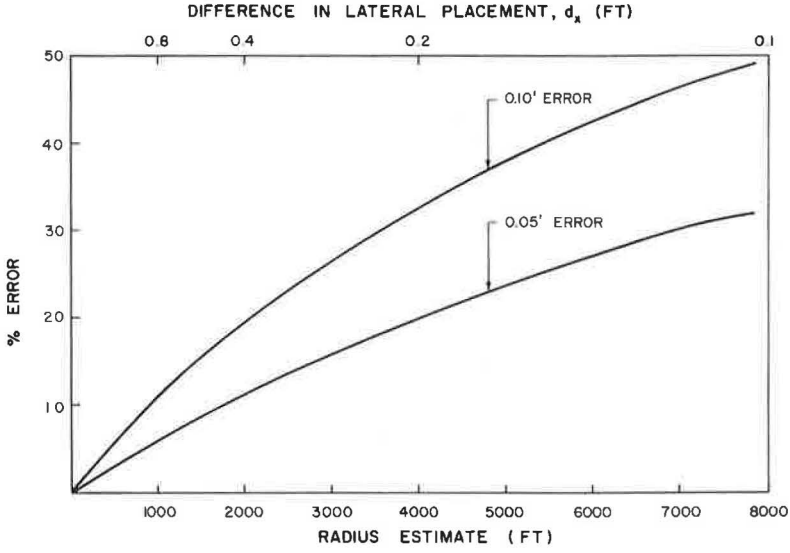

Table 1. Sample data.

Sample No.	Impeding Vehicle Speed	Data and Point of Maximum f			Sample No.	Impeding Vehicle Speed	Data and Point of Maximum f		
		Speed	Radius	f			Speed	Radius	f
Site A—Initial Maneuver					Site B—Initial Maneuver				
40	55	60	963	0.245	64	60	73	1,143	0.308
58	65	82	2,553	0.175	30	65	77	1,461	0.271
20	55	73	3,378	0.104	92	55	55	1,023	0.194
10	50	65	6,218	0.046	116	65	77	3,600	0.110
16	50	55	5,306	0.037	41	60	65	8,685	0.033
Site A—Return Maneuver					Site B—Return Maneuver				
84	50	65	792	0.361	70	60	82	1,177	0.379
19	55	82	1,879	0.238	80	50	60	916	0.258
67	50	73	2,346	0.150	68	50	69	1,566	0.202
64	50	62	2,358	0.110	34	60	94	5,503	0.106
37	55	73	7,150	0.049	30	65	82	11,750	0.038

This point, for most of the samples, coincided with either the point of minimum path radius or the point of maximum speed or both. Sample data, showing the ranges in vehicle speed, radius, and lateral acceleration, are given in Table 1.

Vehicle Speed

Figure 7 shows the distribution of vehicle speeds for the impeding speed, the speed at maximum lateral g acceleration during the initial maneuver, and the speed at maximum lateral g acceleration during the return maneuver. In general, the speed at the critical point of the initial maneuver is about 10 to 12 mph higher than the impeding speed, and the speed at the critical point of the return maneuver is 17 to 21 mph higher than the impeding speed. Also of interest is the fact that only about 12 percent of the samples exceeded the speed limit at the critical point of the initial maneuver.

Vehicle Radius

Plotting scatter diagrams of speed versus vehicle path radius for the two basic maneuvers showed that there was no relationship between the two parameters. This lack of correlation indicated that the distribution of vehicle path radii (at maximum lateral g acceleration) could be expected at any speed within the speed range studied.

Table 2 gives the radius values for the critical end of these distributions. It is important to compare the values in Table 2 with the error sensitivity curve of Figure 6. By doing this, we note that the radius values of Table 2 have a reasonably low error sensitivity.

The values for site B in Table 2 are consistently lower than the values for site A. This may be due to the presence of the horizontal curve at site B, although very few initial or return maneuvers coincided with the horizontal curve. Actually, the few maneuvers that did coincide with the horizontal curve were deleted because of the larger extra effort required to program the transition and curve parameters. Perhaps, however, the horizontal curve had some influence by encouraging drivers to begin or end maneuvers outside the limits of curve to avoid the extra vehicle control problems associated with the curve.

Lateral Acceleration

If the critical side friction requirement is to be determined, a percentile level is needed to ensure that very few vehicles will approach instability. The 10 percent level appears to be a relatively good choice. Using this level would say that only 10 percent of the vehicles would have lower vehicle path radii. To obtain the critical values, we averaged the values for sites A and B. Actually the difference between these two values was not too large and may be simply a sampling variation. The critical vehicle path radii, therefore, are 1,470 ft for the initial maneuver and 1,640 ft for the return maneuver. By using these two values in the centripetal force equation, $f = (V^2/15R) - e$, one can plot the critical relationship between lateral g acceleration and speed for the initial and return maneuvers, as shown in Figures 9 and 10 respectively. It is noted that a negative e was used in computing these two curves inasmuch as most critical vehicle paths were adverse to the pavement cross slope (Fig. 4).

Forward Acceleration

Although no precise measurements of instantaneous vehicle acceleration were possible, some general observations are appropriate. The data indicate that vehicles were almost always accelerating during the initial maneuver and coasting (constant speed) during the return maneuver. Cursory examination of the data indicates an average acceleration range of from 1 to 3 ft/sec^2 for the initial maneuver. Inasmuch as these are averages over fairly long intervals (200 to 500 ft), instantaneous accelerations could be considerably higher.

Figure 7. Speed distributions for various portions of the passing maneuver at both sites.

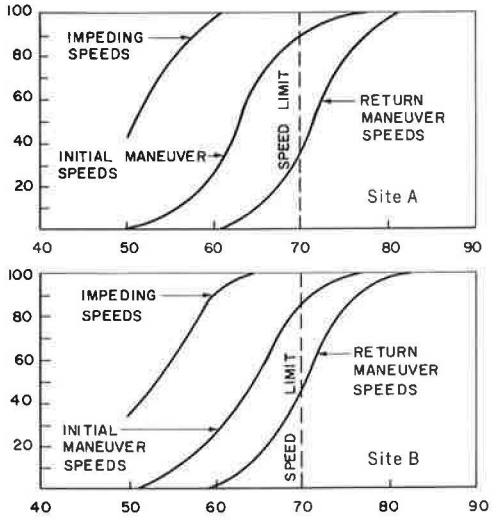

Table 2. Distribution of vehicle path radii.

Percentage of Vehicles Having a Smaller Radius	Radius of Path (ft)			
	Site A		Site B	
	Initial Maneuver	Return Maneuver	Initial Maneuver	Return Maneuver
5	1,500	1,380	1,130	1,320
10	1,650	1,700	1,290	1,580
15	2,010	1,910	1,430	1,770

Figure 8. Total friction requirement for the initial maneuver.

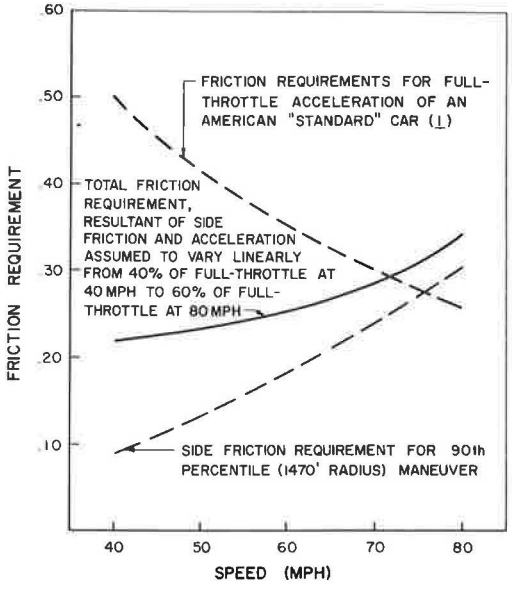

Figure 9. Total friction requirement for the return maneuver.

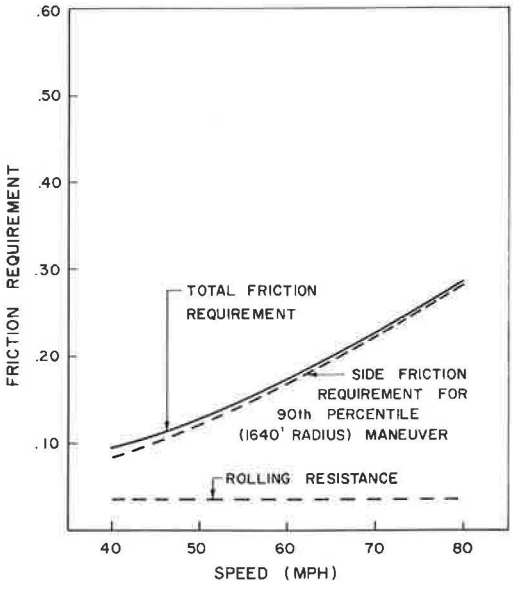

Critical Friction Demand

Kummer and Meyer (1) state that the total friction demand, f_T, is a resultant of lateral, f_l, and forward, f_f, accelerations, such that $f_T = \sqrt{f_l^2 + f_f^2}$. They also report the forward friction demand of a standard American vehicle accelerating at full throttle. The friction demand of an American "hot" car accelerating at full throttle is considerably greater and of compact cars somewhat less.

To arrive at a reasonable estimate of the total friction demand we assumed the forward acceleration of the passing vehicle during the initial maneuver to vary linearly between 40 percent of full throttle at 40 mph and 60 percent of full throttle at 80 mph. For a 4,000-lb vehicle, this corresponds to an acceleration of 6.4 ft/sec^2 at 40 mph and an acceleration of 5.0 ft/sec^2 at 80 mph. The total friction demand estimate for the initial maneuver is shown on Figure 8. For the return maneuver, the only friction component in the forward direction is 0.035 contributed by rolling resistance. The total friction demand estimate for the return maneuver is shown on Figure 9. Comparing the total friction demand curves of Figures 8 and 9 reveals that the initial maneuver creates the critical friction demand, varying from 0.22 at 40 mph to 0.34 at 80 mph.

APPLICATION OF RESULTS

Of all the normal (nonemergency) maneuvers performed on our rural two-lane highways, passing probably accounts for the highest frequency of critical tire-pavement friction demands. If there is to be a reasonably low loss-of-control frequency for passing maneuvers (and other maneuvers) during wet weather, then the critical friction demand level must be met. The frictional requirements developed in the previous section, therefore, have an application to a skidding accident prevention program that incorporates minimum skid resistance levels and wet-weather speed limits.

Although specific program recommendations cannot be offered, it is important to look at the potential effect of the suggested frictional requirements. Figure 10 shows a percentile distribution of skid numbers in one state and will be used for illustration. Also plotted in Figure 10 is the suggested frictional requirement (assuming SN =100f). The percentage of pavements that satisfy the frictional requirement at various speeds is as follows:

Speed (mph)	Percentage of Pavements
80	42
70	60
60	75
50	85
40	93

As was found in the analysis of field data, only about 12 percent of the passing vehicles exceeded the posted speed limit at the critical point in the passing maneuver. Therefore, the critical speed may be equated with the speed limit for determining minimum skid resistance levels and wet-weather speed limits.

Table 3 compares the effect of using the suggested frictional requirements for various programs in the state depicted in Figure 10. Two assumptions were applied to derive Table 3. First, the statewide speed limit is 70 mph, and, second, the pavements that were improved by not satisfying the minimum skid resistance requirement have the same percentile distribution of skid numbers as the unimproved pavements.

Table 3 shows the advantage of having a minimum skid resistance requirement. It is probably undesirable (and maybe ineffective) to have wet-weather speed zones below 50 mph on highways normally signed for 70 mph. This would suggest an absolute minimum skid number of about 27 at 40 mph for the state depicted in Figure 10. If wet-weather speed limits were not desirable or feasible, then this state should have a minimum skid number requirement of 35 at 40 mph.

Figure 10. Percentile distribution of relation between skid number and speed for 500 pavements.

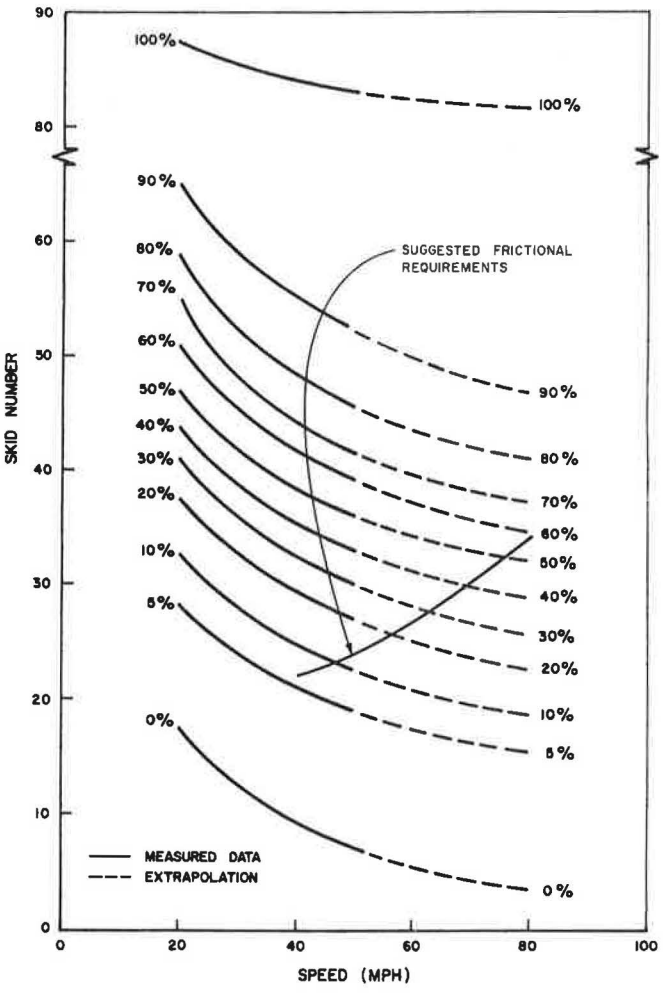

Table 3. Percentage of pavements on roads with posted wet-weather speed limits having minimum skid resistance requirements.

Wet-Weather Speed Limit	Minimum Skid Number Requirement at 40 mph				
	None	20	25	30	35
40	9	4	—	—	—
45	4	5	4	—	—
50	5	6	6	—	—
55	7	6	8	7	—
60	7	8	8	9	—
65	8	8	8	9	—
70	60	63	67	75	100
Below 70[a]	40	37	33	25	0

[a]Percentage of pavements with wet-weather speed limit below the 70-mph statewide limit.

The above discussion illustrates program considerations. Of course, to apply the frictional requirements to an individual section of pavement necessitates a skid number versus speed plot for that pavement.

REFERENCES

1. Kummer, H. W., and Meyer, W. E. Tentative Skid Resistance Requirements for Main Rural Highways. NCHRP Rept. 37, 1967.
2. Weaver, G. D., and Glennon J. C. Passing Performance Measurements Related to Sight Distance Design. Texas Transportation Institute, Res. Rept. 134-6, June 1971.

A STUDY OF VARIABLES ASSOCIATED WITH WHEEL SPIN-DOWN AND HYDROPLANING

J. E. Martinez, J. M. Lewis, and A. J. Stocker, Texas Transportation Institute, Texas A&M University

Vehicles operating on wet pavements suffer impairment of their steering and braking capabilities. Tests have shown that this condition worsens as the vehicle speed increases and that at a critical ground speed the vehicular wheel is separated from the pavement by a layer of fluid. This is said to be hydroplaning. When this occurs the steering ability of the vehicle is completely lost, and the braking capability is greatly diminished. The spin-down (reduction in wheel speed) of a wheel is an indication of a loss in the tire-ground frictional force and is regarded by researchers as a manifestation of hydroplaning. Spin-down occurs when the hydrodynamic lift effects combine to cause a moment that opposes the normal rolling action of the tire caused by the drag forces. As ground speed increases, the tire becomes detached from the pavement, which decreases the ground friction on the tire. Also as ground speed increases, the center of hydrodynamic uplift forces moves forward of the axle, which causes a moment that opposes the drag forces on the tire; as this moment increases, spin-down begins. This report uses wheel spin-down as a criterion for evaluating the wet-weather properties of a portland cement concrete pavement and a bituminous surface and considers the effects of water depth, tire inflation pressure, tire tread depth, and wheel load. The study was performed by conducting full-scale tests on a hydroplaning trough 800 ft long, 30 in. wide, and 4 in. deep. Water depths up to 0.8 in. can be maintained in the trough.

•TIRE HYDROPLANING or aquaplaning comes about from fluid pressures that are developed at the tire-pavement interface. When these pressures become large and the total hydrodynamic force developed on the tire from these pressures equals the total load the tire is carrying, hydroplaning occurs. At this instant, theoretically the tire loses contact with the pavement and skims over the surface in the same manner that a water skier glides along a water surface. The hydroplaning condition, as manifested by wheel spin-down (reduction in speed of wheel), occurs at a particular vehicular speed that is a function of the pavement surface, fluid properties, and various physical and geometrical wheel parameters.

The hydroplaning phenomenon undoubtedly causes a loss in the directional stability of a vehicle and can be considerably aggravated if the vehicle is traveling on a curve or is exposed to high cross winds. Further, as is reported in the literature, the application of brakes to the hydroplaning vehicle does not improve conditions because the braking-friction coefficients approximate free-rolling coefficients at ground speeds approaching the critical hydroplaning speed. Tests have shown that once spin-down begins, the required decrease in ground speed that caused hydroplaning can be sizable before "spin-up" occurs.

Sponsored by Committee on Surface Properties-Vehicle Interaction.

Concern about the hydroplaning problem has been limited essentially to the air transportation industry because of the high take-off and touch-down speeds associated with modern aircraft. Consequently, a large majority of the research done on the hydroplaning problem has been by people associated with agencies like the Langley Research Center of the National Aeronautics and Space Administration (NASA). These people have made significant theoretical and experimental contributions (1, 2, 3). Due to their primary objectives, most of the research concerned airplane tires, which differ in construction and inflation pressures from ground vehicle tires. The tests were usually aimed at investigating the overall problem and analyzing the effects caused by displacing the water on the pavement. A vast amount of research concerning the variables associated with hydroplaning and particularly friction characteristics and effects of pavement texture and material has been conducted by British researchers (4, 5, 6). A review of the works more nearly associated with the research investigation reported in this paper is presented in the original report.

SELECTION OF PARAMETERS

Pavements

Two pavements were selected for the study. The first pavement was a burlap drag-finished concrete pavement with an average texture of 0.018 in. as measured by the silicone putty method. This type of pavement was considered typical of existing concrete pavements of low macrotexture. The second pavement was a bituminous surface treatment with rounded river gravel and stone between -$^5/_8$ in. and +No. 4 used as cover stone. An average texture of 0.146 in. as measured by the silicone putty method was obtained. This pavement was selected because it represents as coarse a pavement as the driving public tolerates, the criterion being noise level.

Water Depths

Various water depths were considered, and values were selected so that the influence of this variable could be adequately evaluated. Consequently the depth selected for the concrete pavement varied from 0.12 to 0.70 in., whereas the depth selected for the bituminous surface treatment varied from 0.25 to 0.70 in. Lower water depths were considered for this pavement, but the vehicular ground speed that would produce spin-down was not achievable.

Tire Inflation Pressures

Tire inflation pressures varying from 18 to 36 psi in 6-psi increments were selected for both pavements. It was felt that these values not only were representative of pressures found in the tires of most ground vehicles but also would provide a good basis for studying the effect of this parameter. Higher pressures were not selected because the test tow vehicle was unable to attain a high enough ground speed to produce sufficient data for these regions.

Wheel Load

Wheel loads of 800 and 1,085 lb were selected in the evaluation on the concrete pavement. The latter load was used because of its specification as the ASTM skid trailer standard and the former because it represented a realistic wheel load and provided a wide enough variation to detect the effects of this parameter. Only the 1,085-lb load was used in the evaluation of the bituminous surface treatment inasmuch as no appreciable variation in the results was observed in the evaluation of the concrete pavement when the 800-lb load was used.

Tires

Eight tires were selected for the study and are given in Table 1. It was felt that a wide range of tires would provide an adequate evaluation of the effects of tire geometry, stiffness, and tread depth.

EXPERIMENTATION

The tests were conducted on a sloped trough shown in Figures 1 and 2 (7). The trough is 800 ft long, 30 in. wide, and 4 in. deep. No difficulty in obtaining water depths of up to 0.7 in. above the pavement asperities was encountered with the two pavements. To be able to better interpret the data, we took water depth readings (Fig. 2) at various trough locations. The variation in the readings was more pronounced for the bituminous surface treatment. Ideal conditions involving no wind were difficult to achieve, so the data collected contain the influence of winds varying from 5 to 15 mph. This did not seem to affect the data because adequate water recovery times to reach equilibrium conditions between tests were allowed.

The tow truck and instrumented test trailer are shown in Figure 3, and a photograph of a typical test is shown in Figure 4. From these photographs it can be seen that the trailer is positioned so that, as the tow vehicle proceeds down the trough, straddling it, the test trailer has one of its wheels in the trough. The ground speed from the fifth wheel and the speed of the test wheel of the trailer are sensed by identical tachometer generators. The output from the generators is fed into a Hewlett-Packard 320 recorder that contains its own amplifier circuits. The two wheel speeds are simultaneously recorded as analog traces on a strip chart. The fifth-wheel speed is also displayed to the driver on a digital voltmeter.

DISCUSSION OF RESULTS

The critical or "total" hydroplaning speed is the speed at which the hydrodynamic pressure force is in equilibrium with the load carried by the tire. However, this speed is not necessarily the speed at which wheel spin-down is initiated, and, according to Horne and Dreher (2), wheel spin-down can commence at ground speeds considerably lower than the critical hydroplaning speed. In fact, according to them the front wheel spin-down for tandem wheels occurred at 70 percent of the predicted hydroplaning speed. These researchers reached the same conclusions in another report (1) and stated that total spin-down for their data, which included aircraft tires, takes place between 80 and 120 percent of the predicted hydroplaning speed. This report also points out that further increases in ground speed resulted in less tire-fluid exposure time in the trough due to the increased ground speed and a more uniform hydrodynamic pressure in the tire-ground contact region when hydroplaning prevails. This latter effect causes a reduction in the wheel spin-down torque. Thus, spin-down should be regarded as a manifestation of hydroplaning and not as the only criterion to determine the critical hydroplaning speed. To determine this speed more precisely requires that the effects of the braking force, yaw or side force, and fluid drag force be investigated.

For the experimentation conducted on the Texas Transportation Institute's hydroplaning trough, wheel spin-down was the only criterion used to indicate hydroplaning. For this reason, we decided to evaluate the two pavements discussed previously and to discuss the effects of the various hydroplaning parameters on the basis of several spin-down percentages.

Figure 5 shows a comparison of the results obtained at 10, 32, and 60 percent spin-down and the equation presented by Horne and Dreher (2). Even though the data for a treaded tire were selected, the water depth was greater than the tire tread depth, thus making the results fall within the stated limitations of the Horne equation. The curves show that the values of 32 and 60 percent spin-down bound Horne's values and that the 10 percent values are within 70 percent of the values predicted by the equation. It can also be seen that the curves of experimental results have approximately the same slope as Horne's values. This makes the results quite encouraging.

Figure 6 shows the results obtained for a smooth tire and for Horne's equation. For these data, the agreement was not so good as it had been for the previous case. Here, even at 100 percent spin-down, the hydroplaning speed predicted by Horne's equation cannot be reached. Also, even though the slopes of three experimental curves are nearly the same, they tend to differ from that of the equation. However, it should be emphasized that spin-down is only a manifestation of hydroplaning and that even for 10

Table 1. Tires selected for study.

Tire No.	Manufacturer	Size	Type
1	A	7.75 by 14	Bias ply, full tread depth
2	A	7.75 by 14	Bias ply, ½ tread depth
3	A	7.75 by 14	Bias ply, smooth
4	B	F70-14	Wide tire, full tread depth
5	C	7.75 by 14	Bias ply, full tread depth
6	ASTM[a]	7.50 by 14	Full tread depth
7	D	7.75 by 14	Bias ply, full tread depth
8	D	7.75 by 14	Bias ply, smooth

[a] ASTM E-17 traction standard.

Figure 1. Hydroplaning trough.

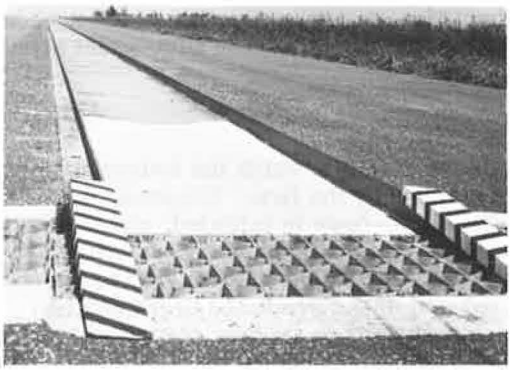

Figure 2. Typical water depth reading taken before test on hydroplaning trough.

Figure 3. Tow truck and instrumented test trailer.

Figure 4. Typical test run on hydroplaning trough.

Figure 5. Comparison of experimental results and Horne and Dreher's equation for full-tread depth tire.

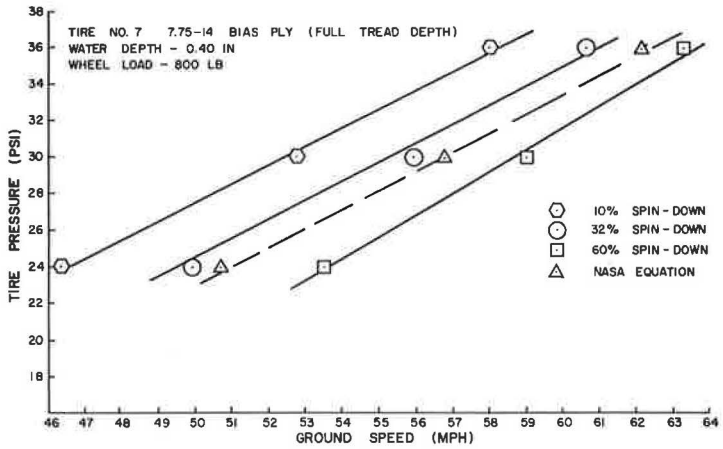

Figure 6. Comparison of experimental results and Horne and Dreher's equation for smooth tire.

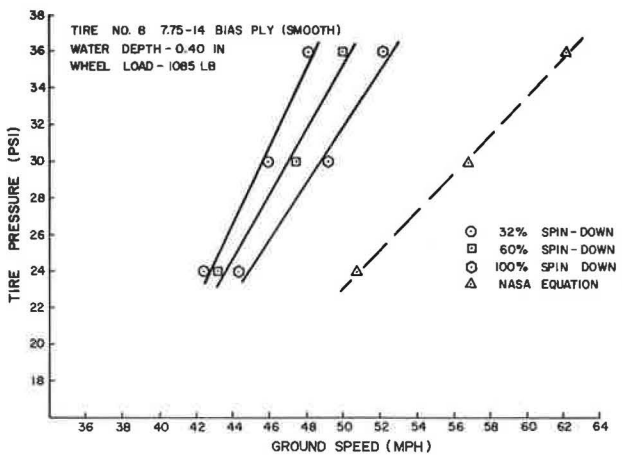

percent spin-down the ground speed is at least 70 percent of the predicted hydroplaning speed. Results obtained for other tires tend to follow similar patterns.

Figures 7, 8, and 9 show plots of vehicle ground speed versus percentage of spin-down for tire No. 4 when various inflation pressures, water depths, and pavements are considered. Figure 7 shows some of the effects of increasing the tire inflation pressure. For example, a pressure increase of 6 psi requires an increase of approximately 4 mph to cause a 20 percent spin-down; however, this is not true for the 18-psi pressure at which no spin-down was obtained for vehicle speeds up to 64 mph. This may be attributed to the fact that a decrease in the inflation pressure does not necessarily worsen a tire's hydroplaning behavior because the effect of the decreased contact pressure due to a larger contact area may be offset by a longer contact length. However, it should not be concluded that a hazardous condition does not prevail. It is possible for the tire frictional force to be reduced significantly without having the spin-down torque overcome the spin-up torque. Consequently, no spin-down will occur. For these cases, it might be desirable to perform skid tests and measure the friction coefficient for several tire inflation pressures. This would give the variation of the friction coefficient with tire inflation pressure and could indicate that a hydroplaning condition can be approached without any wheel spin-down.

Figures 10 and 11 show the effect of varying the wheel load from 800 to 1,085 lb. The results for the smooth tire are plotted in Figure 10 and indicate that an increase in the wheel load increases the ground speed that is required to produce a 10 percent spin-down of the wheel. However, Figure 11 indicates that, for a tire with full tread depth, the reverse takes place. This type of behavior is possible inasmuch as spin-down is closely associated with tire characteristics.

Figure 12 shows a comparison of tires No. 4 (wide tire) and No. 7 (bias ply). The results indicate that, to produce the same spin-down, the bias ply tire required greater ground speeds than did the wide tire. This tends to agree with studies performed by other researchers, which indicate that the hydroplaning speed decreases with a decrease in the tire aspect ratio (height/width).

Figure 13 shows the effects of tire tread depth on spin-down. The data, taken for smooth and full-tread depth bias ply tires (tires No. 7 and No. 8), show that a new tire requires a significantly larger ground speed to produce the same spin-down as a smooth tire. For example, in order to produce 10 percent spin-down for a water depth of 0.4 in. and a tire inflation pressure of 36 psi, the tire with the full tread depth required a ground speed of 57 mph, whereas the smooth tire only required a speed of 46.5 mph.

Figures 14 and 15 show the effects of the two pavements tested. Figure 14 shows the results obtained for a bias ply (tire No. 1), full-tread depth tire and shows that spin-down was obtained without difficulty on the concrete pavement and that realistic trends were demonstrated when the tire inflation pressure and water depth were varied. For the bituminous surface treatment, spin-down was only obtained at a water depth of 0.7 in. If spin-down is to be taken as an indication of hydroplaning, it can be concluded that a hazardous condition will not normally occur when typical water depths found on most well-drained roads are encountered. A water depth of 0.7 in. can be regarded as being high.

Figures 10 through 15 contain plots of water depth versus ground speed for various parameters. These curves show that the ground speed required to produce 10 percent spin-down always increases with a decrease in the water depth. This fact indicates that there is a low enough water depth for which wheel spin-down and probably hydroplaning do not occur.

From the electronic instrumentation data it was observed that wheel spin-down began almost immediately after the test trailer entered the hydroplaning trough. The trailer travel distance in the trough before the maximum spin-down was obtained for a particular test varied mainly with the trailer speed upon entering the trough. For example, when tire No. 4 with an inflation pressure of 24 psi was tested on the bituminous pavement with a water depth of 0.7 in., it took approximately 80 ft to reach a total spin-down of 20 percent when the vehicle speed upon entering the trough was 48 mph. How-

Figure 7. Effect of vehicle ground speed on wheel spin-down with water depth of 0.25 in.

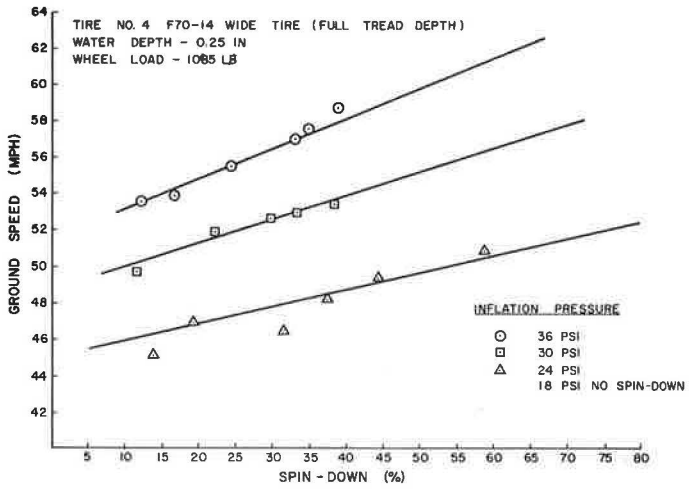

Figure 8. Effect of vehicle ground speed on wheel spin-down for concrete pavement with water depth of 0.40 in.

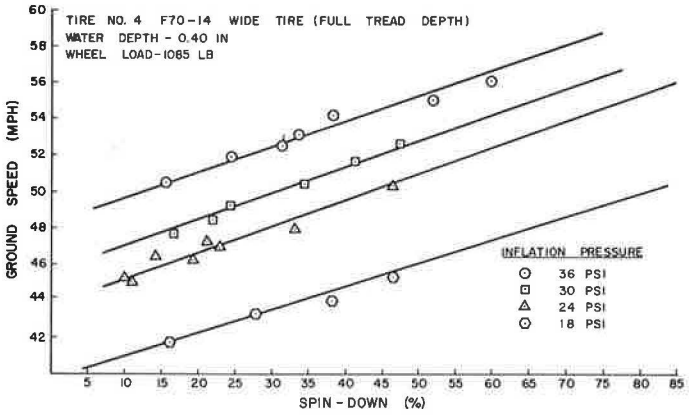

Figure 9. Effect of vehicle ground speed on wheel spin-down for bituminous surface treatment.

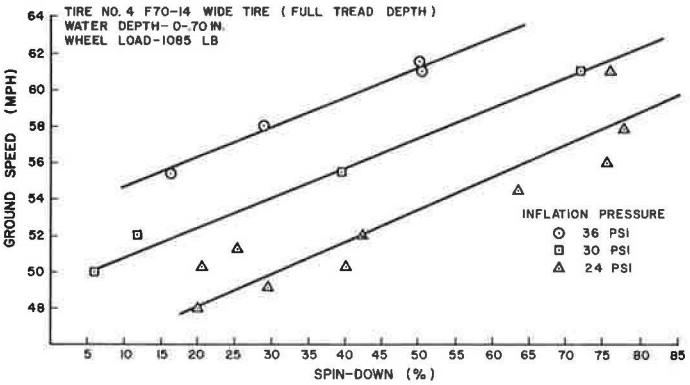

Figure 10. Effect of water depth and wheel load on ground speed required to produce 10 percent spin-down (tire No. 8).

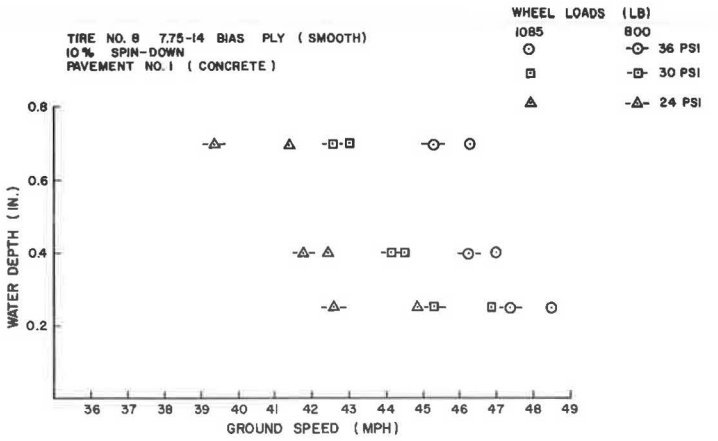

Figure 11. Effect of water depth and wheel load on ground speed required to produce 10 percent spin-down (tire No. 7).

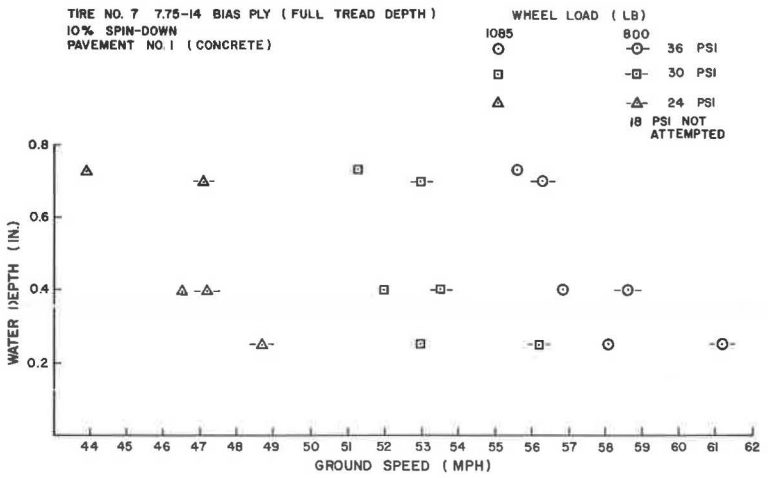

Figure 12. Effect of water depth and tire aspect ratio on speed required to produce 10 percent spin-down.

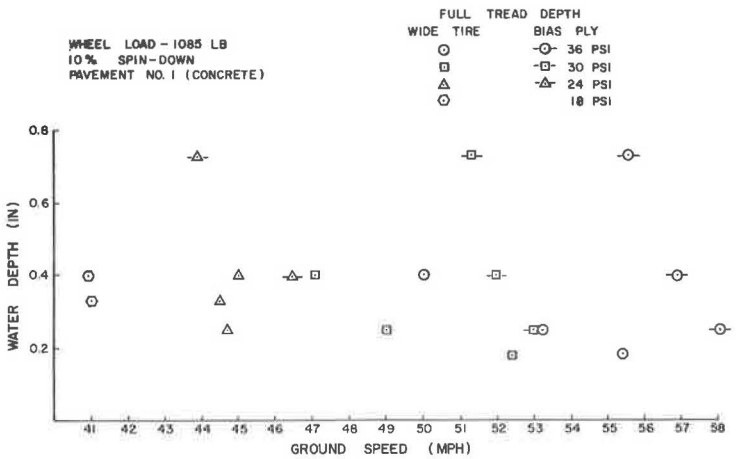

Figure 13. Effect of water depth and tread depth on speed required to produce 10 percent spin-down.

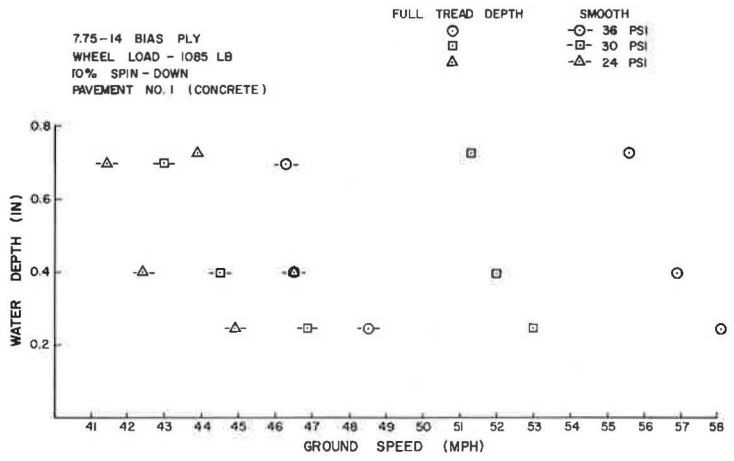

Figure 14. Comparison of concrete and bituminous surface treatment (tire No. 1).

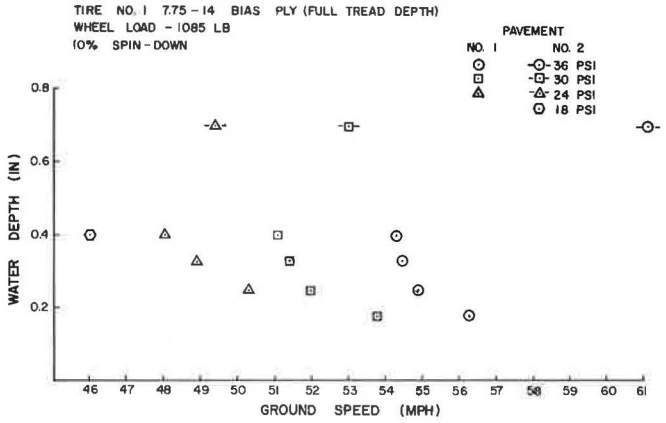

Figure 15. Comparison of concrete and bituminous surface treatment (tire No. 4).

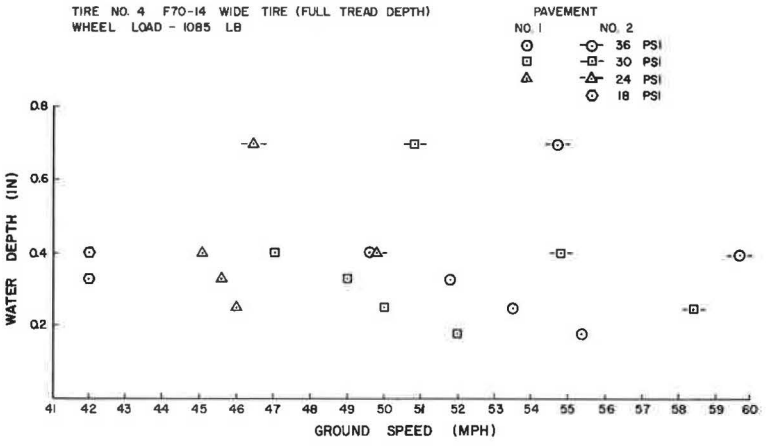

ever, when the entry speed was increased to 58 mph, it took 240 ft of travel before the final spin-down of 78 percent was attained; after 80 ft the tachometer generator traces indicated a wheel spin-down of approximately 20 percent.

Thus, it can be concluded that loss of traction occurs as soon as the wheel of a vehicle comes in contact with a flooded pavement. If the flooded portion of pavement is not long and the vehicle is not subjected to abnormal maneuvers, the tractive force can probably be regained without a hazardous condition existing. For a given vehicular ground speed that is high enough to cause wheel spin-down, the possibility of a hazardous condition existing increases with increasing length of flooded pavement.

APPLICABILITY TO SAFE WET-WEATHER SPEEDS

In recent legislative action, the state of Texas has given authority to the highway commission to set wet-weather speed limits at specific places on Texas highways. Although by no means encompassing all the factors that should be considered in determining safe speeds, the current data on hydroplaning give indications of the speeds that result in a potentially marginal condition with regard to vehicle control. Hydroplaning is only one of the many factors that must be considered in determining safe speeds. It is limited to the case in which a significant depth of water is encountered on the roadway due to an exceptionally high-intensity rain or to poor drainage, puddles, wheel ruts, low cross slope, and the like.

In the discussion presented in this section, it is assumed that a 10 percent spin-down of a free-rolling automobile wheel signifies the approach of a control problem, due to either a loss of stopping capability or a loss in directional control. In this section the 10 percent spin-down speed will be called the "critical speed."

Figures 16, 17, and 18 show approximate curves representing the data developed at this time. The effects of pavement texture, tire pressure, and tire type or condition are shown by these curves. Several tires are used to illustrate the various effects.

Tires 7 and 8 represent full tread depth and smooth bias ply respectively. Tire No. 4 is a full tread depth with a wide tire configuration. The wheel load in all cases is 1,085 lb.

The influence of pavement texture on partial hydroplaning speed (as indicated by 10 percent spin-down) is significant. An increase in critical speed from 47 to 60 mph is indicated at a water depth of $\frac{1}{4}$ in. when the macrotexture is increased from 0.018 to 0.145 in. This difference apparently decreases slightly as water depth increases. These macrotextures are average values determined by the silicone putty method.

The effect of tire pressure is shown in Figure 17. The tire pressures of 24 to 36 psi shown in this figure account for approximately 70 percent of the range of tire pressures observed in a study of 501 wet-pavement accidents in Texas (8).

Figure 17 shows that, at a water depth of 0.1 in., the critical speed increases by approximately 10 mph (from 48 to 58 mph) as tire pressure increases from 24 to 36 psi. This difference becomes much smaller at greater water depths.

The effect of three different tires on critical speed is shown in Figure 18. Unlike the effects of texture and pressure, the differences between these tires increase as the water layer becomes thicker. At a water depth of $\frac{1}{2}$ in. the critical speed varies from 43 to 51 mph. It is notable that the full-tread depth, wide tire falls between the bias ply, smooth and bias ply, full-tread depth as related to critical speed.

Figure 19 shows the consolidation of individual wheel tire pressure graphs (8). Although it is obvious from the curves presented that there is no one critical speed that is appropriate for the range of pavement, pressure, and tire parameters investigated, it is obvious that partial hydroplaning, and thus some loss of control, results at speeds significantly below the usual speed limit on major rural highways in Texas. No critical speeds below 40 mph were found, and a speed of 50 mph seems to be the roughly approximated median value for all parameters investigated.

It is therefore suggested that a reduction of speed to 50 mph be considered on any section of highway where water can accumulate to depths of 0.1 in. or more during wet periods. Further improvements in the safety of these sections can be made if a high-macrotexture surface can be produced and maintained.

Figure 16. Effect of texture on hydroplaning.

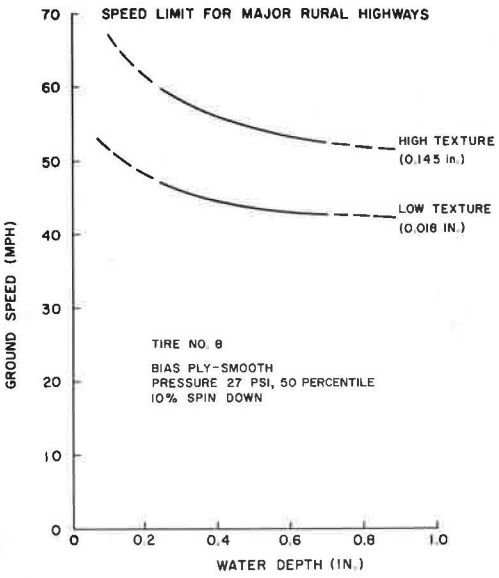

Figure 17. Effect of tire inflation pressure on hydroplaning.

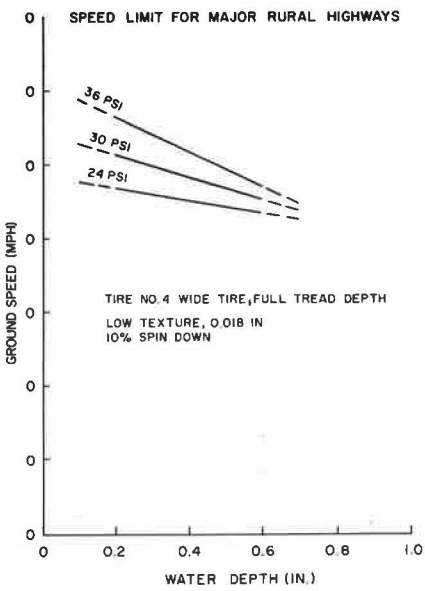

Figure 18. Effect of tire type on hydroplaning.

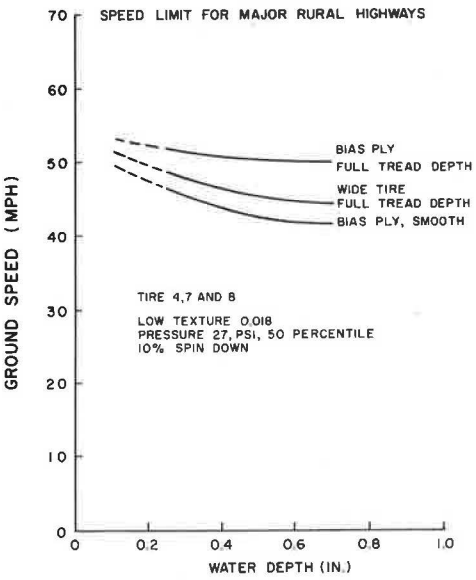

Figure 19. Comparison of tire pressures—accident sample.

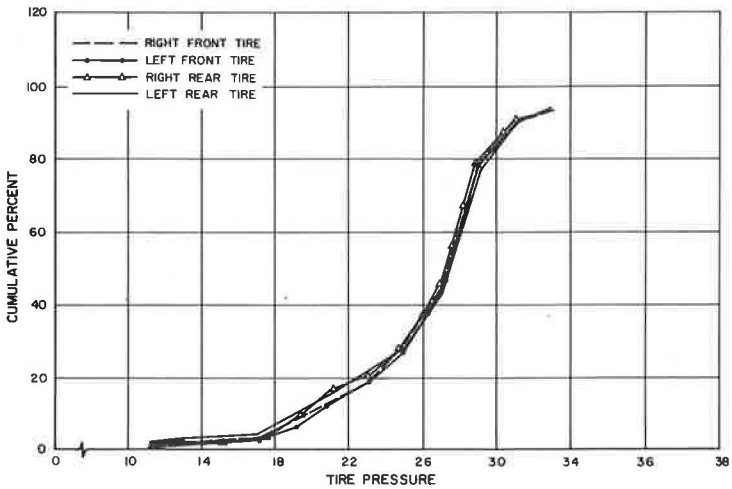

CONCLUSIONS

The following general conclusions are based on the data obtained from the tests and the criterion that 10 percent spin-down causes a sufficient reduction in the frictional coefficient such that vehicle stability is affected.

1. Wheel spin-down is normally initiated at a ground speed that falls within 70 percent of the critical hydroplaning speed predicted by Horne and Dreher's equation.
2. The ground speed required to initiate spin-down on full-tread depth tires is higher than the speed required with smooth tires.
3. Decreasing the tire inflation pressure normally has the effect of lowering the ground speed at which a certain amount of spin-down occurs.
4. Decreasing the tire aspect ratio (height/width) causes a decrease in the ground speed required to initiate spin-down.
5. Increasing the wheel load while maintaining the same inflation pressure for a smooth tire increases the gound speed at which spin-down is initiated. The reverse takes place for a full-tread depth tire.
6. An increase in the water depth decreases the speed at which wheel spin-down is initiated.
7. The bituminous surface treatment requires a higher ground speed to cause spin-down than the concrete pavement.
8. Total spin-down (wheel stops rotating) may occur at ground speeds lower than those predicted by Horne's equation.
9. Even though a tire may not have reached the total hydroplaning speed as predicted by Horne's equation, a hazardous condition may exist when the wheel has spun down and its frictional characteristics have been impaired.
10. Many factors must be considered in determining safe wet-weather speeds. From a hydroplaning standpoint, it is suggested that a reduction of speed to 50 mph be considered on any section of highway where water can accumulate to depths of 0.1 in.

ACKNOWLEDGMENTS

These tests and evaluations were sponsored by the Texas Highway Department in cooperation with the U.S. Department of Transportation, Federal Highway Administration. The opinions, findings, and conclusions expressed in this report are those of the authors and not necessarily those of the sponsor.

REFERENCES

1. Dreher, R. C., and Horne, W. B. Ground-Run Tests With a Bogie Landing Gear in Water and Slush. National Aeronautics and Space Administration, Tech. Note D-3515, July 1966.
2. Horne, W. B., and Dreher, R. C. Phenomena of Pneumatic Tire Hydroplaning. National Aeronautics and Space Administration, Tech. Note D-2056, Nov. 1963.
3. Horne, W. B., and Leland, T. J. W. Influence of Tire Tread Pattern and Runway Surface Condition on Braking Friction and Rolling Resistance of a Modern Aircraft Tire. National Aeronautics and Space Administration, Tech. Note D-1376, Sept. 1962.
4. Allbert, B. J. Tires and Hydroplaning. Society of Automotive Engineers, Automotive Engineering Congress, Detroit, Jan. 8-12, 1968.
5. Allbert, B. J., Walker, J. C., and Maycock, G. Tyre to Wet Road Friction. Proc. Institution of Mechanical Engineers, Vol. 180, Part 2A, No. 4, 1966.
6. Gough, V. E., and Badger, D. W. Tyre and Road Safety. Presented at Fifth World Meeting of the International Road Federation, London, Sept. 18-24, 1966.
7. Stocker, A. J., and Gregory, R. T. Construction of a Facility to Study Variables Associated With Hydroplaning. Texas Transportation Institute, Texas A&M University, Progress Report No. 1, March 1971.
8. Hankins, K. D., Morgan, R. B., Ashkar, B., and Tutt, P. R. The Degree of Influence of Certain Factors Pertaining to the Vehicle and the Pavement on Traffic Accidents Under Wet Conditions. Texas Highway Department, Departmental Research, Rept. 133-3F, Sept. 1970.

THE EFFECTS OF SALTS ON ROAD DRYING RATES, TIRE FRICTION, AND INVISIBLE WETNESS

Thomas P. Mortimer, Pratt and Whitney, East Hartford, Conn.; and
Kenneth C. Ludema, Department of Mechanical Engineering, University of Michigan

Roads may be slippery even though they are not visibly wet. Water films of invisible thickness cause substantial reductions in skid resistance on some road surfaces. This hidden wetness exists for a short time whenever surfaces are drying from the visibly wet state. Road salts slow the drying rate, which prolongs the condition of hidden wetness. Calcium chloride solutions may produce a very persistent invisible slippery film, depending on atmospheric conditions. Equations are given for predicting fluid film drying rates and the influence on skid resistance.

•TIRE FRICTION on road surfaces is usually measured in the fully wetted condition or in the "dry" condition because these two conditions are thought to represent the lower and upper extremes of tire friction. Very little attention has been given to the condition of intermediate wetness (1, 2), even though this condition is more common than fully wetted roads and may be as dangerous.

Road wetness is usually judged in a subjective manner, but sometimes attempts are made to measure the amount of liquid on the road surface. The depth or thickness of liquid on actual road surfaces varies considerably with location. On rain-wetted roads, the average liquid film thickness is typically 10^6 to 10^7 Å (1 Å = 10^{-8}cm) or 4×10^{-3} to 4×10^{-2} in. At the other extreme, clean, dry road surfaces are covered with water films whose thickness is typically 10 to 100 Å or 4×10^{-8} to 4×10^{-7} in. The latter are adsorbed films and are invisible.

This paper is a report of an investigation of tire friction on road surfaces wetted by fluid films with an average thickness less than the fully wetted thickness. It is oriented to the problem of the transition of tire friction from low to high values as the road surface dries from the very wet state. Three points are emphasized here: Whereas water films may evaporate and thin in a regular and continuous manner, tire friction increases rather abruptly in a certain range of fluid film thickness. Second, the film thickness range at which tire friction increases does not necessarily correspond with the disappearance of the observed wetness. That is, roads that appear dry do not necessarily show dry friction characteristics. Finally, it was found that salt additives on roads have a profound effect on the time and rate of transition of tire friction from low to high values and, furthermore, that salts lower the general level of tire friction below the plain water-wetted value.

The work reported here begins with a description of the method used to obtain fluid films of desired thicknesses. The film thicknesses of greatest interest are invisible and therefore difficult to measure. The method described begins with visible fluid films. After some period of water evaporation, light interference patterns, which give a good indication of film thickness, are observed. Further évaporation produces continued film thinning until an equilibrium film thickness is reached. The equilibrium thickness is a function of surface type, atmospheric temperature, relative humidity (3), and type and concentration of salt in the film. All of these factors are considered in the evaporation model developed in the next section.

Sponsored by Committee on Surface Properties-Vehicle Interaction.

EVAPORATION MODEL

In the simple evaporation model (4) the road surface is assumed to be flat and smooth and initially covered with a uniform liquid film of thickness h_o (in Å) and molar salt concentration M_o. Note that rainwater may be taken to be a salt solution of very low molar concentration. At any instant of time t (min) after the salt film has lost some water due to evaporation, the instantaneous film thickness decreases to h_f and the molar salt concentration increases to M.

Salt additives in water decrease the evaporation rate by lowering the bulk water vapor pressure of the solution P_s (in mm Hg). Figure 1a shows P_s as a function of M for NaCl and $CaCl_2$ salts. In the model, the solution temperature and air temperature are assumed equal; so the following linear approximation can be made for P_s:

$$P_s = KM + P_o \tag{1}$$

where K (mm Hg/molar) is the slope constant, which is a function of salt type and temperature T (in deg F), and P_o (mm Hg) is the saturated water vapor pressure of the air, which is also a function of T (Fig. 1b).

Assuming that the total atmospheric pressure is 760 mm Hg, we can express the evaporation of the salt solution film as

$$t = (6 \times 10^{-6}\, M_o h_o)/(0.031 + 0.0135\, V)\left((M - M_o)/[MM_oP_o(1 - H)] + \{K/[P_o(1 - H)]^2 \ln_e\}\{M_o[KM + P_o(1 - H)]\}/\{M[KM_o + P_o(1 - H)]\}\right) \tag{2}$$

where V is the horizontal wind velocity (m/sec) and H is the relative humidity of the air expressed as a fraction. Given the atmospheric conditions (i.e., T, H, and V), the salt type (i.e., K), and the initial conditions (i.e., h_o and M_o), the time t required for the solution to evaporate from salt concentration M_o to M can be calculated by using Eq. 2. Figure 2 shows families of curves for $\log_{10} M$ versus t for various initial concentrations of NaCl and $CaCl_2$ solutions with h_o = 3,000 Å at the atmospheric conditions indicated. The Xs on the NaCl solution curves denote the points at which the solutions begin to crystallize. $CaCl_2$ is deliquescent with these atmospheric conditions; these solutions therefore reach an equilibrium salt concentration instead of crystallizing.

The instantaneous salt solution film thickness can be calculated by using the expression,

$$h_f = h_o\,(M_o/M) \tag{3}$$

Figure 3 shows curves for h_f versus t corresponding to the solutions and conditions shown in Figure 2. Note that the film thinning is fairly regular and continuous. Also note that the 1.0 M_o $CaCl_2$ solution approaches an equilibrium film thickness of about 650 Å.

Given the ability to calculate fluid film thickness and molar salt concentration as a function of time, we can calculate the viscous drag force of smooth rubber sliding over smooth glass with a known fluid film between. Because we used a smooth rubber slider mounted on a British portable tester (Fig. 4) to check the model calculations, the viscous drag force was converted to units of British portable number (BPN), the average coefficient of friction multiplied by 100. The viscous drag force F was calculated by using Newton's law (5),

$$F = \eta Av/h \tag{4}$$

where

η = bulk viscosity of the salt solution film,
A = contact area,
v = relative sliding velocity, and
h = total film thickness.

Figure 1. Water vapor pressure versus (a) M and (b) T.

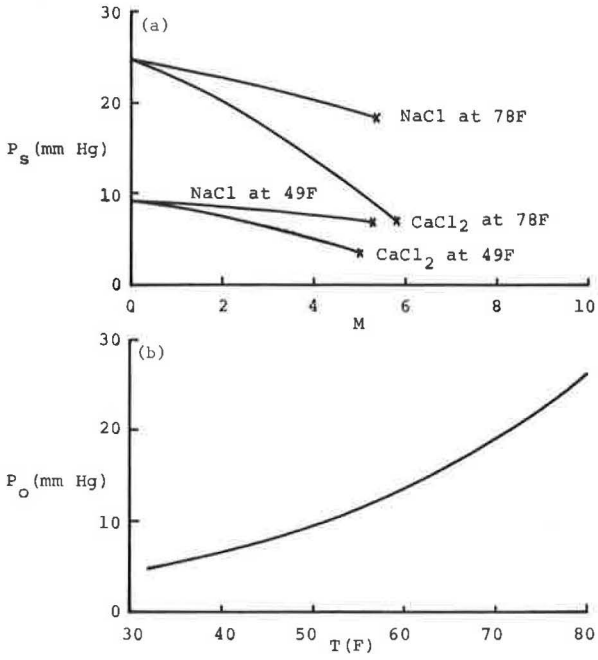

Figure 2. Evaporation model $\log_{10}M$ versus t for h_o = 3,000 Å at T = 78 F, H = 0.50, and V = 0.5 m/sec.

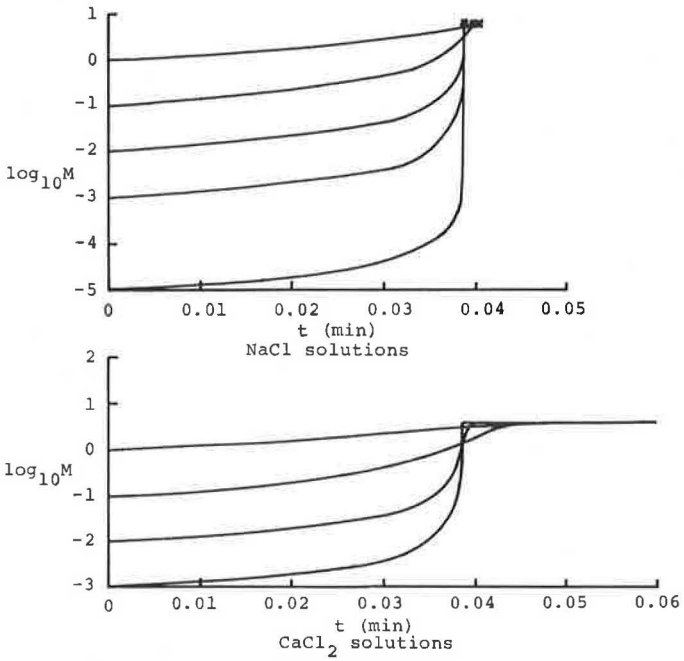

It is recognized that this simple viscous drag equation does not represent the actual case of a tire sliding over a textured road surface, but it was helpful in checking the validity of the evaporation model. The values of A and v corresponding to the British portable tester were 0.108 in.^{2} and 121 in./sec (6.9 mph). The instantaneous value of η corresponding to M was obtained from Figure 5, which shows the bulk viscosity of the salt solution divided by the bulk viscosity of pure water η/n_o as a function of M. Finally, the value of h was defined as

$$h = h_f + h_a \tag{5}$$

where h_a is the adsorbed film thickness on the clean surface. For the type of glass used in the experiments, the reference value of h_a with $\eta/n_o = 1.0$ was 89 Å at 78 F and 132 Å at 49 F.

Figures 6, 7, and 8 show the evaporation model curves of BPN versus t. The 10^{-5} M_o NaCl solutions are the approximate equivalent of distilled water. The curves in Figure 6, which correspond to those in Figures 2 and 3, show that the rate of transition of BPN is rather rapid for low initial concentrations and is more gradual for high initial concentrations. Figure 7 shows curves for 10^{-5} M_o NaCl, 1.0 M_o NaCl, and 1.0 M_o $CaCl_2$ at low and high humidity. Note that neither salt is deliquescent at low humidity, whereas both are at high humidity. The curves in Figure 7 show that, as humidity increases, the time of transition of BPN is longer and the rate of transition of BPN is less rapid. Comparison of the 1.0 M_o curves at either humidity shows that the $CaCl_2$ solution has a longer time of transition and a less rapid rate of transition than the NaCl solution. The same is true of these two salt types for any other atmospheric condition or initial concentration, but the difference is less noticeable with low humidities and initial concentrations. The difference between the 10^{-5} M_o and 1.0 M_o solutions is also less pronounced with low humidities. Figure 8 shows how temperature and wind velocity affect the transition of BPN. Note that the wind velocity affects the time and rate of transition but not the equilibrium BPN.

These evaporation model curves were checked by experiment in the following manner. A glass plate surface was first wetted with an excess of solution and then wiped with a rubber-bladed window squeegee. It was deduced that $h_o \cong 3{,}000$ Å from the fact that light interference patterns appeared almost immediately after wiping with the squeegee. The first British portable test swing was made just after wiping, and subsequent test swings were made at 0.5-min intervals without rewetting the test surface.

From a comparison of the experimental data of BPN versus t with the evaporation model curves, the following conclusions were made:

1. The evaporation model predicts correctly the relative effects on the time and time rate of transition of BPN of salt type (NaOH, NaBr, NaI, KCl, and LiCl as well as NaCl and $CaCl_2$), initial salt concentration, and atmospheric conditions.
2. The times predicted by the evaporation model are approximately 10 times faster than those that actually occur (i.e., the predicted evaporation rate is faster than the actual rate). This discrepancy is thought to be caused by four conditions not accounted for in the simple evaporation model: (a) a decrease of the liquid film temperature below air temperature due to the cooling effect of the evaporation process, (b) a salt concentration gradient in the thickness direction in which the liquid at the air surface is salt-rich, (c) a decrease of the water vapor pressure of thin films due to the absorbate surface force fields, and (d) a decrease of the water vapor pressure of thin films due to the capillary effect of a microscopically rough surface.

EVAPORATION TESTS AND TRANSITIONS IN SKID RESISTANCE AS MEASURED BY THE BRITISH PORTABLE TESTER

Evaporation tests were made on five textured road surfaces to determine if the evaporation model predicts the relative effects of salt type, salt concentration, and atmospheric conditions on the time and rate of transition of BPN on real roads as well as on glass. Pictures of the five test surfaces are shown in Figure 9. All but the Dorset pebble surface were worn under actual traffic conditions. For a

Figure 3. Evaporation model h_f versus t for h_o = 3,000 Å at T = 78 F, H = 0.50, and V = 0.5 m/sec.

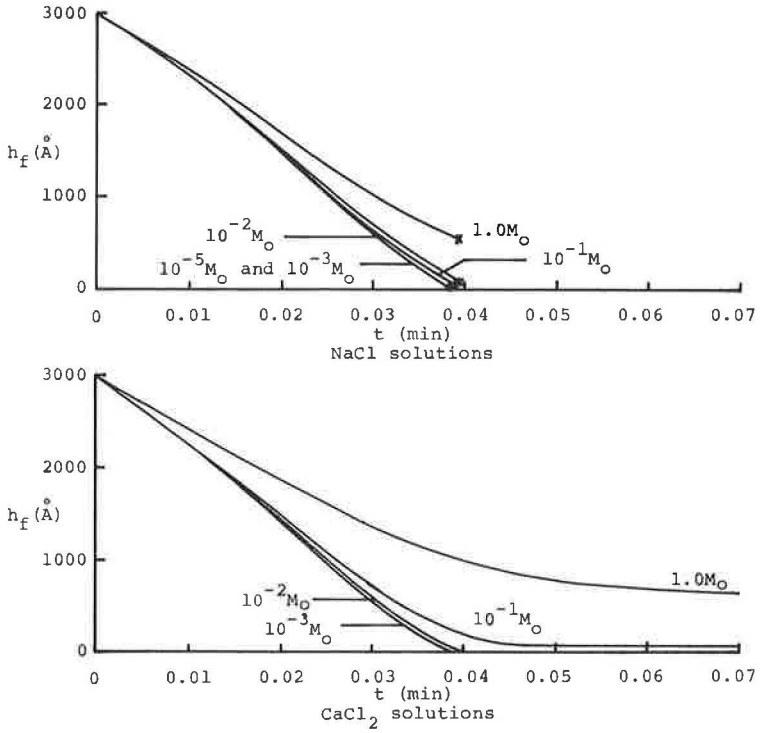

Figure 4. British portable tester.

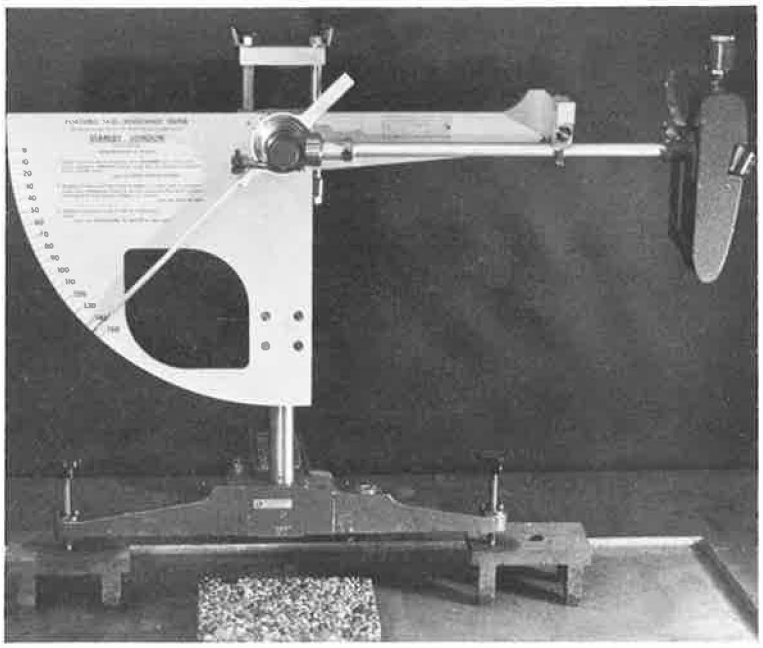

Figure 5. η/η_o **versus M (at T = 78 F,** η_o **= 0.008817 poise; at T = 49 F,** η_o **= 0.013077 poise).**

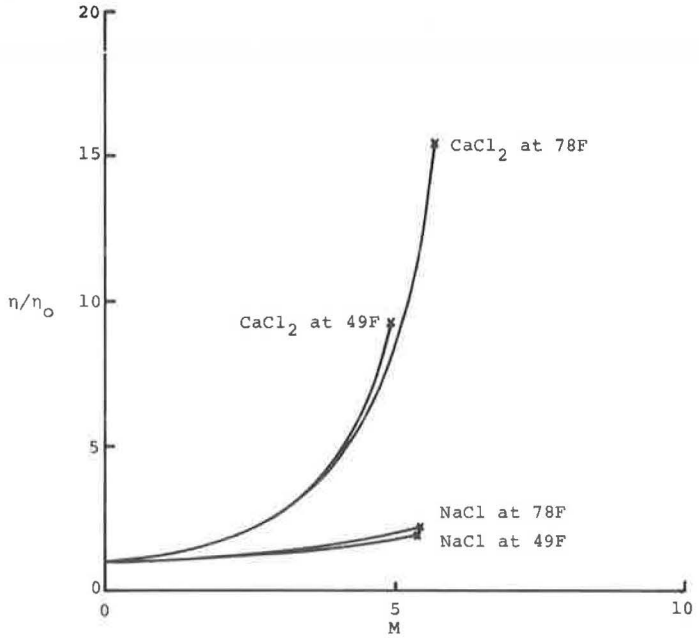

Figure 6. Evaporation model BPN versus t for h_o **= 3,000 Å at T = 78 F, H = 0.50, and V = 0.5 m/sec.**

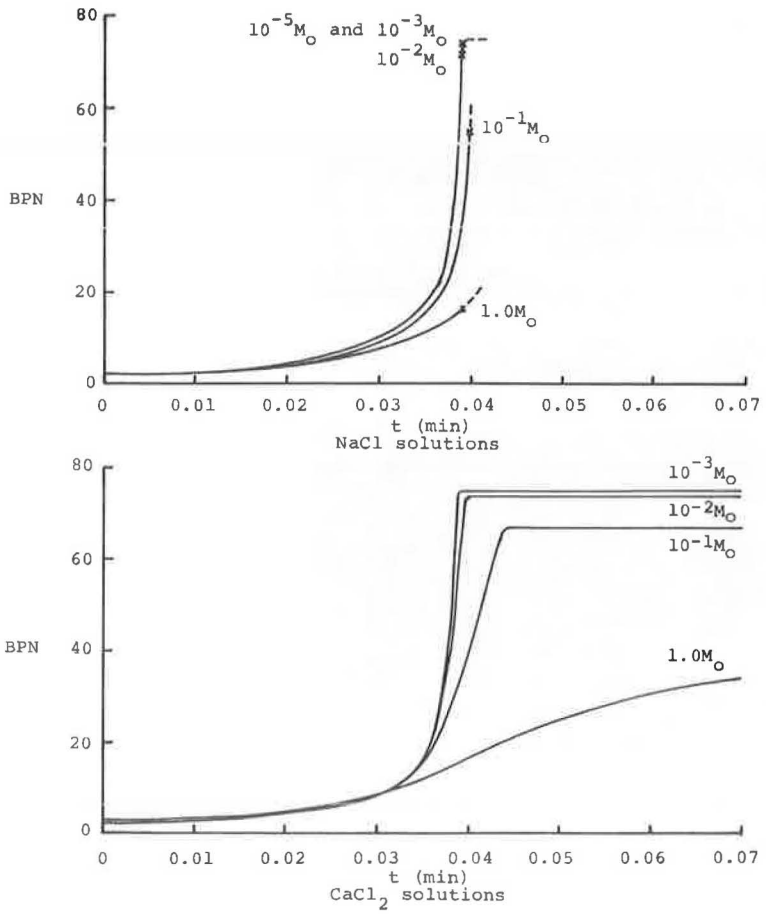

Figure 7. Evaporation model BPN versus t for h_o = 3,000 Å at T = 78 F and V = 0.5 m/sec.

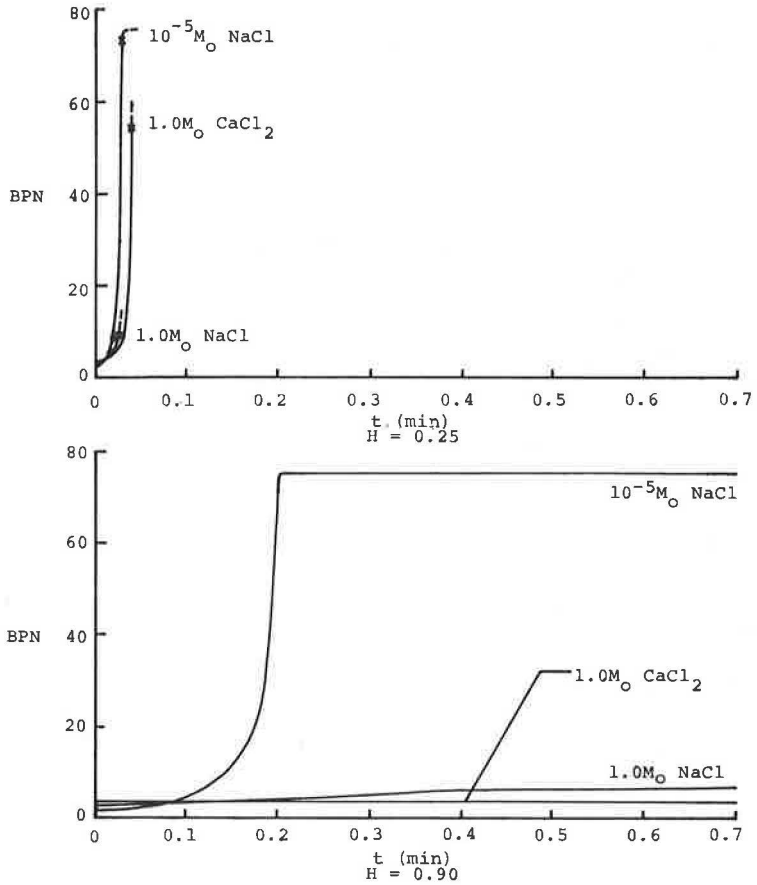

Figure 8. Evaporation model BPN versus t for h_o = 3,000 Å at T = 49 F, H = 0.62, and V = 1.0 or 0.0 m/sec.

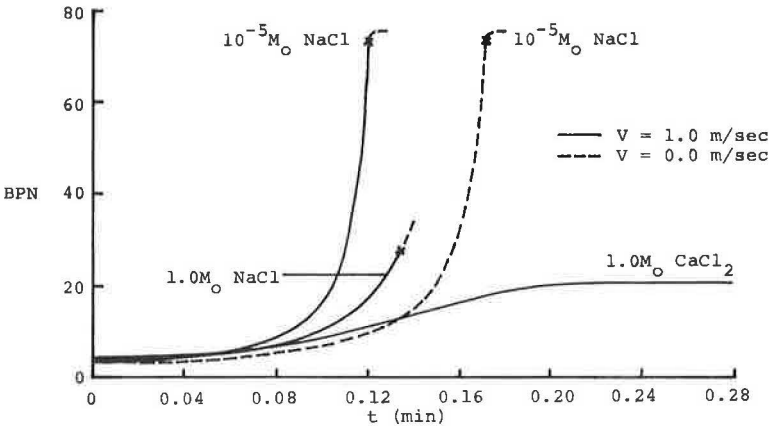

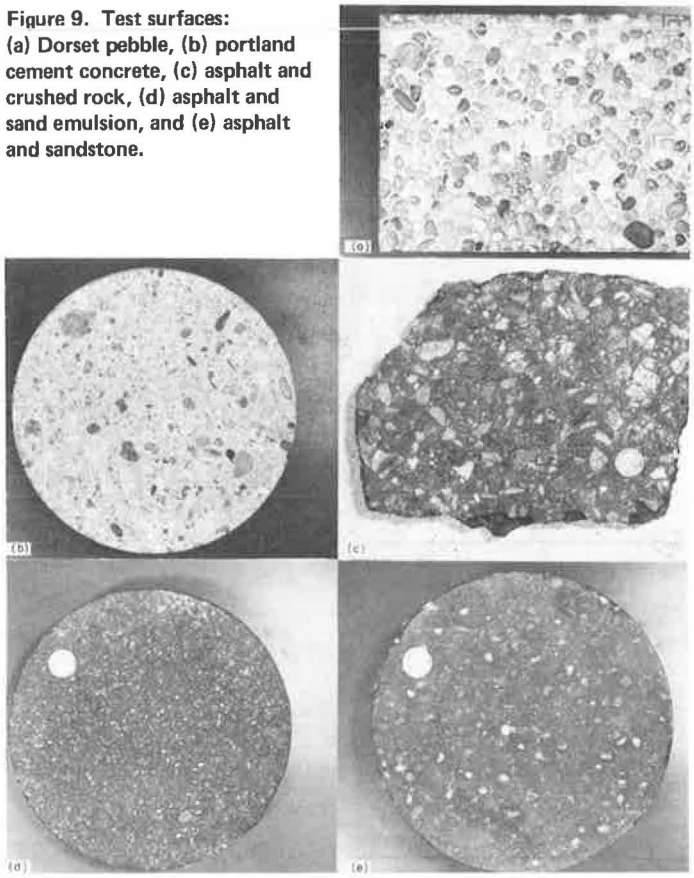

Figure 9. Test surfaces: (a) Dorset pebble, (b) portland cement concrete, (c) asphalt and crushed rock, (d) asphalt and sand emulsion, and (e) asphalt and sandstone.

Figure 10. Dorset pebble BPN versus t.

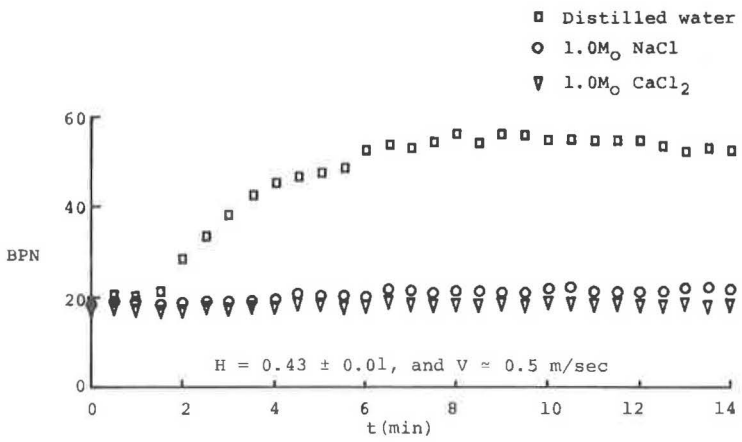

reference, the BPNs from a standard test (i.e., using distilled water, a 5-in. slide length, and a standard natural rubber slider) were measured at 78 F and are as follows: Dorset pebble, 24; portland cement concrete, 58.3; asphalt and crushed rock, 52.5; asphalt and sand emulsion, 57; and asphalt and sandstone, 62.

In the evaporation tests a slide length of 4 in. was used, and the rubber sliders were made from Royalene 505, a styrene-butadiene experimental tread stock. At the beginning of the tests, 30 ml of distilled water 1.0 M_o NaCl or 1.0 M_o $CaCl_2$ solution was spread over the clean dry test surface. The amount of salt per unit area spread on the test surface in the 1.0 M_o salt solution tests is approximately equal to that spread on road surfaces to melt ice and snow (approximately 300 to 500 pounds per lane-mile). Test swings were made without rewetting at 0.5-min intervals with the Dorset pebble surface and at 5.0-min intervals with the other road surfaces. The test data of BPN versus t are shown in Figures 10 through 14. The S and F in these figures denote the approximate start and finish of the driving of the surface as was carefully observed from directly overhead. In comparing Figures 10 through 14 with the evaporation model curves, we see that the time scales of the BPN versus t data are considerably different from the model. Part of this difference is due to the fact that the initial film thicknesses are considerably greater than 3,000 Å. Other possible causes besides the four already put forth for the glass plate tests are rewetting due to splashing from trapped liquid pools; increased liquid spreadability due to the fine scale surface texture (3); and changed air circulation patterns at the liquid surfaces, which affects the local evaporation rates. Despite this difference of the time scales, the evaporation model does predict the relative effects of salt type, initial concentration, and atmospheric conditions on the time and time rate of transition of BPN with these textured test surfaces.

EVAPORATION TESTS AND TRANSITIONS IN TIRE FRICTION AS MEASURED BY A SKID TRAILER

BPN skid resistance as usually measured on fully water-wetted roads has been shown to correlate with locked-wheel tire friction for car speeds from 20 to 50 mph (6). It was not known, however, if such a correlation exists for road surfaces of transition wetness, or film thickness, such as exist in the evaporation tests. For this reason, the validity of the findings from the evaporation tests with the British portable tester on textured surfaces was checked by performing similar evaporation tests on a real road surface and by measuring tire friction directly with the two-wheeled skid trailer (ASTM Standard E 274-65T) of the Michigan Department of State Highways. The skid trailer tires (ASTM Standard E 249-66) had a vertical load of approximately 800 lb each. Pictures of the test vehicle and the trailer tire are shown in Figures 15 and 16. The test site chosen was the outer lane of a uniform, level stretch of a 15-year-old portland cement concrete divided highway in southern Michigan. The road surface is similar in appearance to the test surface shown in Figure 9b. For a reference, the BPN from a standard test on this road surface at 47 F was 59.8.

In these evaporation tests, the test lane was blocked off to traffic, and three separate 60- by 10-ft sections were wetted, one with 15 gal of tap water, one with 1.0 M_o NaCl solution, and one with 1.0 M_o $CaCl_2$ solution. The volume of solution per unit area spread on the road surface was approximately the same as that used in the evaporation tests. The average coefficient of tire friction μ in full skidding at 40 mph of the three wetted test sections was periodically measured. To minimize the contamination of one solution by the others required that the skid trailer wheels be washed between each test run. Throughout the test the sky was overcast, and the atmospheric conditions remained nearly constant. Figure 17 shows μ as a function of t, which is the total elapsed time since the solution in that section was first tested.

It is seen from the curves that the relative times and time rates of transition of μ are in agreement with the transitions of BPN in the other evaporation tests and with the evaporation model. Because the evaporation model is based on viscous drag, the test data suggest that fluid viscous effects are prominent in tire friction in the transition film thickness range.

The skid trailer data confirmed the findings of British portable tests, which showed that salt additives decrease the general level of friction in the fully wetted condition.

Figure 11. Portland cement concrete BPN versus t.

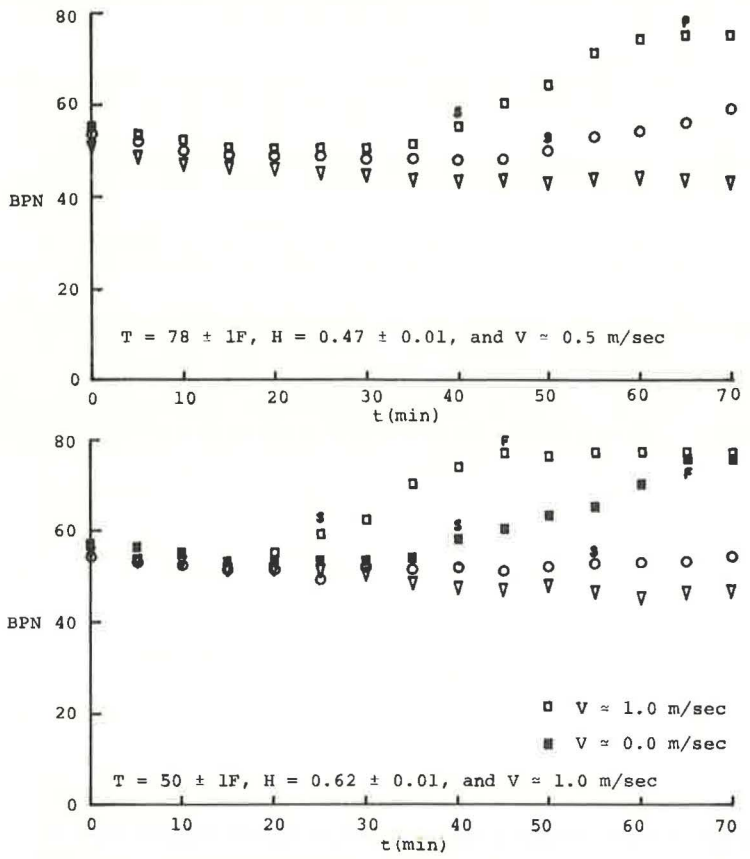

Figure 12. Asphalt and crushed rock BPN versus t.

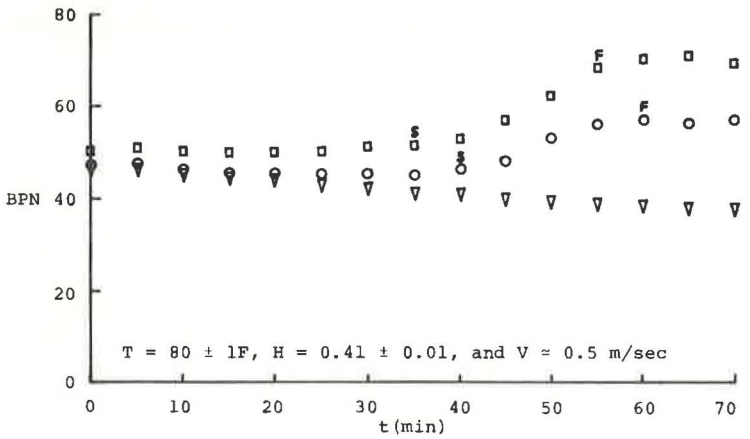

Figure 13. Asphalt and sand emulsion BPN versus t.

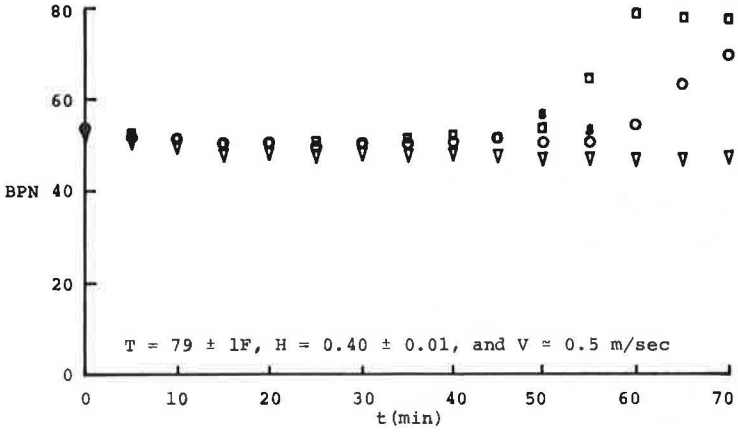

Figure 14. Asphalt and sandstone BPN versus t.

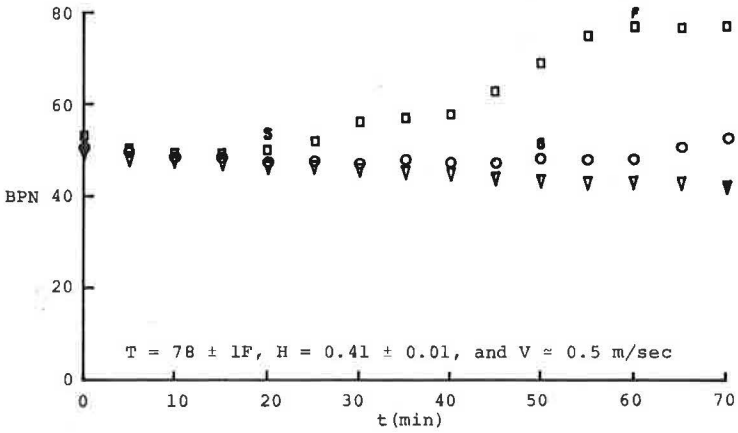

Figure 15. Test vehicle.

Figure 16. Trailer tire.

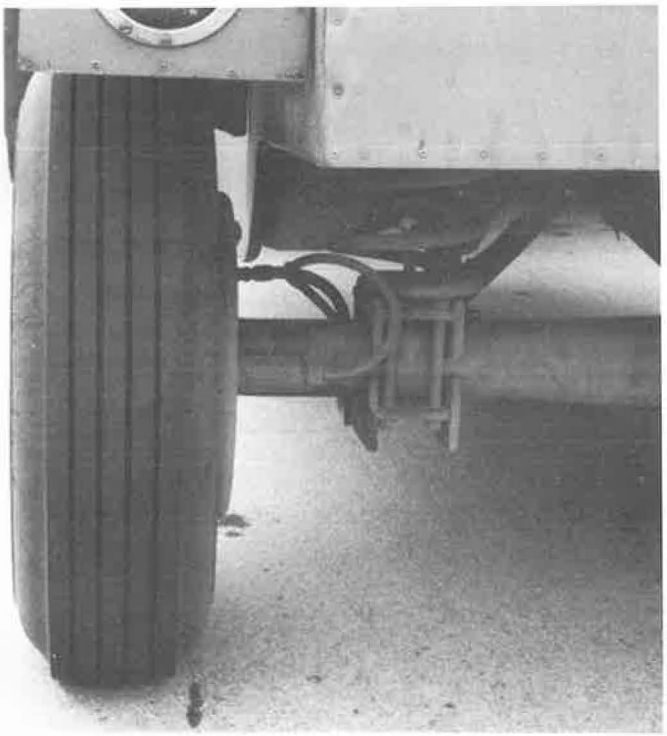

Figure 17. Portland cement concrete μ versus t.

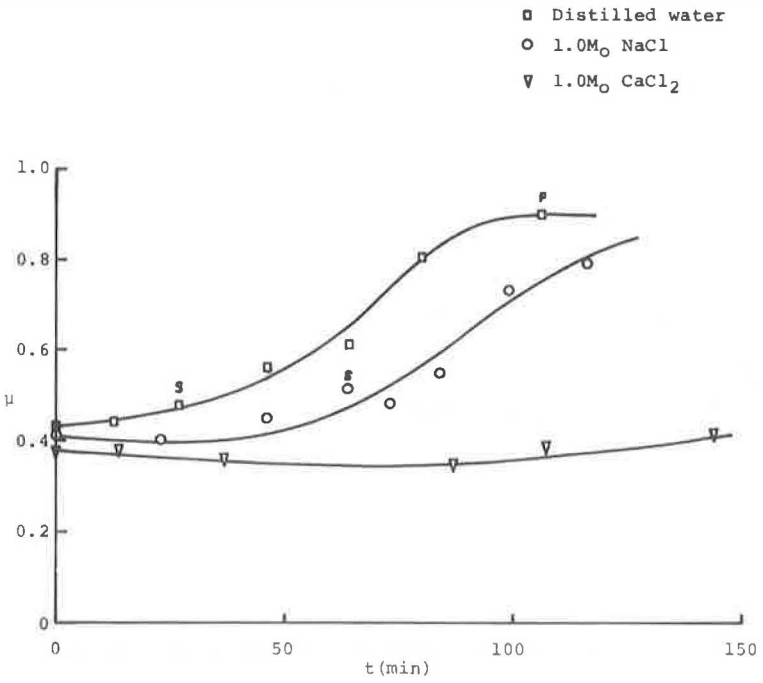

The probable reason is that the squeeze film between the tire and road surface is thicker for the salt solutions because they have a bulk viscosity greater than pure water (Fig. 5). Csathy (2) tested real road surfaces with a British portable tester and reported a BPN decrease of 7 to 10 percent with 4.65 M NaCl solution and 12 to 15 percent with 2.5 M $CaCl_2$ solution. A BPN decrease of similar magnitude was observed in the evaporation tests reported in this paper. The skid trailer tire friction data showed an initial decrease of 4.7 percent for 1.0 M_o NaCl solution and 11.6 percent for 1.0 M_o $CaCl_2$ solution. After some evaporation had taken place and the bulk viscosity of the salt solution had increased, the value of μ with the salt solutions reached a minimum, and the decrease below the plain water-wetted value was 7.0 percent for the NaCl solution and 18.6 percent for the $CaCl_2$ solution.

INVISIBLE WETNESS

In the evaporation tests on the glass plate surface, the liquid films were directly visible at first, then interference fringes were seen, and after this no evidence of water was apparent. The minimum light interference film depth was calculated to be approximately 1,700 Å (4). Thinner films were invisible, and yet the BPN value continued to increase with time just as predicted by the evaporation model. The BPN value when the glass plate first appeared dry was approximately 30. In contrast, the maximum dry value for the clean plate was over 84. The condition in which a surface appears dry but has a friction value significantly below the clean, dry value is termed "invisible wetness." The evaporation test data on the glass plate showed that one of the effects of salt additives in solution is to temporarily or indefinitely delay the decrease in film thickness and the increase in BPN, i.e., to prolong the condition of invisible wetness.

Invisible wetness poses a problem for drivers who mistakenly perceive a road surface to be dry when in fact the actual tire friction is significantly below the expected clean, dry level. In the evaporation experiments on the textured road surfaces, there was some evidence that under certain conditions invisible wetness does in fact occur. For the Dorset pebble and portland cement concrete road surfaces, which have porous cement binders and nonporous road stone aggregates, the driver usually determines road wetness from the cement binder appearance. The road is perceived to be dry when the binder is light and wet when dark. Evaporation tests with the British portable tester showed, however, that the matrix does not always reveal the true wetness. For example, in evaporation tests with 10^{-1} M_o $CaCl_2$ solutions, the porous cement binder absorbed the solution after 15 to 30 min and began to appear light, which is characteristic of a dry surface. The nonporous road stones over which the rubber surface slides maintained relatively thick but invisible liquid films, however. In this condition of invisible wetness, the Dorset pebble BPN was about 35 compared to the dry upper limit of 85, and the portland cement concrete BPN was about 65 compared to the dry upper limit of 75.

The asphalt binder of the three asphalt surfaces was much darker than the cement binder, and the change in darkness from the wet to the dry condition was much less pronounced than with the cement binder. The asphalt matrix tended to be less porous, however, which kept the matrix wet longer and helped to offset the difficulty in detecting the binder wetness. The degree of danger from invisible wetness with the asphalt road surfaces is about the same as that with the portland cement concrete surface.

CONCLUSIONS

Salt additives in the solution wetting a road surface have the effect to temporarily or indefinitely delaying the drying of the surface and thereby delaying the transition of tire friction from the wet to the dry value. The evaporation model described in this paper predicts the relative effects on the transitions of tire friction of salt type, salt concentration, and atmospheric conditions. Three significant effects are as follows:

1. $CaCl_2$ delays the transition more than the equivalent molar concentration of NaCl and is therefore a more undesirable road contaminant in terms of tire friction.
2. The greater the concentration of a particular salt type is, the slower is the transition from the wet to the dry friction level.

3. The higher the air humidity is, the greater is the effect that salt contaminants have in prolonging the transition from the wet to the dry friction level.

Salt contaminants in the solution wetting road surfaces can decrease tire friction below the uncontaminated water-wetted value. This decrease is as large as 7.0 percent for NaCl and 18.6 percent for $CaCl_2$. Also, salt contaminants on road surfaces increase the equilibrium film thickness and thereby promote the condition of invisible wetness in which the road surface appears dry but in fact has a level of tire friction significantly below the clean, dry value.

ACKNOWLEDGMENTS

We thank David Sapper of the Uniroyal Tire Company, Detroit, Michigan, for supplying the Royalene 505 rubber used in the experiments.

REFERENCES

1. Moyer, R. A. Skidding Characteristics of Road Surfaces. HRB Proc., Vol.13, Pt. 1, 1934, pp. 123-168.
2. Csathy, T. I. A Study of the Skid-Resistance of Pavement Surfaces. Department of Highways, Ontario, DHO Rept. 32, 1963, pp. 9-14.
3. Holland, L. The Properties of Glass Surfaces. Chapman and Hall, London, 1964, pp. 227, 349-351.
4. Mortimer, T. P. The Effects of Ions in Aqueous Solution on Wet Rubber Friction. PhD thesis, Univ. of Michigan, 1971, pp. 118-130, 141-143.
5. Hersey, M. D. Theory and Research in Lubrication. John Wiley and Sons, New York, 1966, p.26.
6. Mahone, D. C. Pavement Friction as Measured by the British Portable Tester and by the Stopping-Distance Method. Materials Research and Standards, Vol. 2, No. 3, March 1962.

THE RELATIVE EFFECTS OF SEVERAL FACTORS AFFECTING RAINWATER DEPTHS ON PAVEMENT SURFACES

Bob M. Gallaway, Jerry G. Rose, and R. E. Schiller, Jr.,
Texas Transportation Institute, Texas A&M University

Reported are the results of a study concerned with determining the amount of water that can be expected to exist on various pavement-surface types under normal ranges of pavement cross slopes, rainfall intensities, surface textures, and drainage lengths. Equations are developed that relate these variables and their relative effects to water depth. Background information and pertinent past research pertaining to hydraulics of water flow over paved surfaces are given. Increases in pavement cross slope and surface texture resulted in decreased water depths, whereas increases in rainfall intensity and drainage length increased water depths. The findings and conclusions contained herein will be useful to highway engineers in determining proper geometric designs and paving materials commensurate with acceptable pavement friction characteristics and service demands. Suggestions for further research are also included.

•SAFETY on our nation's highways is a topic of utmost importance to the driving public. Concern for the prevention of traffic accidents is evidenced in every responsible agency from the Department of Transportation at the federal level to local highway authorities. The causes of traffic accidents are numerous, but the results are the same: costly destruction of property, incalculable human suffering, and an annual death toll exceeding 50,000 lives. Trends in the causes of traffic accidents have been discovered; research has been, and will continue to be, conducted in an effort to solve the problems that bring about this senseless loss of resources.

Among those topics that have received considerable attention during the past 30 or 40 years is the problem of producing roadway pavement surfaces that provide adequate tire-gripping capabilities under all operating conditions, thus reducing the occurrence of accidents attributed to skidding. Skidding occurs when frictional demands on the vehicle wheels exceed that available; such loss results in increased stopping distance, loss of directional stability, and loss of operator control.

Characteristically, a pavement becomes slippery when the prevailing conditions are such that water lubricates the tire-road interface, when the inherently high skid resistance of a new surface has been worn and polished away by traffic, and/or when vehicle speeds during wet-pavement driving are high enough to hydrodynamically reduce or eliminate the tire-surface contact (hydroplaning), and thus the available friction, below the level required for safe vehicle maneuvers (1). Dearinger and Hutchinson (2) suggest that, although the details of the slipperiness-skid resistance problem are quite complex, most automobile accidents involving skidding are simply due to the unfortunately common combination of a wet pavement and an attempt by the driver to perform a maneuver (braking, cornering, or accelerating) at a speed too high for the conditions. The frequency of occurrence of this combination or circumstances has risen sharply in the past few years with continuing increases in traffic volumes and higher average vehicle speeds.

Sponsored by Committee on Surface Drainage of Highways and Committee on Operational Effects of Geometrics.

Numerous research studies have indicated that, neglecting contamination, all pavement surfaces exhibit adequate skid resistance for normal stopping and cornering maneuvers when dry and clean. When wet, however, this condition is no longer in effect for certain conditions and surface types, the only different condition being the presence of water between tire and pavement. Studying the factors affecting water-film thickness is, therefore, of paramount importance.

The research reported here deals with the effect of several variables on pavement water depth on full-scale elements of nine different pavement surface types under simulated rainfall of various intensities.

OBJECTIVES

The following were the objectives of this research:

1. To examine the relative effects of various rainfall intensities, pavement cross slopes, drainage lengths, and surface textures on resultant pavement water depths;
2. To develop an equation that relates rainfall intensity, pavement cross slope, drainage length, and surface texture to pavement water depth; and
3. To recommend means by which the findings and conclusions contained herein can be implemented by the highway engineer in determining proper geometric designs and paving materials commensurate with acceptable pavement friction characteristics and service demands.

BACKGROUND

Review of the Literature

Recognized research on the hydraulics of water flow evolved in 1775 with the investigations of Chezy (3). Manning (4) extended this research in 1891. During the early 1900s, the so-called "rational formula" (5) was introduced.

The first significant research on the hydraulics of water flow across paved surfaces was that of Horton in 1938 (6). He derived a theoretical formula describing the runoff hydrograph. In 1946, Izzard (7) reported on extensive, practical experiments of overland flow and developed equations for calculating time to equilibrium flow, amount of equilibrium flow, and volume of water in detention at equilibrium. Izzard also determined that the form of the overland flow hydrograph could be presented as a dimensionless graph, thus offering a means by which one might design street and parking lot structures.

Recently, researchers at the British Road Research Laboratory conducted experiments on actual road surfaces to determine relations between rainfall intensity, length of drainage path, slope, and water-film depths for the surface types most common on high-speed roads in the United Kingdom (8, 9, 10). A general equation relating these variables was developed. The tests were limited to extremely coarse-textured surfaces.

Nature of the Problem

Rainwater forms a layer of increasing thickness as it flows to the edge of a sloped pavement surface (Fig. 1). This water is a hazard to motorists due to the reduced frictional drag between the tires and the wet surface and due to the poor visibility caused by splash and heavy spray. The need to remove rainwater quickly from roads is even more important on multilane highways where greater water depths can be expected in the outside lanes. In addition, providing adequate texture in the road surface to allow escape of the remaining water under the tire is very important to achieve necessary tire-pavement mating, particularly on high-speed highways.

A lane of a modern highway surface is normally constructed to a slight plane cross slope. In practice, however, highways are not perfectly plane and do not always possess cross slopes. Water will flow across a surface along a line, the resultant slope of which depends on the transverse cross slope or superelevation and longitudinal gradient. An indication of the effects of various transverse cross slope and longitudinal gradient combinations on drainage lengths for a 24-ft wide pavement are given in

Table 1 (10, 11, 12). It can be seen that steep longitudinal gradients and flat cross slopes markedly increase drainage lengths.

The existence of longitudinal gradient not only increases the flow-path length but also increases the water depth along the lower side of the road relative to the flat longitudinal gradient. The problem is further complicated by horizontal and vertical curves and combinations thereof as well as at-grade intersections. A major benefit of steep cross slopes is the reduction in the volume of water that can collect in pavement deformations. This is particularly important on surfaces that exhibit wheel-track rutting and localized deformations.

All road surface types will drain surface water rapidly and reasonably completely if cross slopes are steep enough. However, the slope must not be steeper than that acceptable from general considerations for road safety, design, drivability, and appearance. Driving on steep, tangent cross slopes presents a safety hazard, with the vehicle tending to veer toward the low edge of the pavement. According to the American Association of State Highway Officials (13), cross slopes up to $\frac{1}{4}$ in./ft (1 in 48) are barely noticeable in relation to vehicle steering. AASHO guidelines for cross slope with regard to surface type recommend that cross slopes never be flatter than $\frac{1}{8}$ in./ft.

Hydraulics of Water Flow

When a rainfall of constant intensity falls over a pavement surface, the following series of events takes place (Fig. 2):

1. Initially a certain amount of water is required to fill the interstices of the surface before runoff occurs. This amount is referred to as "depression storage" and is measured in volume per unit area or average depth in inches. It depends on the initial wetness of the surface, amount of surface texture, deformation in the surface, and cross slope.
2. After the amount of water required for depression storage is satisfied, runoff begins. The runoff rate increases to an equilibrium value, and for an impermeable surface this rate is equal to the rainfall intensity. It is during this interval that the amount of water detained on the surface increases to a maximum value. The thin sheet of water on the surface at the time of constant runoff, excluding that required for depression storage, is called "surface detention." It has the same units as depression storage and can also be expressed as a value at a point or an average over an area. Surface detention depends primarily on the cross slope and rainfall intensity.
3. When the rainfall ceases, the runoff rate momentarily increases and then decreases to zero while the depth of water held by surface detention also decreases to zero.
4. Water that is contained in depression storage decreases by surface evaporation.

Yu and McNown (14) and Izzard (7) have reported that a momentary increase in runoff occurs immediately after the cessation of rainfall. This in effect indicates that raindrop impact increases the turbulence and hence increases the resistance to water flow over the surface during the period of rainfall.

When flow of thin films of water is laminar and steady, the resistance to flow is solely due to viscous shear. It has been experimentally determined (15), however, that free surface flow becomes unstable when the Froude number $V/\sqrt{gd}$ exceeds 2 and the Reynolds number Vd/ν exceeds 500. In these expressions V is the average flow velocity, d is water depth, and ν is the kinematic viscosity. Thus on slopes greater than 1 in 42 where the water depth is greater than 0.08 in., the water flow will tend to be nonlaminar even on perfectly planar surfaces. With the combination of rough texture and the disturbing effect of raindrops on pavement surfaces, water flow is generally turbulent after a short length of flow.

TEST FACILITIES AND PROCEDURES

Surface Types

Nine test surfaces were placed on individual 28½-ft long by 4-ft wide, double T, prestressed concrete beams. Each surface represented a section of a highway surface 2 lanes wide taken perpendicular to the direction of travel (Fig. 3).

Figure 1. Water flow over an impermeable road surface.

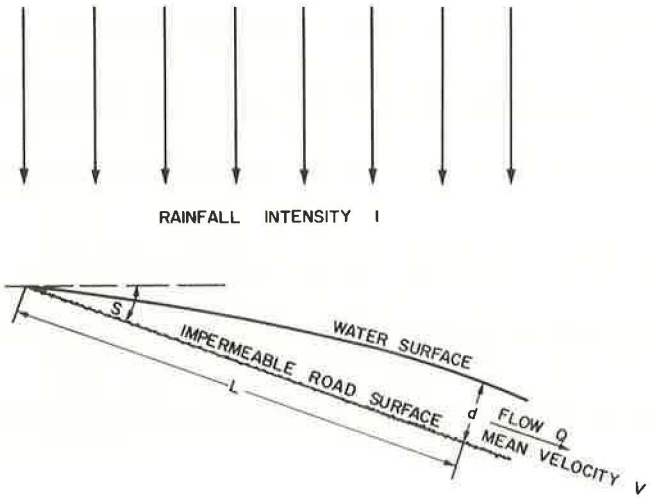

Figure 2. Rainfall runoff hydrograph.

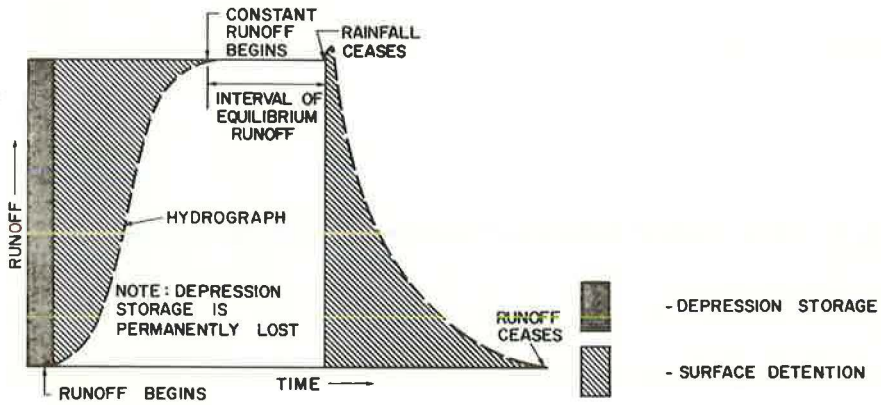

Table 1. Effect of cross slope and longitudinal gradient on drainage length.

Transverse Cross Slope (in./ft)	Longitudinal Gradient (percent)	Drainage Length (ft)	Increase in Drainage Length[a] (percent)
1/16	0	24	—
	1	52	117
	2½	118	390
	5	232	866
	10	461	1,820
3/8	0	24	—
	1	25	4
	2½	31	29
	5	45	88
	10	80	233

[a]With respect to a zero longitudinal gradient.

Figure 3. Surface element.

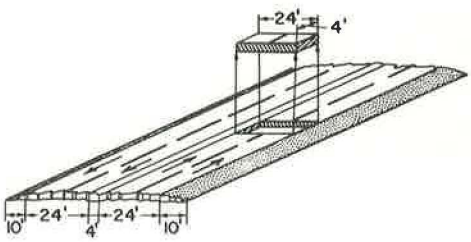

Descriptions of the surfaces are given in Table 2. The surfaces that were chosen contain the range of textures found on Texas highway pavements. Previous research had indicated that, on a random sample of 41 Texas highway pavements, textures ranged from 0.00 to 0.07 in. (16). Photographs of the surfaces are shown in Figure 4.

Equipment

A general view of the test equipment is shown in Figure 5. The tests were conducted inside a former airfield hangar in order to minimize wind effects. Following are descriptions of the various components.

The two 30-ft long by 9-ft high frames used to support the 58 U.S. Forest Service Type F nozzles were composed of 4-in. wide by 1-in. deep channel iron. The upper horizontal channels were attached to the vertical channels in such a manner that the upper channels could be pivoted, thus permitting the water spray from the nozzles to be directed over the test surface. The nozzles, located approximately 1 ft to the sides and 5 ft above the test surface, were equally spaced 1 ft apart on the two frames. The orifices were placed so that every fourth nozzle had the same orifice size. This same pattern was followed on the opposite side; however, the spacing of similar orifices was offset by two nozzles so that, when nozzles of a given orifice size were operating, the rainfall spray would tend to be more uniform on the surface.

The two-hose nozzles were placed directly over the test surface. One was centered at the upper end and the other centered 9 ft from the lower end of the surface. The nozzles, located 15 ft above the surface, sprayed a circular pattern, only part of which fell on the test area and thereby contributed to the intensity. Half-in. pipes attached to the top of the frame served as support for the nozzles.

Two 10-ft long, 10-in. diameter metal pipes sealed at both ends served as manifolds. Connections between the ½-in. hose and manifolds were ¾-in. pipe couplings. Gate valves were placed between each coupling and hose. The upper ends of the hose were attached to the upper channels.

Water was supplied to the manifolds through a 2-in. diameter pipe. Flow and pressure were controlled by both a gate valve and a butterfly valve. Another butterfly valve was used for an instant bleeder valve. Water pressure gauges were placed in both manifolds to monitor the water pressure.

The end of the test surface, which was to simulate the outer or lower edge of the pavement, was placed 4 ft above the floor on a specially designed stand. This stand was bolted to the concrete floor to prevent the beam from moving. The other end of the beam was placed directly on two 2-ft high, 5-ton mechanical jacks. The jacks had a throw of 12 in. It was therefore necessary to use a 2-in. spacer between the jack and beam in order to achieve the desired range of cross slopes.

Redwood strips, 6 in. wide and 1 in. thick, were attached to each side and to the upper end of the beam. The strips extended 2 in. above the surface. The strips were required to prevent the water from running off the side of the flat beam and thus confine it to the 4-ft wide surface. The space between the strips and the surface was sealed with caulking compound. An aluminum flume was placed on the lower end of the beam for the purpose of directing the water into the collecting tank.

A 3-ft square by 2-ft deep metal tank was used to collect the water at the lower end of the beam. An auxiliary tank with similar dimensions was connected to the tank and used in combination during the heavier rainfalls. For the lower rainfall rates only one tank was needed because the capacity was sufficient to accommodate the discharge.

A special order Stevens Type F Recorder was used for maintaining a graphic record of the time rate of water-level rise in the tank. The smallest time scale division of the recorder chart was equal to 37.5 sec, and the scale could be estimated to the nearest 3.75 sec. In operation, the horizontal chart drum is turned in response to a large diameter float action, which is equal to changes in water levels. The large float allowed water surface measurements to the nearest 0.005 ft. The stylus is moved across the width of the chart paper at a clock-controlled constant speed. After the rate of water rise in the tank becomes constant, the rainfall intensity over the surface can be deduced from the time rate of water-level rise in the tank. The recorder was positioned directly over the collecting tank, and a stilling well was used to protect the float from turbulence.

Table 2. Descriptions of the surfaces tested.

Surface Number	Surface Type	Maximum Size of Aggregate (in.)	Average Texture Depth[a] (in.)
1	Portland cement concrete, rounded siliceous gravel, transverse drag[b]	3/4	0.035
1A	Portland cement concrete, rounded siliceous gravel, longitudinal drag[b]	3/4	0.036
2	Clay-filled tar emulsion (jennite) seal, no aggregate		0.009
3	Hot-mixed asphalt concrete, crushed limestone aggregate, terrazzo finish	1/2	0.003
4	Hot-mixed asphalt concrete, crushed siliceous gravel	1/4	0.019
5	Hot-mixed asphalt concrete, rounded siliceous gravel	5/8	0.039
6	Rounded siliceous gravel surface treatment, chip seal	1/2	0.141
7	Synthetic lightweight aggregate surface treatment, chip seal	1/2	0.164
8	Hot-mixed asphalt concrete, synthetic lightweight aggregate	1/2	0.020

[a]Obtained by putty impression method (17). [b]With respect to direction of vehicular travel.

Figure 4. Photographs of the surfaces.

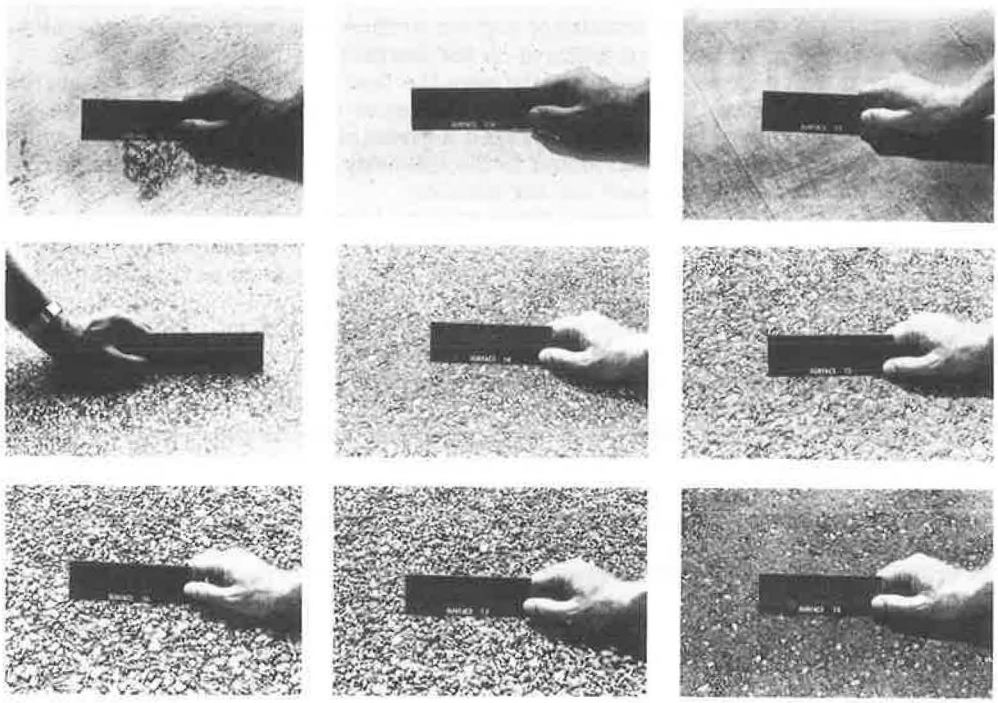

Figure 5. General view of test equipment.

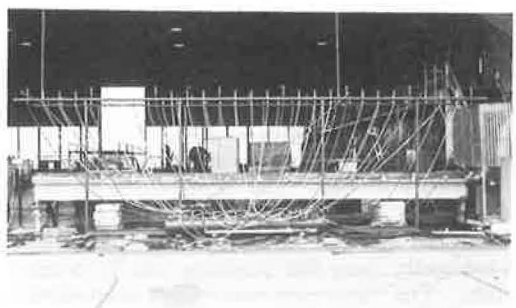

Figure 6. Point gauge used for measuring water depth.

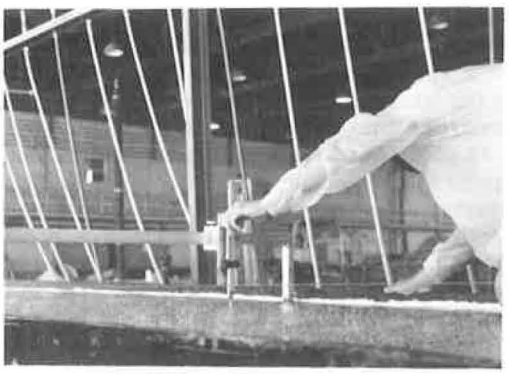

A Leupold and Stevens point gauge was used for measuring the water depths on the surfaces. The metric scale vernier can be read directly to the nearest 0.2 mm. The gauge was attached to a 46-in. long stand as shown in Figure 6 and could be moved along the full length of the stand. Measurements were taken accordingly.

The silicone putty impression method was used for assessing the degree of surface macrotexture (Fig. 7). This method was initially developed as a means of providing surface-texture correction factors for nuclear density measurements and has also been used in pavement friction research (17, 18). The equipment consisted of a 6-in. diameter by 1-in. thick metal plate with a 4-in. diameter, $\frac{1}{16}$-in. deep recess machined into one side and a 15.90-gram ball of silicone putty. When placed on a smooth surface, 15.90 grams of putty will smooth out to a 4-in. diameter circle, $\frac{1}{16}$ in. deep, thus completely filling the recess.

The silicone putty is formed into an approximate sphere and placed on the pavement surface. The recess in the plate is centered over the putty, and the place is pressed down in firm contact with the road surface. The more irregular the surface texture (the higher the macrotexture) is, the smaller the resulting putty diameter will be because more material is required to fill the surface texture. Average texture depth, based on volume per unit area, is calculated from an average of four diameter measurements.

Testing Procedure

A methodical test procedure was used for each surface. Five water depth measurements, spaced equidistant across the width of the surface, were taken at four locations (approximately 6-ft intervals) along the drainage length of the surface. Measurements were taken at approximately 6, 12, 18, and 24 ft as measured from the upper end of the drainage area. These 20 measurements were repeated for each cross slope-rainfall intensity combination. Table 3 gives 25 series that were used. An additional five series at a cross slope of 1 in./ft (1:12) were taken on three surfaces. A minimum of 500 depth measurements was taken on each surface.

Zero measurements were first taken at each test spot. These were necessary in order to establish a datum plane at the top of the texture from which subsequent water-depth measurements could be referenced. Both positive (i.e., above top of texture) and negative (i.e., below top of texture) water depths were recorded.

It was desirable for the raindrop size to increase as the rainfall intensity was increased. This requirement necessitated the use of different nozzle orifice sizes; the larger orifices produced higher intensities and correspondingly larger drop sizes. The intensity could also be varied by regulating the water pressure and changing the number of nozzles. The hose type of nozzle was used for the lowest rainfall intensity.

ANALYSIS AND DISCUSSION OF TEST RESULTS

The water-depth data for each surface were analyzed by using a computerized multiple regression program to obtain the best fit of the data. Equations were derived for determining water depths based on both the top and bottom of the texture datum planes. Because a logarithmic model was used, the equations based on the top of the texture datum plane are only valid for water depths greater than zero. (Logarithmic models do not accept zero or negative values.) When the water depth above the texture approaches zero or becomes negative, equations based on a datum plane at the bottom of the texture must be used with appropriate average texture depths subtracted from the resulting water depths. The subtraction shifts the datum plane to the top of the texture.

Tabular representations and graphical plots of the relative effects of the variables on water depths are given in Table 4 and shown in Figure 8 respectively. These values were determined from the highest correlation, overall experimentally obtained equation:

$$d = 3.38 \times 10^{-3} (1/T)^{-0.11} (L)^{0.43} (I)^{0.59} (1/S)^{0.42} - T$$

Figure 7. Putty impression method for measuring surface macrotexture.

Figure 8. Water depths versus variables for combined surfaces.

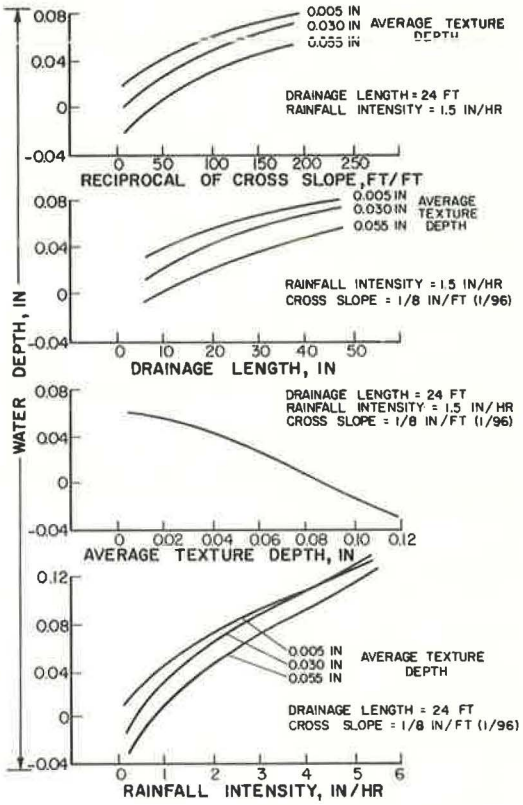

Table 3. Testing series.

Series	Cross Slope In./Ft	Cross Slope Ft/Ft	Approximate Rainfall Intensities (in./hr)
A1-A5	1/16	1/192	0.50, 1.00, 2.00, 3.50, 5.50
B6-B10	1/8	1/96	0.50, 1.00, 2.00, 3.50, 5.50
C11-C15	1/4	1/48	0.50, 1.00, 2.00, 3.50, 5.50
D16-D20	3/8	1/36	0.50, 1.00, 2.00, 3.50, 5.50
E21-E25	1/2	1/24	0.50, 1.00, 2.00, 3.50, 5.50
F26-F30[a]	1	1/12	0.50, 1.00, 2.00, 3.50, 5.50

[a]Only taken on three surfaces.

Table 4. Effects of variables on water depth.

Constant	Variable	Resultant Water Depth (in. at 24 ft)	Change (percent)
Texture, 0.03 in., length, 24 ft, intensity, 1.5 in./hr	Cross slope, in./ft		
	1/16	0.074	
	1/8	0.048	-35
	1/4	0.028	-62
	3/8	0.021	-72
	1/2	0.013	-82
	1	0.002	-97
Length, 24 ft, intensity, 1.5 in./hr, cross slope, 1/8 in./ft	Texture, in.		
	0.005	0.059	
	0.015	0.057	-3
	0.030	0.048	-19
	0.050	0.038	-36
	0.075	0.011	-81
	0.125	-0.034	-158
Intensity, 1.5 in./hr, cross slope, 1/8 in./ft, texture, 0.03 in.	Drainage length, ft		
	6	0.013	
	12	0.028	115
	18	0.039	200
	24	0.048	269
	36	0.062	377
	48	0.074	469
Texture, 0.03 in., length, 24 ft, cross slope, 1/8 in./ft	Intensity, in./hr		
	5.5	0.138	
	3.5	0.098	-29
	2.0	0.062	-55
	1.0	0.031	-77
	0.5	0.011	-92
	0.1	-0.014	-110

where

d = average water depth above the top of texture, in.;
T = average texture depth, in.;
L = length of drainage path, ft;
I = rainfall intensity, in./hr; and
S = cross slope, ft/ft.

In its original form the equation was based on a datum plane at the bottom of the texture; however, subtraction of texture depth from the obtained depth shifts the datum plane to the top of the texture. The equation is valid for all water depths with negative values, which indicate water depths below the top of the texture.

As given in Table 4, increases in cross slope result in corresponding decreases in water depths. The effect is more pronounced at the flatter cross slopes. For example, increasing the cross slope from $\frac{1}{6}$ in./ft ($\frac{1}{192}$ ft/ft) to $\frac{1}{4}$ in./ft ($\frac{1}{48}$ ft/ft) will decrease the corresponding water depth by 62 percent of its $\frac{1}{16}$-in./ft value in the outside wheelpath. Note, however, that cross slopes in excess of $\frac{1}{4}$ in./ft do not affect resultant water depths as much, particularly when the magnitudes of the cross-slope increments are given consideration.

An inverse relationship between macrotexture and water depth was also found. The effect increased at the higher macrotexture levels and was more pronounced at macrotexture levels greater than 0.050 in.

As expected, water depths increased as drainage lengths increased. Also as expected, water depths decreased as rainfall intensities decreased. A rainfall intensity of about 0.3 in./hr would be required to encapsulate the asperities on a pavement surface having 0.03-in. texture, 24-ft drainage length, and $\frac{1}{8}$-in./ft cross slope.

In addition to the previous discussion of the relative effects of cross slope on water depth, another major benefit of a steeper cross slope would be the reduced volume of water that could collect in pavement deformations. This is particularly so on flexible pavements where a certain amount of wheel-track depression often occurs because of compaction in the base and the surface. The use of paved shoulders generally reduces the subsidence of the outside one-third of the right traffic lane. Such subsidence was caused by less construction compaction near the pavement edge and subsequently greater permanent deformation during service. Where highly compacted shoulders are used, permanent deformation can still occur in the traveled lanes; thus, after a period of time, a portion of the cross slope can be lost. Steeper cross slopes will reduce the effect.

It was observed during the experimental tests that, after the cessation of rainfall, the steeper cross slopes drained the remaining surface water more quickly than did the flatter slopes. This is another benefit of steep cross slopes, particularly in areas of high humidity, low wind speed, low ambient temperatures, or combinations of these. These conditions serve to increase the drying time and thus the length of the time the surface is wet. Steeper cross slopes not only would serve to remove the bulk of the water more quickly but also would facilitate drainage of low areas and deformations.

Another possible means of reducing the wet-pavement exposure time would be the use of a permeable surface that could absorb some of the rainfall and also permit water to drain through the permeable layer and then laterally to the pavement edge. Admittedly, this concept has some disadvantages, but under certain circumstances these would be more than offset by improved safety. Results of field experiments by the Texas Highway Department and the Texas Transportation Institute on permeable pavements will be the subject of a separate paper.

SUMMARY OF FINDINGS AND RESULTS

Nine surfaces were tested. The surfaces were placed on individual beams, and a uniform rainfall intensity was applied to the surfaces. Water-depth measurements were taken at several drainage lengths for various combinations of rainfall intensity and pavement cross slope. Multiple regression analyses were used to determine the best fit of the relationships.

An experimentally determined equation relating water depth to surface texture, length of drainage path, rainfall intensity, and pavement cross slope was developed.

Increased surface texture resulted in a decrease in water depth as measured from the top of the surface texture for a given rainfall intensity, cross slope, and drainage length. This effect was more pronounced at the flatter cross slopes and lower rainfall intensities.

Greater drainage lengths increased water depths; however, the rate of increase in water depth became smaller as drainage lengths increased. Greater water depths were associated with high rainfall intensities. (Even at the lower rainfall intensities, the adverse effect of rainfall intensity was quite pronounced.)

Increases in pavement cross slope resulted in reduced water depths. This effect was very significant at the flatter cross slopes where a slight increase in cross slope resulted in a pronounced reduction in water depth.

CONCLUSIONS AND RECOMMENDATIONS

Increases in the minimum rates of pavement cross slopes are warranted. It is recommended that cross slopes ranging from $\frac{1}{8}$ in./ft ($\frac{1}{96}$) to $\frac{1}{4}$ in./ft ($\frac{1}{48}$) be used on high-speed rural highways. The higher cross slope of $\frac{1}{4}$ in./ft should be favored in areas with greater potential for wet-weather accidents. This not only will reduce the water depth on pavements for a given rainfall intensity but also will assist in providing for drainage of low areas and depressions that tend to lower the effectiveness of built-in cross slopes. Steeper cross slopes will offer a margin of safety against ponding and concomitant long wet-pavement exposure times.

Essentially smooth-textured, dense-graded surfaces should not be used on high-speed rural highways. Slight amounts of precipitation will result in water depths above the texture peaks and thus in poor effective drainage on these types of surfaces. If such surfaces are used, an ample degree of permeability should be built into the surface. The surface aggregate should be capable of puncturing the water film, or drainage of the water into the surface should be possible.

It is suggested that research be conducted to determine the relative influences of ambient temperatures, wind velocities, and relative humidities on the drying rates of various pavement surface types after rainfall has ceased. Rainfall records based on observations at 10-min intervals would be desirable, if not necessary. Drying rates are indicative of the time during which the pavement surface is wet after cessation of rain. It is assumed that high relative humidity, low wind velocity, and low ambient temperature all contribute to increased exposure times and thus decreased drying rates for a given surface. Their relative effects and significance need to be determined. From such data it may very well be possible to estimate inclement weather accident potential, considering, of course, several other important contributing factors including speed, pavement surface characteristics, and geometrics. Allocation of funds for improvement of highways subject to skidding accidents could then be scheduled according to a more reasonable plan.

Additional research currently in progress proposes to furnish field data on the effect of wind velocity and direction on pavement water depths for the nine surfaces used in this study.

ACKNOWLEDGMENTS

This paper is based on research sponsored by the Texas Highway Department in cooperation with the Federal Highway Administration. The assistance of maintenance personnel of District 17 of the Texas Highway Department and Kenneth D. Hankins of Texas Highway Research, Austin, is gratefully acknowledged. The opinions, findings, and conclusions expressed or implied in this report are those of the research agency and not necessarily those of the Texas Highway Department or the Federal Highway Administration.

REFERENCES

1. Kummer, H. W., and Meyer, W. E. Tentative Skid-Resistance Requirements for Main Rural Highways. NCHRP Rept. 37, 1967.

2. Dearinger, J. A., and Hutchinson, J. W. Traffic Control and Roadway Elements—Their Relationship to Highway Safety, Rev. Ed. Highway Users Federation for Safety and Mobility, Washington, D.C., 1970, Ch. 7.
3. Albertson, M. L., et al. Fluid Mechanics for Engineers. Prentice-Hall, Englewood Cliffs, N.J., 1960.
4. Manning, R. On the Flow of Water in Open Channels and Pipes. Trans., Inst. of Civil Eng., Ireland, Vol. 22, 1891.
5. Bernard, J. Discussion of paper by Gregory, R. L., and Arnold, C. E., Run Off—Rational Run Off Formulas. Trans., ASCE, Vol. 96, 1932.
6. Horton, R. E. The Interpretation of Run Off Plot Experiments With Reference to Soil Erosion Problems. Proc., Soil Sci. Soc. Amer., 1938.
7. Izzard, C. F. Hydraulics of Runoff From Developed Surfaces. HRB Proc., Vol. 26, 1946, pp. 129-150.
8. Watkins, L. H. An Investigation of the Hydraulics of Run-Off From Road Surfaces: First Report. Gt. Brit. Road Research Laboratory, Note LN/418/LHW, Sept. 1963.
9. Watkins, L. H. An Investigation of the Hydraulics of Run-Off From Road Surfaces: Second Report. Gt. Brit. Road Research Laboratory, Note LN/699/LHW, Oct. 1964.
10. Ross, N. F., and Russam, K. The Depth of Rain Water on Road Surfaces. Gt. Brit. Road Research Laboratory, RRL Rept. LR 236, 1968.
11. Rose, J. G. The Effects of Rainfall Intensity, Pavement Cross Slope, and Surface Texture on Water Depths and Resultant Friction Properties of Various Pavements. Texas A&M Univ., College Station, PhD dissertation, May 1971.
12. Gallaway, B. M., Schiller, R. E., Jr., and Rose, J. G. The Effects of Rainfall Intensity, Pavement Cross Slope, Surface Texture, and Drainage Length on Pavement Water Depths. Texas Transportation Institute, Texas A&M Univ., Res. Rept. 138-5, Jan. 1971.
13. A Policy on Geometric Design of Rural Highways—1965. American Association of State Highway Officials, 1966.
14. Yu, U. S., and McNown, J. S. Runoff From Impervious Surfaces. U.S. Army Engineer Waterways Experiment Station, Contract Rept. 2-66, Feb. 1963.
15. Rouse, H., ed. Engineering Hydraulics. John Wiley and Sons, New York, 1950.
16. Gallaway, B. M., and Rose, J. G. Macrotexture, Friction, Cross Slope and Wheel Track Depression Measurement on 41 Typical Texas Highway Pavements. Texas Transportation Institute, Texas A&M Univ., Res. Rept. 138-2, June 1970.
17. Rose, J. G., Gallaway, B. M., and Hankins, K. D. Macrotexture Measurements and Related Skid Resistance at Speeds From 20 to 60 Miles Per Hour. Highway Research Record 341, 1970, pp. 33-45.
18. Gallaway, B. M., and Rose, J. G. Highway Friction Measurements With Mu-Meter and Locked Wheel Trailer. Texas Transportation Institute, Texas A&M Univ., Res. Rept. 138-3, June 1970.
19. Gallaway, B. M., Epps, J. A., and Tomita, H. Effects of Pavement Surface Characteristics and Textures on Skid Resistance. Texas Transportation Institute, Texas A&M Univ., Res. Rept. 138-4, Sept. 1971.

DISCUSSION

T. Y. Kao and J. W. Hutchinson, University of Kentucky

The information presented concerning runoff water depths on pavement surfaces is very useful. The empirical equation obtained by the authors provides highway engineers with a new criterion for estimating the relative effects of pavement surface texture, cross slope, drainage length, and rainfall intensity on pavement surface water depths. The contribution of the authors' work is highly significant.

However, for completeness of the information, consideration should be given to the effects of wind and raindrop impact on water runoff. The former has not been included in the paper, whereas only the gross effect of the latter is included implicitly and then only with respect to zero lateral velocity of the raindrops.

EFFECT OF WIND ON SURFACE RUNOFF

Intuitive conjecture and direct observations suggest that flow of a liquid will be retarded to a certain degree if the air flow above it is in the opposite direction and will be further accelerated if the air flows in the direction of the liquid. These phenomena can be readily illustrated in terms of fluid dynamics.

The wind profile near a boundary can be described logarithmically and is often written in the form of the law of Wall

$$[u(y)/u_*] = (1/0.4) \ln (u_* y/\nu_a) + \text{const}$$

where

$u(y)$ = velocity of air as a function of distance measured upward from the boundary,
$u_* = \sqrt{\tau_o/\rho_a}$ = shear velocity at the boundary,
y = distance measured from the boundary, and
ν_a = kinematic viscosity of air.

The numerical value, 0.4, represents Karman's constant. The constant to be determined in this equation depends on the boundary characteristics. Values ranging from +6.1 to -7.0 have been observed by Plate, Chang, and Hidy (20) during laboratory experiments on wind-generated waves. Their work also indicated that, when the velocity of air relative to the surface drift current velocity u_s is used in the equation for the case where no significant wave exists, the constant obtained for air flowing over a solid boundary, 5.6, can be used. The equation, therefore, can be written as

$$[u(y) - u_s/u_*] = (1/0.4) \ln (u_* y/\nu_a) + 5.6$$

According to the definition of boundary layer thickness, δ, at $y = \delta$, $u(\delta) = 0.99\, u_\infty$. Here u_∞ is the speed of the wind. Based on the Plate, Chang, and Hidy data, a smooth wind with a velocity of 8.2 mph produces a surface drift velocity of 0.35 fps in the direction of the wind. When turbulence is introduced to the air flow, an even higher drift current velocity will result.

Assuming a linear velocity distribution in the water gives an average drift velocity for water ponded on a flat surface of 0.175 fps. To illustrate the effect of drift current velocity on pavement surface water depth, we may use the following rough approximation.

Employing the data provided by the authors, for L = 24 ft, S = 1/96, T = 0.055 in., and i = 5 in./hr gives a water depth of approximately 0.12 in. At this rainfall intensity the equilibrium discharge is 0.00278 cfs/ft at the end of the drainage length. The average velocity of flow without wind effect is 0.278 fps. When the wind effect is superimposed on water flow velocity, the average water flow velocity will be

$$V_w^+ = V_w + U_s = 0.453 \text{ fps}$$

for wind in the direction of flow, and

$$V_w^- = V_w - U_s = 0.103 \text{ fps}$$

for wind in the negative direction of flow. The water depth will be 0.0736 in. for positive direction wind and 0.324 in. for negative direction wind as compared to d = 0.12 in. without wind effect.

Clearly, this analysis should only be used as a qualitative illustration. The actual system is much too complicated to be handled analytically. For instance, in addition to the shear effect considered, momentum exchange also occurs at the wind-water interface, adding to the total effect of the wind. This is especially important when waves are generated. Furthermore, when water is flowing on a slope, air flow approaches at an angle above the plane parallel to the water surface. The greater the cross slope (crown) of the pavement is, the greater the confrontation of the wind will be and the greater the momentum exchange on the upwind side of the pavement will be for a given wind velocity. The authors' tabular amounts of decrease in water depth

that accompanies various increases in pavement cross slope would therefore be lessened considerably, even by mild cross winds. Water depths at least two or three times greater than those in Table 4 would be required to present realistic rainfall conditions along highways. Determination of the actual magnitude of combined wind and cross slope effects should be an objective in future research. Furthermore, the effects of wind on the authors' tabular amounts of increase in water depth due to increased drainage length need investigation; the greater the drainage length (pavement width) is, the greater the fetch of the wind will be and the greater the probability of air flow turbulence and wave production will be, which add respectively to the shear and momentum exchange effects of the wind.

EFFECT OF RAINDROP IMPACT ON SURFACE RUNOFF

The effect of raindrop impact on runoff water is to cause a logarithmic type of velocity distribution at Reynolds number below 1,000 where the flow would normally be laminar (21). This can be characterized by flow retardation near the free surface due to the impact turbulence. For a fixed rate of discharge, such retardation would result in increased water depth. This effect is included in the authors' work because actual (zero wind) rainfall simulation has been used.

However, when this effect is expressed in terms of flow resistance on a smooth surface, Wenzel (22) reported that rainfall intensity increases the resistance to flow only for Reynolds numbers below approximately 2,000. Above this value the effect of rainfall intensity decreases rapidly until it becomes insignificant. Therefore, the relation between water depth d and the rainfall intensity i is not a monotonous one. Care should be taken not to make application of the authors' equation to describe flows with larger Reynolds numbers. Nevertheless, in predicting runoff water depths on pavements, such uncertainty does not exist because the Reynolds number for this type of flow is almost always below the value 2,000.

Neither Wenzel's work nor that of the authors considered the effect of wind, which, undoubtedly, will vary the effect of drop impact and momentum exchange between the raindrop and the water flow. Further study to include this effect should be of great interest.

References

20. Plate, E. J., Chang, P. C., and Hidy, G. M. Experiments on the Generation of Small Water Waves by Wind. Jour. Fluid Mech., Vol. 35, Part 4, 1969, pp. 625-656.
21. Yoon, Y. N. The Effect of Rainfall on the Mechanics of Steady Spatially Varied Sheet Flow on a Hydraulically Smooth Boundary. Univ. of Illinois, Urbana, PhD thesis, 1970.
22. Wenzel, H. G. The Effect of Raindrop Impact and Surface Roughness on Sheet Flow. Univ. of Illinois, Water Resources Center, Res. Rept. 34, 1970.

AUTHORS' CLOSURE

The complimentary remarks of Kao and Hutchinson are sincerely appreciated. The authors are well aware of the effects of wind on water. Recent hurricanes such as Carla left little doubt in the minds of many Texans!

It is pleasing to see the very neat mathematical treatment presented by Kao and Hutchinson concerning the positive and negative effects of wind on pavement water depths. These calculations are necessarily based on "a smooth wind" from a fixed direction, neither condition being at all likely but still a definite possibility.

Indeed much more work needs to be done to fully evaluate the range of conditions that repeatedly transpire on our highways during rains with wind and to attach practical significance to these findings.

The effect of raindrop impact is recognized, and general reference to this effect was mentioned in the paper; however, within the range of variables investigated, it was not considered to have an appreciable effect.

Kao and Hutchinson are to be commended for adding their discussion.

SPONSORSHIP OF THIS RECORD

GROUP 2—DESIGN AND CONSTRUCTION OF TRANSPORTATION FACILITIES
John L. Beaton, California Division of Highways, chairman

GENERAL DESIGN SECTION
F. W. Thorstenson, Minnesota Department of Highways, chairman

Committee on Surface Drainage of Highways
Lester A. Herr, Federal Highway Administration, chairman
Alvin G. Anderson, John J. Bailey, Jr., Harry H. Barnes Jr., Mike Bealey, Allen L. Cox, Glenn W. Decker, C. R. Edgerton, Kenneth S. Eff, Gene R. Fiala, Samuel V. Fox, Harry C. Green, John G. Hendrickson, Jr., Philip V. King, Robert A. Norton, Byron M. Parker, Ralph M. Peterson, Arthur L. Pond, Jr., William O. Ree, Brian M. Reich, James K. Searcy, William P. Somers, F. W. Thorstenson, Adrianus Van Kampen, A. Mainard Wacker

PAVEMENT DESIGN SECTION
John E. Burke, Illinois Department of Transportation, chairman

Committee on Surface Properties-Vehicle Interaction
W. E. Meyer, Pennsylvania State University, chairman
Malcolm D. Armstrong, Glenn G. Balmer, F. Cecil Brenner, Arthur D. Brickman, William F. R. Briscoe, William C. Burnett, A. Y. Casanova, III, Blaine R. Englund, William Gartner, Jr., Ralph C. G. Haas, Douglas I. Hanson, Robert N. Janeway, David C. Mahone, B. F. McCullough, Robert B. McGough, Paul Milliman, Alexander B. Moore, Desmond F. Moore, E. W. Myers, F. William Petring, Bayard E. Quinn, John J. Quinn, Frederick A. Renninger, Rolands L. Ritzenbergs, Hollis B. Rushing, Richard K. Shaffer, Elson B. Spangler, W. E. Teske, M. Lee Webster, Ross G. Wilcox, Dillard D. Woodson

GROUP 3—OPERATION AND MAINTENANCE OF TRANSPORTATION FACILITIES
Harold L. Michael, Purdue University, chairman

Committee on Operational Effects of Geometrics
John W. Hutchinson, University of Kentucky, chairman
E. N. Burns, Stanley R. Byington, Arno Cassel, Robert R. Coleman, B. K. Cooper, Joseph C. Corradino, James J. Crowley, Harley T. Davidson, John A. Dearinger, John Drake, Julie Anna Fee, George F. Hagenauer, Rajendra Jain, Janis H. Lacis, Richard A. Luettich, William A. McConnell, Joseph M. McDermott, Thomas E. Mulinazzi, John D. Orzeske, Stuart R. Perkins, Eugene F. Reilly, Neilon J. Rowan, Sheldon Schumacher, James J. Schuster, Robert B. Shaw, James Correll Spencer, Kenneth A. Stonex, Vasant H. Surti, Paul R. Tutt, Walter C. Vodrazka, Jason C. Yu

Lawrence F. Spaine and Kenneth B. Johns, Highway Research Board staff

The sponsoring committee is identified by a footnote on the first page of each report.